European Journal of Taxonomy 1084: 1–71
https://doi.org/10.5852/ejt.2026.1084.3314

europeanjournaloftaxonomy.eu
ISSN 2118-9773
2026 · Valencia J.H. *et al.*

Received: 5 July 2025 • *Accepted: 23 June 2026* • *Published: 11 August 2026*

Topic editor: Magalie Castelin • *Section editor: Aurélien Miralles* • *Desk editor: Lizeth Alonso*

Monograph

urn:lsid:zoobank.org:pub:01CC9D46-CDFC-442B-9D48-352C5D40055B

Integrative review of cis-Andean monadal coralsnakes of the genus *Micrurus* (Elapidae: Serpentes) reveals considerable overestimation of species diversity

Jorge H. VALENCIA[1,*], Eric N. SMITH[2], Biraj SHRESTHA[3], Juan C. CHÁVEZ-ARRIBASPLATA[4], Pablo J. VENEGAS[5], Walter QUILUMBAQUIN[6], Alejandro ESPINOSA DE LOS MONTEROS[7], Omar TORRES-CARVAJAL[8], Juan C. CHAPARRO[9], Andrés LIRA-NORIEGA[10] & H. Mauricio ORTEGA-ANDRADE[11]

[1,9] Red de Estudios Moleculares Avanzados, Instituto de Ecología, A.C., carretera antigua a Coatepec 351, El Haya, Xalapa, 91073 Veracruz, México.
[2,3] Department of Biology, The University of Texas at Arlington, Arlington, Texas, USA.
[1,6,11] Laboratorio de Biología Integrativa, Grupo de Investigación en Biogeografía y Ecología Espacial, Universidad Regional Amazónica Ikiam, Tena, Ecuador.
[4,5] Instituto Peruano de Herpetología (IPH), Augusto Salazar Bondy 136, Urb. Higuereta, Surco, Lima, Perú.
[7] Rainforest Partnership, 4005 Guadalupe St., Austin, Texas 78751, USA.
[7] Red de Biología Evolutiva, Instituto de Ecología A.C., carretera antigua a Coatepec 351; El Haya; Xalapa, 91073 Veracruz, México.
[8] Museo de Zoología, Biología, Pontificia Universidad Católica del Ecuador, Avenida 12 de Octubre 1076 y Roca, Quito, Ecuador.
[9] Departamento de Herpetología, Museo de Biodiversidad del Perú (MUBI), Cusco, Perú.
[10] Research Fellow, Secretaría de Ciencia, Humanidades, Tecnología e Innovación (SECIHTI), México.
[11] División de Herpetología, Instituto Nacional de Biodiversidad (INABIO), Quito, Ecuador.

[*] Corresponding author: jorge.valencia@posgrado.ecologia.edu.mx
[2] Email: e.smith@uta.edu
[3] Email: biraj.shrestha@uta.edu
[4] Email: juancarlos.chavez@cordidi.org
[5] Email: sancarranca@yahoo.es
[6] Email: walter.quilumbaquin@ikiam.edu.ec
[7] Email: alejandro.espinosa@inecol.mx
[8] Email: lotorres@puce.edu.ec
[9] Email: jchaparroauza@yahoo.com
[10] Email: aliranoriega@gmail.com
[11] Email: mauricio.ortega@ikiam.edu.ec

Abstract. Coralsnakes of the genus *Micrurus* Wagler, 1824 contain approximately 89 species distributed from the United States to Argentina. The genus *Micrurus* comprises numerous species and presents important taxonomic challenges, particularly in lineages where morphological similarity among species complicates species delimitation. Many species have been described based on subtle morphological differences and/or inadequate molecular analyses. In this study, we focused on cis-Andean monadal coralsnakes using an integrative taxonomic approach that combines a multilocus dataset of mitochondrial (mtDNA) and nuclear (nDNA) gene fragments with morphological data, ecological niche models (ENMs), and extent of occurrence (EOO) analyses to assess species boundaries and infer phylogenetic relationships. Maximum Likelihood and Bayesian phylogenies revealed discrepancies between morphology-based taxonomy and molecular data. Among our findings, we support the junior synonymization of *M. petersi* Roze, 1967, *M. peruvianus* Schmidt, 1936, *M. steindachneri* (Werner, 1901), and *M. tikuna* Feitosa, Da Silva Jr., Pires, Zaher & Prudente, 2015, with *M. ornatissimus* (Jan, 1858), and of *M. albicinctus* Amaral, 1926, *M. annellatus annellatus* (Peters, 1871), *M. a. balzani* (Boulenger, 1898), and *M. bolivianus* Roze, 1967, with *M. corallinus* (Merrem, 1820). In contrast, our results confirm the distinctiveness of *M. langsdorffi* (Wagler, 1824) and *M. medemi* Roze, 1967 as separate evolutionary lineages, warranting their recognition as valid species. Multivariate analyses of morphometric traits showed limited differentiation among the three focal species in both sexes. Discriminant analysis of localities in environmental niche space showed an overall classification accuracy of 92.2%. The distributions of *M. langsdorffi* and *M. ornatissimus* broadly overlap, indicating sympatry, whereas both species are allopatric with respect to *M. corallinus*. Both occur between the Amazon and Negro rivers, whereas *M. corallinus* is distributed south of the Amazon River, with an isolated population in the Brazilian Atlantic Forest. These disjunctions are consistent with Wallace's Riverine Barrier Hypothesis, suggesting river systems as major isolating factors. *Micrurus medemi* occurs along the eastern Andean foothills of Colombia. These results indicate that past morphology-based and/or organellar DNA-based taxonomic studies have overestimated species diversity. Our study highlights the importance of integrative taxonomy for accurately delimiting species and improving our understanding of the evolutionary history of monadal coralsnakes.

Keywords. Biogeography, coloration pattern, morphology, niche modeling, phylogenetic relationships, South America, systematics, taxonomy.

Valencia J.H., Smith E.N., Shrestha B., Chávez-Arribasplata J.C., Venegas P.J., Quilumbaquin W., Espinosa de los Monteros A., Torres-Carvajal O., Chaparro J.C., Lira-Noriega A. & Ortega-Andrade H.M. 2026. Integrative review of cis-Andean monadal coralsnakes of the genus *Micrurus* (Elapidae: Serpentes) reveals considerable overestimation of species diversity. *European Journal of Taxonomy* 1084: 1–71. https://doi.org/10.5852/ejt.2026.1084.3314

Introduction

Species delimitation refers to the process of identifying species-level biological diversity (Carstens *et al.* 2013). The assignment of individual organisms to pre-existing species or higher-level categories, and the designation of new species with proper diagnoses to distinguish them, were for a long time roles performed by taxonomists using traditional morphology and/or somatic characters (Jörger & Schrödl 2013; Rannala 2015). Understanding morphological variation among different groups of organisms is key to identifying diagnostic characters that facilitate taxonomic delimitation (Rannala 2015). Nevertheless, this task may be hindered by phenotypic plasticity among individuals or by the lack of clearly distinctive morphological traits among closely related species (Bickford *et al.* 2007; Carstens *et al.* 2013), making species delimitation based solely on morphology difficult (DeSalle *et al.* 2005). In such cases, morphologically similar but genetically distinct lineages may remain unrecognized as cryptic species (Bickford *et al.* 2007). As a result, multiple evolutionary lineages may remain hidden under a similar external appearance and a single taxonomic name until alternative sources of evidence and thorough analyses reveal deep evolutionary divisions among them (Sites & Marshall 2004).

Likewise, species are sometimes described based on limited geographic sampling, which can lead to the underestimation of intraspecific variation and the neglect of phenotypic plasticity or population genetic structure. These factors may contribute to taxonomic confusion and the overestimation of biodiversity (Dayrat 2005). Therefore, evolutionary relationships should be treated as hypotheses requiring validation through multiple lines of evidence, including morphological, molecular, ecological, and behavioral data (Padial *et al.* 2010). This comprehensive approach, known as integrative taxonomy, promotes more robust and transparent species delimitation (Padial *et al.* 2010; Samadi & Barberousse 2006; de Queiroz 2007). This is especially important for highly specialized taxa, where morphological convergence in the absence of a phylogenetic framework can be misinterpreted as shared ancestry (Grismer *et al.* 2020).

Our study focuses on coralsnakes of the genus *Micrurus* Wagler, 1824, a group of highly specialized species characterized by their unique venom composition, cryptic behavior, and specific ecological requirements (Roze 1996; Lomonte *et al.* 2016; Jowers *et al.* 2019). *Micrurus* is a genus distributed across the Americas, from the southeastern United States to Argentina (Roze 1996; Campbell & Lamar 2004; Da Silva *et al.* 2016). This genus is the most diverse within the family *Elapidae* Boie, 1827, comprising approximately 89 species (Jowers *et al.* 2023). The traditional taxonomy of *Micrurus* is primarily based on color pattern, morphology, and scale counts (Pires *et al.* 2014; Feitosa *et al.* 2015; Bernarde *et al.* 2018). Current evidence suggests that *Micrurus* comprises two major lineages distinguished by their coloration patterns, specifically the distribution of black rings, either in triads or monads (single black rings followed by white rings) (Slowinski 1995; Gutberlet & Harvey 2004). In addition to color pattern, hemipenial morphology supports the monophyly of the genus (Slowinski 1995; Slowinski & Keogh 2000; Campbell & Lamar 2004). These combined morphological character complexes have been useful in recognizing nearly all currently valid species. Nonetheless, species descriptions based solely on coloration patterns and morphometric data have led to the accumulation of numerous synonyms and questionable taxa (Jowers *et al.* 2019; Reyes-Velasco *et al.* 2020). However, with advances in molecular data, several studies have investigated species diversity within *Micrurus* using mitochondrial DNA (e.g., Jowers *et al.* 2019, 2023), a combination of mitochondrial and nuclear DNA (e.g., Hurtado *et al.* 2021), or a combination of mitochondrial and traditional morphological species delimitation analyses to recognize and/or describe species within cryptic species complexes (e.g., Nascimento *et al.* 2024). Furthermore, genome-wide molecular variation has been used to reveal species limits that are not recognized under traditional taxonomy based on morphological characters or molecular datasets limited to a few mitochondrial and nuclear sequence fragments (e.g., Castoe *et al.* 2012; Streicher *et al.* 2016; Reyes-Velasco *et al.* 2020).

Monadal coralsnakes are characterized by a banding pattern consisting of a single black ring followed by a yellow and a red ring (Savage & Slowinski 1990). In contrast, triad-bearing coralsnakes are a phenetic group characterized by a dorsal pattern consisting of a sequence of three black rings separated from each other by white rings. Some monadal members possess poorly to well-developed accessory black rings (e.g., *Micrurus bocourti* (Jan, 1872), *M. sangilensis* Nicéforo María, 1942), and several species exhibit melanized dorsal patterns (e.g., *M. peruvianus* Schmidt, 1936; *M. steindachneri* (Werner, 1901)), in which the red rings become strongly obscured (Campbell & Lamar 2004; Valencia *et al.* 2016). Likewise, scutellation and scale ornamentation are generally homogeneous across species (Feitosa *et al.* 2015). Nonetheless, the few differences in coloration and morphology have commonly been used to delimit species and subspecies in this group (e.g., Roze 1967, 1989; Pires *et al.* 2014; Bernarde *et al.* 2018).

Coralsnakes are predominantly tropical, with the highest species richness concentrated in northwestern South America (Marques & Sazima 2021; Frateles *et al.* 2025). The Andean and Amazonian regions support the highest diversity within their range (Roze 1996; Campbell & Lamar 2004). Nonetheless, most coralsnake taxa exhibit significant taxonomic uncertainty, including those occurring in these regions. Therefore, we provide an initial phylogenetic framework to: (1) assess the diversity of monadal

coralsnakes occurring east of the Andes (i.e., cis-Andean); (2) clarify phylogenetic relationships within monadal coralsnakes by incorporating a greater number of species, specimens, and geographic samples; (3) determine the phylogenetic placement of species previously unsampled in phylogenetic analyses; and (4) provide insights into the biogeography of cis-Andean monadal coralsnakes.

Material and methods

Molecular methods

DNA was extracted from tissue samples (blood, muscle, or shed skins) preserved using a variety of methods, including ethanol, RNAlater, or detergent buffer, using the Wizard® Genomic DNA Purification Kit (Promega, Madison, WI, USA) or the DNeasy Blood & Tissue Kit (Qiagen). DNA purity and concentration were measured using a NanoDrop™ One/OneC Microvolume UV–Vis Spectrophotometer (Thermo Scientific, Waltham, MA, USA).

We amplified five gene fragments for *Micrurus* species: three mitochondrial genes (*16S rRNA*, cytochrome b, *cytb*; NADH dehydrogenase subunit 4, *ND4*, and associated tRNAs His, Ser, and Leu) and one nuclear gene (*neurotrophin-3*, *NT3*). Initially, fragments of the nuclear gene *cmos* were also planned for inclusion in the phylogenetic analyses. Amplification of this locus was successfully achieved; however, the number of high-quality sequences obtained was insufficient to provide a robust phylogenetic signal. Consequently, *cmos* sequences were excluded from all subsequent phylogenetic analyses, and only the mitochondrial loci (*16S*, *cytb*, and *ND4*) and the nuclear locus *NT3* were used to infer evolutionary relationships among the studied taxa.

Laboratory work was conducted at the University of Texas at Arlington, USA; Universidad Regional Amazónica Ikiam, Ecuador; and Pontificia Universidad Católica del Ecuador, Ecuador. All genes were amplified using previously published primer sets and protocols (Table 1). PCR amplification was performed using GoTaq® Green Master Mix 2× (Promega Corporation) following standard protocols. Thermal cycling was conducted on either an Applied Biosystems™ Veriti™ 96-Well Thermal Cycler or a GeneAmp® PCR System 9700 (Applied Biosystems, Foster City, CA, USA). The *16S* rRNA fragments were amplified with an initial denaturation at 95°C for 5 min, followed by 30 cycles of 30 s denaturation at 95°C, 30 s annealing at 52°C, and 45 s extension at 72°C, with a final extension at 72°C for 5 min. *ND4* fragments were amplified with an initial denaturation at 95°C for 4 min, followed by 38 cycles of 30 s denaturation at 94°C, 45 s annealing at 52°C, and 1 min extension at 72°C, with a final extension at 72°C for 5 min. *cytb* fragments were amplified using an initial denaturation at 95°C for 2 min, followed by two cycles of 30 s denaturation at 94°C, 30 s annealing at 53°C, and 1 min 15 s extension at 72°C; three cycles with annealing at 52°C; five cycles with annealing at 51°C; and 30 cycles with annealing at 50°C, all with 30 s denaturation at 94°C and 1 min 15 s extension at 72°C. A final extension was performed at 72°C for 7 min. *NT3* fragments were amplified with an initial denaturation at 94°C for 1 min 30 S, followed by 5 cycles with annealing at 51°C, 5 cycles at 50°C, 10 cycles at 49°C, and 30 cycles at 48°C. Each cycle included denaturation at 94°C for 30 s and extension at 72°C for 1 min 30 s. A final extension was performed at 72°C for 7 min. PCR products were purified using Exonuclease I and Shrimp Alkaline Phosphatase (New England BioLabs, Ipswich, MA, USA) and subsequently sequenced using the Oxford Nanopore Technology platform.

A second PCR was performed to index a barcode for each sample using the PCR Barcoding Expansion 1–96 kit (EXP-PBC096; ONT, Oxford, UK). The reaction volume was 25 µL and consisted of 1 µL PCR barcode, 11 µL purified PCR product, and 13 µL LongAmp® Hot Start Taq 2× Master Mix (New England BioLabs, Ipswich, MA, USA). The thermal cycling program consisted of an initial denaturation at 94°C for 3 min, followed by 15 cycles of 15 s at 94°C, 15 s at 56°C, and 45 s at 65°C, with a final extension of 10 min at 65°C and cooling to 4°C.

Table 1. Sequences of primers used in this study

Gene	Primer	Primer sequence	Source
16S	16Sar	5' CGCCTGTTTATCAAAAACAT 3'	Palumbi 1996
	16S br	5' CCGGTCTGAACTCAGATCACGT 3'	
ND4	ND4	5' CACCTATGACTACCAAAAGCTCATGTAGAAGC 3'	Arévalo *et al.* 1994
	LEU	5' CATTACTTTTACTTGGATTTGCACCA 3'	
cytb	GLUDG	5' TGACTTGAARAACCAYCGTTG 3'	Parkinson *et al.* 2002
	AtrCB3	5' TGAGAAGTTTTCYGGGTGRTT 3'	
NT3	NT3-F3	5' ATATTTCTGGCTTTTCTCTGTGGC 3'	Noonan & Chippindale 2006
	NT3-R4	5' GCGTTTCATAAAAATATTGTTTGACCGG 3'	

A pool of all barcoded samples was prepared by combining 10 µL of each sample, followed by purification using Mag-Bind® TotalPure NGS (Omega Bio-tek Inc., Norcross, GA, USA) and quantification with a Qubit™ 4 Fluorometer (Invitrogen, Carlsbad, CA, USA). DNA repair, end preparation, and adapter ligation were performed using the NEBNext® FFPE DNA Repair Mix (M6630), NEBNext® Ultra II End Repair/dA-Tailing Module (E7546), and the Ligation Sequencing Kit (SQK-LSK109; ONT, Oxford, UK), following the manufacturer's protocol.

Sequencing was performed on a MinION Mk1B sequencer using a Flow Cell (FLO-MIN106D; ONT, Oxford, UK) preconditioned with the Flow Cell Priming Kit (EXP-FLP002). The final library loaded onto the Flow Cell had a volume of 75 µL and consisted of 37.5 µL sequencing buffer (SQB), 25.5 µL loading beads (LB) and 75 fmol of DNA library in 15 µL (Quilumbaquín *et al.* 2023). Basecalling was performed in real time using Guppy ver. 6.5.7 with the high-accuracy model (450 bps), generating both FAST5 and FASTQ files.

Bioinformatics and sequence analyses

Raw FASTQ reads were processed using Python ver. 3.10.1 and a Docker image in Docker Desktop ver. 4.1 (https://docs.docker.com/) for each sequenced sample. Consensus sequences were generated with NGSpeciesID (Sahlin *et al.* 2021). Quality scores and read lengths were assessed using NanoFilt ver. 2.8.0 (https://github.com/wdecoster/nanofilt). Reads were filtered based on quality scores using NanoFilt, and those with a Phred score < 10 were removed from the dataset. Adapters and index barcodes were trimmed using Porechop ver. 0.2.4 (https://github.com/rrwick/Porechop). Clustering and consensus sequence generation were performed using NGSpeciesID ver. 0.3.1 (https://github.com/ksahlin/NGSpeciesID), which integrates Racon ver. 1.4.3 for error correction (Vaser *et al.* 2017).

Sequences were edited and aligned with Geneious ver. 5.4.7 (GeneMatters Corp.) using MAFFT ver. 7 (Katoh & Standley 2013) under default parameters. The alignment of the resulting consensus sequences was manually inspected and edited for accuracy and translated into amino acid sequences to verify the absence of stop codons in MEGA ver. 11.0.13 (Tamura *et al.* 2021).

For the *ND4* gene, the three tRNAs (histidine, serine, and leucine) were aligned by eye, guided by the model provided by Kumazawa & Nishida (1993) and using pre-aligned tRNAs. In addition, we used the MITOS web server to predict tRNAs (Bernt *et al.* 2013). We increased our dataset with 21 GenBank sequences (accession numbers in Table 2) of the genes *16S*, *ND4*, and *cytb*. All sequences were used in their original format for the alignment, as downloaded from GenBank, except for the *M. corallinus* sequence (AF228424), which corresponds to an early clone obtained from *Escherichia coli*. This sequence contained several artificial mutations introduced during the cloning process, which were

Table 2 (continued on next two pages). GenBank accession numbers for DNA sequences used in the phylogenetic analysis. * = new sequences generated in this study.

Older taxonomy	New taxonomy	voucher	Field / lab number	Locality	*ND4*	*NT3*	*cytb*	*16S*
Micrurus albicinctus	*Micrurus corallinus*	MPEG 19548	M192	Brazil, Amazonas	JF308714	PV877512*	PV849953*	PV826383*
Micrurus albicinctus	*Micrurus corallinus*	MPEG 20372	LJV 7533/ M187	Brazil, Río Formoso	PV877530*	–	PZ688277*	–
Micrurus annellatus	*Micrurus corallinus*	MUBI 11AP	M947	Perú, Abancay	–	PZ688284*	–	–
Micrurus bolivianus	*Micrurus corallinus*	CORBIDI 13726	M823	Perú, Huancavelica, Tayacaja	PV877532*	PZ688289*	–	–
Micrurus bolivianus	*Micrurus corallinus*	CORBIDI 14678	M822	Perú, Huancavelica, Tayacaja	PV877533*	PZ688288*	–	PV826386*
Micrurus annellatus	*Micrurus corallinus*	MHNC 5676	M712	Perú, Puno, Carabaya, Coasa, Chuini, between Socorna y Quitoni	–	PZ688285*	PZ688278*	PZ682995*
Micrurus annellatus	*Micrurus corallinus*	MHNC 9331	M720	Perú, Cusco, Echarate, La Convención	–	PZ688286*	–	PZ682996*
Micrurus annellatus	*Micrurus corallinus*	MHNC 7228	M715	Perú, Pasco, Oxapamba, Palcazu, Paujil	–	PZ688287*	PZ688279*	–
Micrurus annellatus	*Micrurus corallinus*	CORBIDI8953	–	Perú, Cusco, La Convención	PV877541*	PV877523*	–	PV826398*
Micrurus annellatus	*Micrurus corallinus*	CORBIDI 8360	–	Perú, Cusco, La Convención	PV877542*	–	–	PV826399*
Micrurus circinalis	*Micrurus circinalis*	UWIZM 2011.19.7	M708	Trinidad and Tobago, Gaspar Grande Island	MK534170	PV877513*	MK534160	MK534141
Micrurus corallinus	*Micrurus corallinus*	CPEB51	M130	Brazil, Rio do Janeiro, Niteroi, Jurujua	AF228424	–	–	–
Micrurus corallinus	*Micrurus corallinus*	KU 289205	M54	Paraguay, Itapuá	AF228424	–	–	PV826384*

Table 2 (continued). GenBank accession numbers for DNA sequences used in the phylogenetic analysis. * = new sequences generated in this study.

Older taxonomy	**New taxonomy**	**voucher**	**Field / lab number**	**Locality**	***ND4***	***NT3***	***cytb***	***16S***
Micrurus corallinus	*Micrurus corallinus*	USNM 253597	M55	Paraguay, Itapuá, El Tirol	PV877531*	PZ688290*	PV877514*	PV826385*
Micrurus sp.	*Micrurus corallinus*	MPEG 20348	LJV 6756/ M182	Brazil, Amazonas, rio Ituxi	–	PV877516*	PV849954*	PV826388*
Micrurus fulvius	*Micrurus fulvius*	–	M89	USA, Mississippi, Perry Co.	KU754454	PV877515*	KU754353	PV826387*
Micrurus langsdorffi	*Micrurus langsdorffi*	QCAZ 13129	–	Ecuador, Sucumbíos, Cuyabeno	PZ688275*	–	–	–
Micrurus medemi	*Micrurus medemi*	–	M555	Colombia, Meta, Villavicencio	PV877534*	PZ688291*	PZ688280*	PV826389*
Micrurus medemi	*Micrurus medemi*	MICMED8	M565	Colombia, Meta, Villavicencio	–	PV877517*	–	PV826390*
Micrurus mipartitus	*Micrurus mipartitus*	CH5377	M159	Panamá, Coclé	EF137406	–	EF137414	–
Micrurus narduccii	*Micrurus narduccii*	KU 202955	M4	Ecuador, Napo, Tena	EF137404	–	EF137412	–
Micrurus ornatissimus	*Micrurus ornatissimus*	–	M558	Colombia, Meta, 50 km E Villavicencio	PZ688276*	PZ688292*	PZ688281*	PV826391*
Micrurus ornatissimus	*Micrurus ornatissimus*	FHGO 5938	M989	Ecuador, Morona Santiago, Tunantsa	PV877535*	PV877518*	–	–
Micrurus ornatissimus	*Micrurus ornatissimus*	FHGO 6357	M529	Ecuador, Orellana, Dayuma, Tiputini	PV877536*	PV877519*	–	PV826392*
Micrurus ornatissimus	*Micrurus ornatissimus*	FHGO 7137	M778	Ecuador, Morona Santiago, Paantin	KP998033	–	–	–
Micrurus ornatissimus	*Micrurus ornatissimus*	FHGO 7314	M779	Ecuador, Morona Santiago, Makuma	KP998034	PZ688293*	–	PV826393*
Micrurus ornatissimus	*Micrurus ornatissimus*	FHGO 9895	M991	Ecuador, Morona Santiago, Kiim	PV877537*	PV877520*	–	–

Table 2 (continued). GenBank accession numbers for DNA sequences used in the phylogenetic analysis. * = new sequences generated in this study.

Older taxonomy	New taxonomy	voucher	Field / lab number	Locality	*ND4*	*NT3*	*cytb*	*16S*
Micrurus ornatissimus	*Micrurus ornatissimus*	QCAZ 17641	–	Ecuador, Orellana, Cononaco, Aguarico	PV877540*	–	–	PV826395*
Micrurus peruvianus	*Micrurus ornatissimus*	QCAZ 12512	–	Ecuador, Zamora Chinchipe, Zumba	PV877539*	PV877522*	–	PV826396*
Micrurus peruvianus	*Micrurus ornatissimus*	QCAZ 6094	M253	Ecuador, Zamora Chinchipe, Zumba	KP998028	–	PZ688283*	PV826397*
Micrurus psyches	*Micrurus psyches*	ROM 28378	M165	Guyana, Paramakatoi, Rupununi	JF308713	PV877525*	–	–
Micrurus steindachneri	*Micrurus ornatissimus*	FHGO 9888	M992	Ecuador, Napo, Archidona, Zuñac	–	PV877524*	–	PV826400*
Micrurus steindachneri	*Micrurus ornatissimus*	QCAZ 4758	–	Ecuador, Sucumbíos, El Reventador	PV877543*	PV877526*	–	PV826401*
Micrurus steindachneri	*Micrurus ornatissimus*	QCAZ6307	–	Ecuador, Tungurahua, Río Negro	PV877544*	–	–	–
Micrurus steindachneri	*Micrurus ornatissimus*	QCAZ8509	–	Ecuador, Sucumbíos, San Rafael	PV877545*	PV877527*	–	PV826402*
Micrurus tikuna	*Micrurus ornatissimus*	–	M556	Colombia, Leticia	PV877538*	PV877521*	PZ688282*	PV826394*
Micrurus surinamensis	*Micrurus surinamensis*	KU214908	WED 54113/ M6	Perú, Madre de Dios, Cusco Amazónico	JF308709	–	–	EF137422
Micrurus tener	*Micrurus tener*	FTB 2189	–	USA	KR814722	–	KR814692	KR814656
Micruroides euryxanthus	*Micruroides euryxanthus*	–	M41	USA, Arizona, Cochise Co.	EF137408	–	EF137416	PV888692*

subsequently identified and removed during manual sequence alignment. The final matrix was imported into Mesquite ver. 3.70 (Maddison & Maddison 2019). The protein-coding genes were partitioned by gene and codon position; *16S* fragments were not partitioned. Newly generated sequences were deposited in GenBank (accession numbers TBD).

Phylogenetic relationships were inferred using both Maximum Likelihood (ML) and Bayesian Inference (BI). The *16S* and *NT3* fragments were highly conserved and lacked sufficient phylogenetic signal; therefore, they were excluded from the phylogenetic analyses. The best-fit models of evolution were obtained in ModelFinder (Kalyaanamoorthy *et al.* 2017) (Table 3). The best partition strategies and Maximum Likelihood analyses were performed using the IQ-TREE web server (Trifinopoulos *et al.* 2016). Maximum Likelihood analyses were conducted under default settings, with model selection based on the Bayesian Information Criterion (BIC). The resulting tree was displayed using FigTree ver. 1.4.4 (http://tree.bio.ed.ac.uk/software/figtree/). ML analysis was performed on a matrix including four genes. The accuracy of the ML phylogeny was evaluated with the Ultrafast Bootstrap method (1000 replicates) (Hoang *et al.* 2018). IQ-TREE was run five times to check consistency of likelihood scores; all runs yielded the same topology and similar log-likelihood values (within a range of one likelihood unit). Bayesian Inference analysis was implemented in MrBayes ver. 3.2.7 (Ronquist *et al.* 2012), the Markov Chain Monte Carlo runs being performed twice, each run consisting of four chain, for 10 million generations, with trees sampled every 1000 generations, and consensus trees were summarized after discarding the initial 25% as burn-in. The sampled log-likelihood values were visualized using Tracer ver. 1.7.2 (Rambaut *et al.* 2018), and adequate mixing of the chain was assessed using an effective sample size (ESS) >200 and a Potential Scale Reduction Factor (PSRF) value near 1.0 as criteria. We interpreted that a tree node had strong support when its bootstrap value was >75 and its Bayesian posterior probability was at least 0.95, low to moderate support for 50–75 and 0.90–0.95, and weak support or non-resolved for values lower than 50 and 0.90, respectively. Uncorrected genetic *p*-distances were calculated with MEGA ver. 11.0.13 (Tamura *et al.* 2021) and are presented in Appendix 1.

Species delimitation was conducted using Bayesian Poisson Tree Processes (bPTP; Zhang *et al.* 2013) and Assemble Species by Automatic Partitioning (ASAP; Puillandre *et al.* 2021). The maximum-likelihood tree generated in IQ-TREE was used as input for bPTP analysis, which was run with two independent MCMC chains of 500 000 generations (25% burn-in). Independently, ASAP was applied to the Kimura 2-parameter (K2P) distance matrix via the web server, and the partition with the lowest ASAP-score was selected as the primary species hypothesis. The resulting molecular operational taxonomic units (MOTUs), which represent putative species delimited by molecular data, from both methods were compared to evaluate congruence between the two approaches.

Additionally, we constructed a haplotype network to illustrate interspecific and clade-level relationships. DNA sequence polymorphism analyses were conducted in DnaSP ver. 6 (Rozas *et al.* 2017) to generate haplotype data. Subsequent analyses were performed in PopART ver. 1.7 (Leigh & Bryant 2015) using the Minimum Spanning Network inference method. Haplotypes were color-coded by region to visualize their geographic distribution.

Morphology

A total of 402 preserved specimens of monadal coralsnakes of the genus *Micrurus* were examined for this study (see Material examined sections and Appendix 2). Additionally, we reviewed specialized literature for comparative purposes (e.g., Schmidt 1954; Silva-Haad 1994; Roze 1967, 1996; Campbell & Lamar 2004; Feitosa *et al.* 2015; Valencia *et al.* 2016).

The definitions of scale counts, morphological features, and color patterns were taken from Roze (1996), Campbell & Lamar (2004), and Valencia *et al.* (2016). Measurements were taken with a digital caliper

Table 3. Summary of taxon sampling and best-fitting models for combined and individual genes, taxa, and characters. Sites: Total number of positions (nucleotides) included in that partition; Seq: number of sequences; G: gamma distribution; U: Unique sites; PI: Number of parsimony-informative sites; I: Number of invariant sites; C: Number of constant sites (can be subset of invariant sites); LogL: log-likelihood function; AICc: Corrected Akaike Information Criteria; n/d: no data

Name	Best-fitting Model	Sites	Seq	G	U	PI	I	C	LogL	AICc
ND4, 1st	HKY+F+G4	31	280	1.56	191	118	98	98	-1720.1	3452.6
ND4, 2nd	HKY+F+I	31	280	n/d	101	38	213	213	-918.6	1849.5
ND4, 3rd	HKY+F+I	31	280	n/d	59	9	257	257	-532.6	1077.5
NT3, 1st	JC	26	166	n/d	5	0	166	166	-237.6	477.4
NT3, 2nd	K2P	26	165	n/d	7	0	163	163	-248.4	500.9
NT3, 3rd	HKY+F+I	26	165	n/d	10	5	157	157	-305.8	624.2
16S	HKY+F+I	24	506	n/d	24	12	491	491	-841.0	1694.2
cytb, 1st	TN+F	18	237	n/d	156	115	62	62	-1386.7	2785.8
cytb, 2nd	TIM2e+I	18	237	n/d	70	26	179	179	-747.9	1506.2
cytb, 3rd	HKY+F+I	18	237	n/d	44	14	212	212	-523.8	1060.0
cmos, 1st	JC	11	190	n/d	15	0	189	189	-273.6	549.3
cmos, 2nd	JC	11	190	n/d	18	0	187	187	-287.1	576.3
cmos, 3rd	F81+F	11	191	n/d	20	1	186	186	-288.5	585.2

(Truper©) to the nearest 0.1 mm under an optical stereoscope, except for snout–vent length and caudal length, which were taken with a flexible ruler to the nearest millimeter. We recorded quantitative data on external morphology for each specimen, including the following body and head scale measurements (abbreviations in parentheses): frontal length (FL), frontal width (FW), head length (HL), head width (HW), internasal length (INL), internasal width (INW), prefrontal length (PFL), prefrontal width (PFW), rostral length (RL), rostral width (RW), snout–vent length (SVL), total length (TL), tail length (TaL). Color pattern was described following Savage & Slowinski (1992), Roze (1996), and Feitosa *et al.* (2007), with particular attention to the number of black body rings (BBR) and tail rings (BTR). Sex was determined by examining the presence or absence of hemipenes through a ventral incision at the base of the tail. Techniques for hemipenes eversion from preserved specimens followed Dowling & Savage (1960). Additionally, we used original descriptions of hemipenial morphology obtained directly from the laboratory notebooks of K. Schmidt and J. Roze, which are archived at the University of Texas at Arlington. Terminology for hemipenial morphology followed Zaher (1999). Tissue covering the maxillary, pterygoid, and palatine bones was removed, and the number of teeth, as well as empty sockets on the left side, was counted.

We conducted multivariate analyses with morphological measurements to reduce the number of morphometric variables using principal component analysis (PCA). This analysis was performed using the *MASS* package in R (Venables & Ripley 2002). We assessed the contribution of each variable to the total explained variance for males and females separately.

Repositories

AMNH = American Museum of Natural History, New York, USA
ANSP = Academy of Natural Sciences, Pennsylvania, USA
BMNH = British Museum of Natural History, London, UK
CAS = California Academy of Sciences, California, USA
CM = Carnegie Museum, Pennsylvania, USA
CORBIDI = Centro de Ornitología y Biodiversidad, Lima, Perú
DHMECN = Instituto Nacional de Biodiversidad, Quito, Ecuador
FHGO = Fundación Herpetológica Gustavo Orcés, Quito, Ecuador
FMNH = Field Museum of Natural History, Illinois, USA
IB = Instituto Butantan, São Paulo, Brazil
INS = Instituto Nacional de Salud de Colombia, Bogotá, Colombia
INSP = Instituto Nacional de Salud de Perú, Lima, Perú
IRSNB = Institut royal des Sciences naturelles de Belgique, Brussels, Belgium
LSUMZ = Louisiana State University Museum of Natural Science, Louisiana, USA
MBUCV = Museo de Biología, Universidad Central de Venezuela, Caracas, Venezuela
MCZ = Museum of Comparative Zoology, Massachusetts, USA
MLS = Museo del Instituto de La Salle, Bogotá, Colombia
MNHNP = Muséum National d'Histoire Naturelle, Paris, France
MNRJ = Museu Nacional do Rio de Janeiro, Rio de Janeiro, Brazil
MRSN = Museo Regionale di Scienze Naturali, Torino, Italy
MSMN = Museo Civico di Storia Naturale di Milano, Milano, Italy
MSNG = Museo Civico di Storia Naturale di Genova, Genova, Italy
MTD = Senckenberg Naturhistorische Sammlungen Dresden, Dresden, Germany
MUSA = Museo de Historia Natural, Universidad Nacional San Agustín de Arequipa, Arequipa, Perú
MUSM = Museo Universidad Nacional Mayor de San Marcos, Lima, Perú
MUBI = Museo de Biodiversidad del Perú, Cusco, Perú
NHMB = Naturhistorisches Museum, Basel, Switzerland
NHRM = Naturhistoriska Riksmuseet, Stockholm, Sweden
NHW = Naturhistorisches Museum Wien, Vienna, Austria
QCAZ = Pontificia Universidad Católica del Ecuador, Quito, Ecuador
TCWC = Texas Cooperative Wildlife Collection, Texas, USA
UIMNH = University of Illinois Museum of Natural History, Illinois, USA
UMMZ = University of Michigan Museum of Zoology, Michigan, USA
USNM = National Museum of Natural History, Washington D.C., USA
UTA = University of Texas at Arlington, Texas, USA
ZMB = Museum für Naturkunde, Leibniz Institute for Evolution and Biodiversity Science, Berlin, Germany
ZMH = Zoologisches Museum für Hamburg, Hamburg, Germany
ZSM = Zoologische Staatssammlung München, Munich, Germany

Geographic and environmental species delimitation

Occurrence data were obtained from the following sources: (1) scientific collections listed in the Material examined sections and Appendix 2, as well as the Museo de Zoología, Escuela Politécnica Nacional (EPN), Museo de Zoología, Universidad San Francisco de Quito (ZSFQ), and Museo de Zoología, Universidad Técnica Particular de Loja (UTPL); (2) national and global biodiversity databases, such as BioWeb Ecuador (www.bioweb.bio), the Global Biodiversity Information Facility (GBIF, www.gbif.org), and VertNet (www.vertnet.org); and (3) scientific literature (e.g., Schmidt 1954; Silva-Haad 1994; Roze 1996; Campbell & Lamar 2004; Feitosa *et al.* 2015; Valencia *et al.* 2016; Nogueira *et al.* 2019).

We performed the following data-cleaning steps to reduce potential bias in the occurrence dataset (Syfert *et al.* 2013; Cobos *et al.* 2018; Alkishe *et al.* 2020): (1) review and assessment of potential taxonomic errors in the database, removing records likely not corresponding to the taxon in question; (2) removal of occurrences lacking geographic references, records with (0, 0) geographic coordinates, records located in oceans or seas, and duplicate records; and (3) relocation (to the nearest pixel) of records located in the sea but close to the coast (i.e., errors related to pixel resolution). We used the *spThin* package in R (Aiello-Lammens *et al.* 2015) to reduce spatial autocorrelation by applying a buffer with a 15 km radius around each point.

Additionally, we calculated the extent of occurrence (EOO) and generated a convex hull polygon using ArcGIS ver. 10.5 (Esri, Redlands, California, USA). To ensure a comprehensive spatial analysis, we first compiled geographic records of phylogenetically related species. To estimate the EOO, we compiled the geographic coordinates of all known localities and organized them into a shapefile projected in the WGS 1984 datum. For accurate area measurements, we reprojected the data to the appropriate UTM zone using the Project tool in ArcToolbox. We then applied the Minimum Bounding Geometry tool (ArcToolbox > Data Management Tools > Features > Minimum Bounding Geometry), selecting CONVEX_HULL as the geometry type to generate a single convex polygon encompassing all records. Finally, we calculated the area of this polygon in square kilometers by adding a new field to the attribute table and using the Field Calculator.

The bioclimatic layers used to model environmental suitability were obtained from the WorldClim database (http://www.worldclim.org) at a spatial resolution of 30 arc-seconds (~1 km) (Fick & Hijmans 2017). Four variables that combine temperature and precipitation information (BIO8, BIO9, BIO18, and BIO19) were excluded due to known spatial artifacts (Escobar *et al.* 2014; Booth 2021). We then followed two additional steps to select bioclimatic variables prior to model calibration. First, an initial model was created using MaxEnt ver. 3.4.3 (Phillips *et al.* 2006) with default settings and the full set of variables; predictors with zero contribution values were removed from the analysis (Cobos *et al.* 2019a) using two metrics: percent contribution and permutation importance. Subsequently, we used variance inflation factor (VIF) analyses with the *car* package in R to reduce multicollinearity among predictors (Brauner & Shacham 1998). VIF has long been suggested as a method for variable selection (Guisan *et al.* 2002). The ratio of variance in a model with multiple terms to the variance in models based on each individual term indicates how much variance is represented by each predictor. Variables with VIF values < 5 were selected as the best predictors (Cobos *et al.* 2019a).

Prior to model calibration, an accessibility area (M) in the BAM conceptual framework (Barve *et al.* 2011) was delimited based on the terrestrial ecoregions of the world (Olson *et al.* 2001) encompassing the geographic distribution of the validated records of each species. Ecological niche models (ENMs) were constructed using the maximum entropy algorithm implemented in MaxEnt via the "kuenm" package following the protocol proposed by Cobos *et al.* (2019b) in R ver. 4.2.2 (R Core Team 2022). The "kuenm" package allows configuration of the modeling procedure by including different parameterizations to construct multiple candidate models that can be evaluated using several criteria. Candidate models were created by combining sets of environmental variables (three sets) and feature classes (linear = l, quadratic = q, product = p). These models were evaluated based on partial ROC (500 iterations), omission rates (E = 5%), and AICc. From these model sets, the best model was selected using delta AICc values ≤ 2. "The kuenm_ceval" function was used for the evaluation and selection of candidate models, whereas the "kuenm_mod and kuenm_feval" functions were used for the calibration and evaluation of final models. MaxEnt was run with 500 iterations and 10 random replicate analyses, with all other parameters set to the default settings of the "kuenm" package. Final maps were generated using the lower 10th percentile of training presence. All rasters were visualized using ArcGIS ver. 10.5 (Esri, Redlands, California, USA).

We used partial ROC analyses to evaluate the predictive performance of the models. This test estimates the significance of a niche model using the cumulative binomial probability of successfully predicting occurrences based on validation data and the proportional area predicted as suitable in the model (Anderson *et al.* 2003). Partial ROC was run with 1000 bootstrap replicates and a 5% omission error rate (E) (Anderson *et al.* 2003). We then compared the Area Under the Receiver Operating Characteristic Curve (AUC) values from evaluation points against those expected by chance using the "ntbox" package in R (Osorio-Olvera *et al.* 2020).

We performed a linear discriminant analysis (LDA) to identify the environmental traits most informative for distinguishing the ecological niche models of each species using the "factoextra", "ggrepel", and "MASS" packages. A matrix of squared Mahalanobis distances was used to compare differences among species and to determine the number of cases correctly and incorrectly assigned by the LDA using the "psych" package. Classification accuracy and Cohen's kappa were calculated using the "caret" package to assess the discriminatory power and reliability of the LDA model while accounting for chance agreement. All analyses were performed in R ver. 4.2.2 (R Core Team 2022).

Results

Phylogenetic analysis

Genetic diversity

The *NT3* dataset contained both homozygous and heterozygous genotypes. Nucleotide diversity (π) varied considerably among the analyzed genes. The highest value was obtained for *ND4* (π = 0.1014), followed by *cytb* (π = 0.0926). In contrast, lower levels of nucleotide diversity were observed in *16S* (π = 0.0056) and *NT3* (π = 0.0023). These results indicate that mitochondrial genes, particularly *ND4* and *cytb*, exhibit substantially higher genetic variation compared to the nuclear loci analyzed (Table 4).

Phylogenetic relationships

The complete DNA sequence dataset comprises 2490 bp from 34 specimens of *Micrurus*, including *Micruroides euryxanthus* (Kennicott, 1860) as the outgroup. The dataset includes the following gene representation: *ND4* = 32 sequences, *16S* = 24 sequences, *NT3* = 25 sequences, and *cytb* = 18 sequences. The partition summary revealed marked variation in phylogenetic informativeness among loci. Mitochondrial protein-coding genes (*ND4* and *cytb*) exhibited the highest numbers of variable and parsimony-informative sites, particularly in their first codon positions (e.g., *ND4*, 1st codon position with 118 informative sites; *cytb*, 1st codon position with 115), indicating strong phylogenetic signal. In contrast, the ribosomal gene *16S* showed a predominance of invariant sites, reflecting its conserved nature. The *NT3* gene was the least variable, with few or no informative positions across codon sites. These results demonstrate that mitochondrial loci contribute most of the genetic variability and phylogenetic signal in the dataset, whereas nuclear and ribosomal loci remain relatively conserved. The optimal partitioning scheme selected 10 partitions, and the parameter estimates for each gene are summarized in Table 3.

Maximum Likelihood (ML) analysis of the eastern Andean *Micrurus* dataset yielded strong support for most nodes (Fig. 1). According to the Bayesian Information Criterion (BIC), the best-fit model for the ML analysis was HKY+F+G4 (LnL = −3154.001). Bayesian inference recovered moderately to strongly supported clades (0.79–1.00 PP) (Fig. 1). The harmonic means of the two replicate runs were −7423.64 and −7423.80, with a 95% credible set comprising 17 346 trees. A burn-in of 25% of the samples was considered sufficient. The average effective sample size (ESS) exceeded 1000 for all parameters, and the average standard deviation of split frequencies at the end of the run was < 0.001. The ratio of successful Metropolis-coupled chain swaps was 0.676–0.677 for both runs, well within the recommended range of 0.20 to 0.70.

Table 4. Basic summary statistics for *Micrurus* Wagler, 1824 sequence alignments.

loci	Taxa	No. Sequences	No. Sites (bp)	No. Polymorphic sites	No. Parsimony Informative Sites	No. of Haplotypes	π
16S	*M. corallinus*	10	505	12	10	4	0.0083
	M. langsdorffi	–	–	–	–	–	–
	M. medemi	2	505	0	0	1	0.0000
	M. ornatissimus	10	505	3	1	5	0.0017
cytb	*M. corallinus*	7	710	28	10	7	0.0135
	M. langsdorffi	–	–	–	–	–	–
	M. medemi	1	710	0	0	1	0.000
	M. ornatissimus	3	710	22	0	3	0.0214
ND4	*M. corallinus*	9	779	33	19	8	0.0168
	M. langsdorffi	1	779	21	13	1	0.0000
	M. medemi	1	779	0	0	1	0.0000
	M. ornatissimus	13	779	17	10	10	0.0081
NT3	*M. corallinus*	10	495	1	0	2	0.0004
	M. langsdorffi	1	–	–	–	–	–
	M. medemi	2	495	2	0	2	0.0004
	M. ornatissimus	8	495	5	3	5	0.0029

Uncorrected *p*-distances between lineages and species are detailed in Appendix 1, ranging from 2.2–3.8% (mean 3.1±0.4 SE). Overall, *ND4* yielded the highest estimates of genetic distance. This discrepancy may result from the limited polymorphism observed in loci such as *16S* and *NT3*, as well as variation in the number of samples successfully amplified per locus. Based on phylogenetic analyses, we recognize four well-supported lineages that correspond to distinct operational taxonomic units (OTUs): the *Micrurus corallinus* (Merrem, 1820) lineage, the *M. langsdorffi* (Wagler, 1824) lineage, the *M. medemi* Roze, 1967 lineage, and *M. ornatissimus* (Jan, 1858).

The *Micrurus corallinus* lineage includes samples of *M. corallinus* from the Atlantic Forest of Paraguay and Brazil, *M. albicinctus* from the lowland forests of the Brazilian states of Mato Grosso and Amazonas, and *M. annellatus*, represented by specimens exhibiting three dorsal coloration patterns: a bicolored black-and-white pattern, a bicolored red-and-white pattern, and the monadal black–white–red pattern, corresponding to *M. a. annellatus* and *M. a. bolivianus*, both taxa from the eastern Andean slopes of Peru. Genetic distances between species in this group are low. Intraspecific distances range from 0.2–2.4% (mean 1.3±0.5 SE), with distances between *M. corallinus* and *M. albicinctus* ranging from 1.8–2.3% (mean 2.1±0.2 SE), and between *M. corallinus* and the *Micrurus annellatus* species complex from 0.2–1.8% (mean 1.4±0.6 SE) (Fig. 2).

The *Micrurus langsdorffi* group is a clade recognized herein that includes *M. langsdorffi*, *M. medemi*, and *M. ornatissimus* lineages (Fig. 1). Genetic distances among these lineages range from 2.0–3.4% (mean 2.4±0.2 SE). The *M. medemi* lineage includes only samples from Villavicencio, Meta, Colombia. Uncorrected *p*-distances within this lineage are zero (0), indicating no sequence divergence among sampled individuals (Fig. 2).

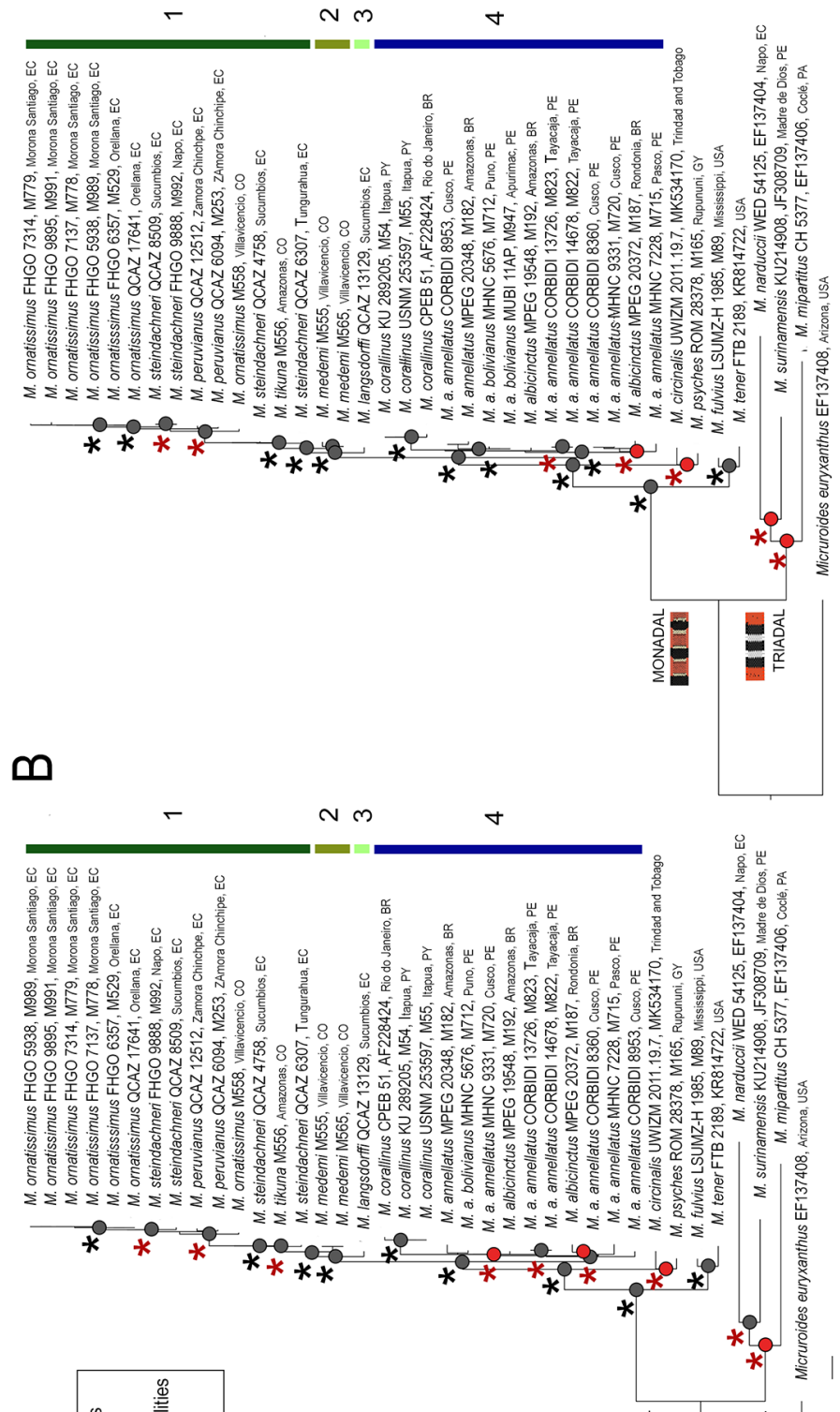

Fig. 1. Phylogenetic relationships of cis-Andean monadal species of the genus *Micrurus* Wagler, 1824. **A**. Tree based on complete and partial sequences of three mitochondrial genes (*ND4, 16S, cytb*). **B**. Tree based on the concatenated dataset of three mitochondrial genes (*ND4, 16S, cytb*) and a nuclear gene (*NT3*). 1=*M. ornatissimus* (Jan, 1858) (green); 2 = *M. medemi* Roze, 1967 (olive green); 3 = *M. langsdorffi* (Wagler, 1824) (light olive); 4 = *Micrurus corallinus* (Merrem, 1820) (blue).

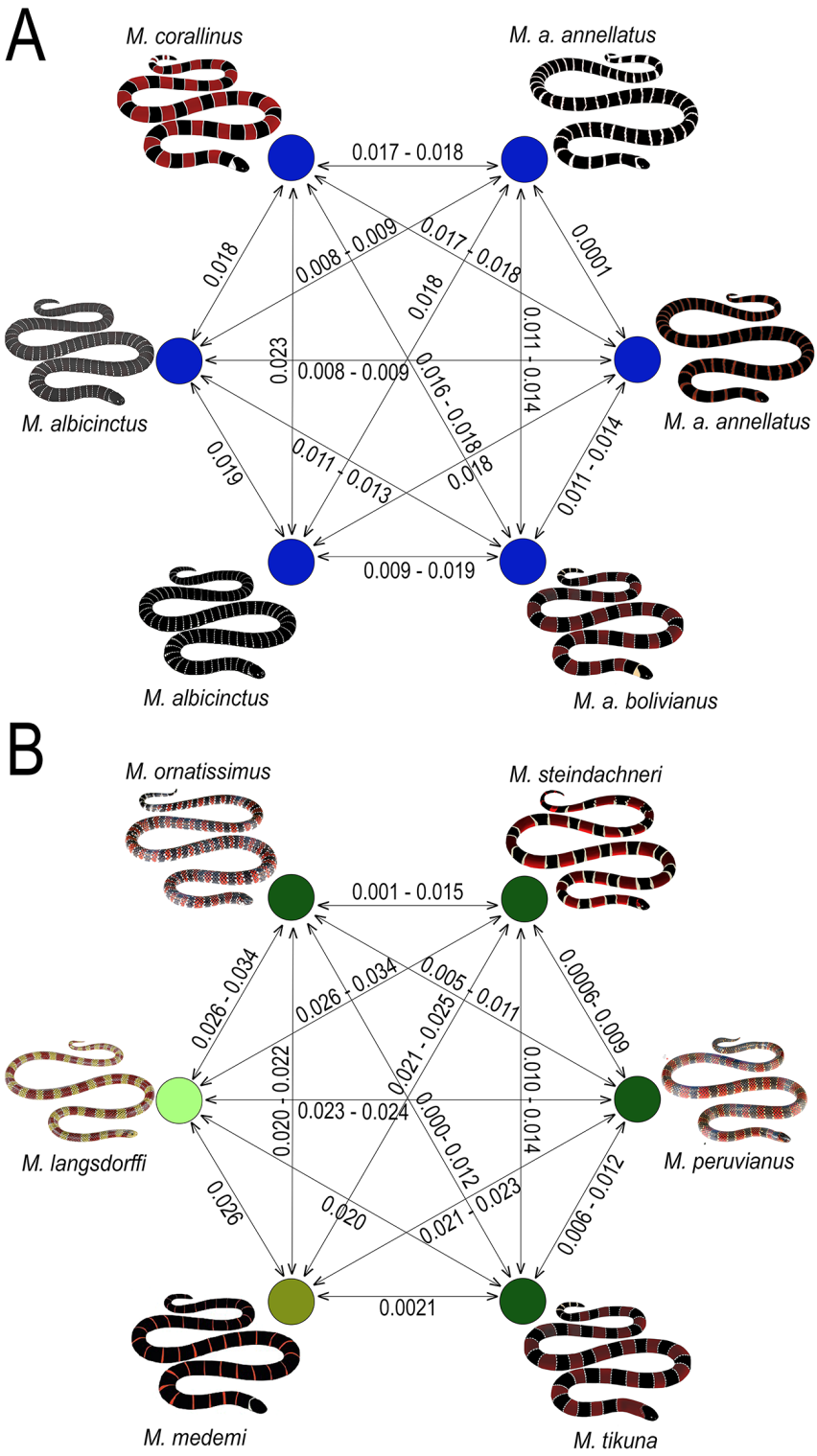

Fig. 2. Diagrams illustrating the range of *p*-distances among lineages and samples of cis-Andean monadal coralsnakes included in the phylogeny. **A**. *Micrurus corallinus* (Merrem, 1820) (blue). **B**. *M. langsdorffi* (Jan, 1858) (light green), *M. medemi* Roze, 1967 (olive green) and *M. ornatissimus* (Jan, 1858) (dark green).

The *Micrurus ornatissimus* lineage comprises samples of *M. langsdorffi* (brown pattern), *M. ornatissimus* from the Amazonian lowlands of Ecuador, *M. peruvianus* from the inter-Andean dry forests of Ecuador, *M. steindachneri* from the eastern Andean slopes of Ecuador, and *M. tikuna* from Leticia, Colombia. Overall, uncorrected *p*-distances among these species are low. Intraspecific variation ranged from 0.4–1.47% (mean 1.2±0.5 SE). Distances between *M. ornatissimus* and *M. peruvianus* ranged from 0.5–1.2% (mean 1.0±0.2 SE). Additional comparisons showed distances of 0.1–1.6% (mean 1.1±0.5 SE) between *M. ornatissimus* and *M. steindachneri*, 0.0–1.3% (mean 1.1±0.5 SE) between *M. ornatissimus* and *M. tikuna*, 0.1–1.1% (mean 0.4±0.5 SE) between *M. steindachneri* and *M. tikuna*, 0.6–0.9% (mean 0.8±0.1 SE) between *M. steindachneri* and *M. peruvianus*, and 0.5–0.6% (mean 0.6) between *M. peruvianus* and *M. tikuna* (Fig. 2).

Mitochondrial haplotype networks (*16S*, *ND4*, and *cytb*) consistently revealed two deeply divergent, completely disconnected lineages separated by several mutational steps: one exclusive to *Micrurus corallinus* and the other comprising all *M. langsdorffi*, *M. ornatissimus* and *M. medemi* haplotypes, which formed a single, closely related group connected by a few mutational steps. The nuclear haplotype network (*NT3*) showed no genetic structure. *NT3* exhibited a single star-like network with a central haplotype shared by *M. corallinus*, *M. langsdorffi*, *M. ornatissimus* and *M. medemi* (peripheral haplotypes differing by 0–3 steps). These results demonstrate strong and congruent mitochondrial lineage sorting but complete nuclear genetic homogeneity among *M. corallinus*, *M. langsdorffi*, *M. ornatissimus*, and *M. medemi* (Fig. 3).

Species delimitation using the Bayesian Poisson Tree Process (bPTP) and Assemble Species by Automatic Partitioning (ASAP) recovered Maximum Likelihood partitions of six species, although

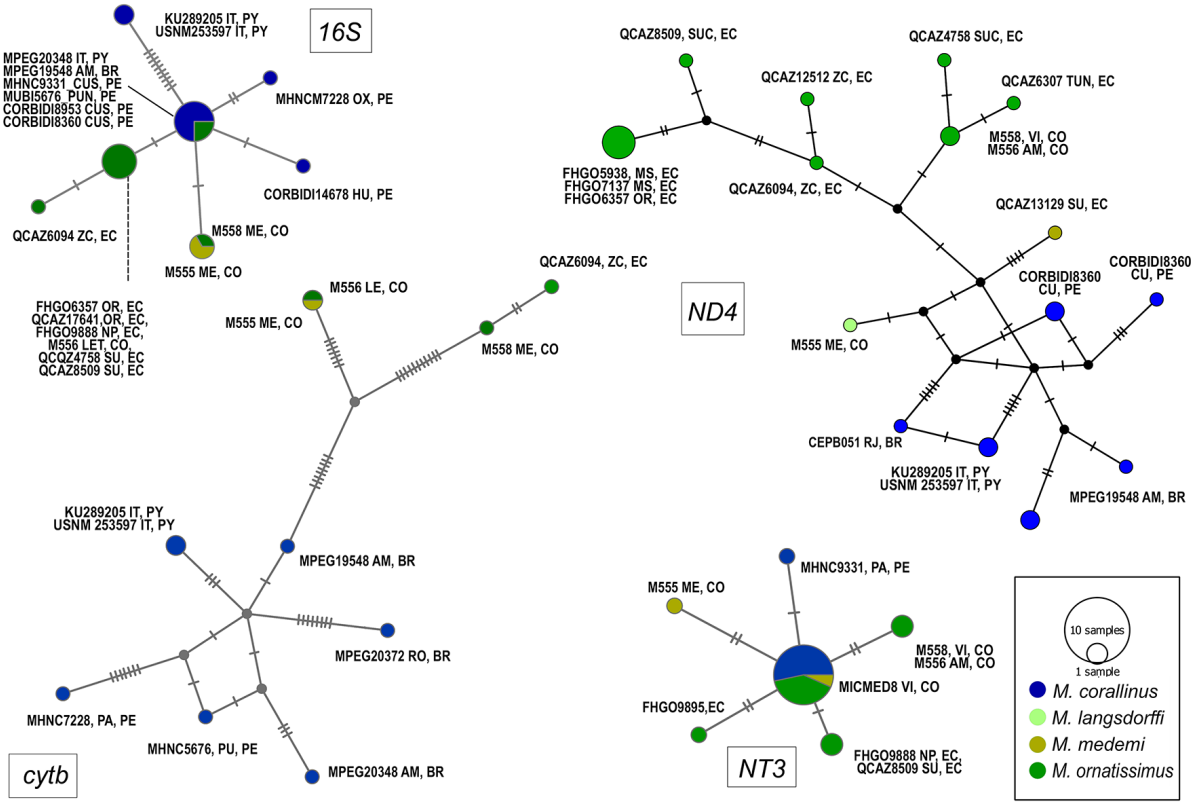

Fig. 3. Haplotype networks for *16S*, *ND4*, *cytb* and *NT3* genes of *Micrurus corallinus* (Merrem, 1820), *M. langsdorffi* (Wagler, 1824), *M. medemi* Roze, 1967 and *M. ornatissimus* (Jan, 1858).

with generally low support. All specimens of *Micrurus ornatissimus* were grouped as a single putative species with moderate support (0.085), whereas *M. medemi* and *M. langsdorffi* were recovered as distinct, highly supported lineages (0.971 and 0.984, respectively). Within the *M. corallinus* lineage, three putative species were delimited, but support was low to moderate (0.243–0.542), suggesting that these subdivisions likely represent intraspecific variation rather than fully independent species.

Morphology analysis

A summary of the descriptive morphometric measurements of males and females of *Micrurus* species is presented in Table 5. Projections of morphometric variables in morphological space are shown, and the importance of components, given by standard deviation, proportion of variance, and cumulative proportion for males and females, is provided in Fig. 4.

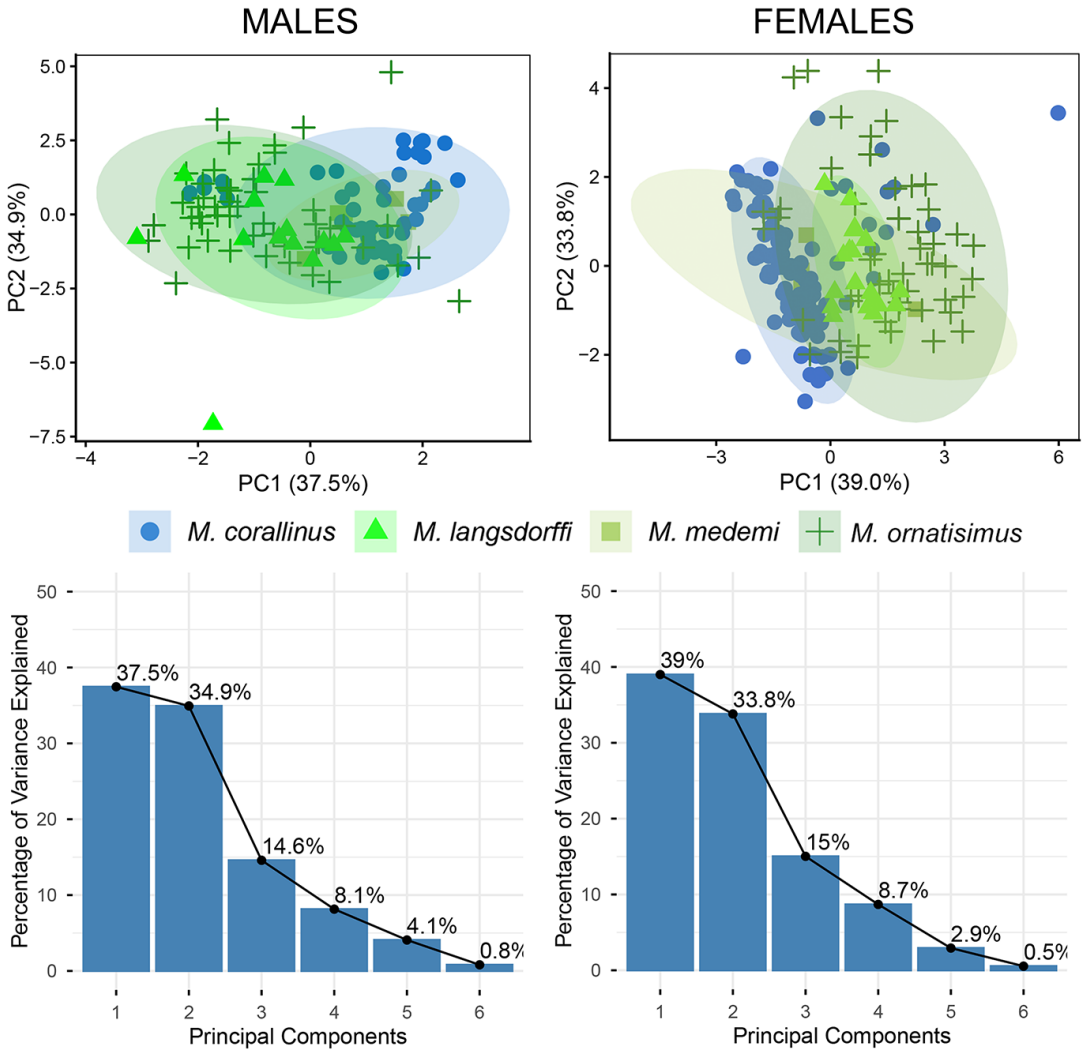

Fig. 4. Principal Component Analysis biplot (top) and variance explained (bottom) of morphometric variables in *Micrurus corallinus* (Merrem, 1820), *M. langsdorffi* (Wagler, 1824), *M. medemi* Roze, 1967 and *M. ornatissimus* (Jan, 1858). Morphometric variables include number of black body rings, number of black tail rings, and scale counts for males and females.

Table 5 (continued on next two pages). Selected characters of monadal coralsnakes of the genus *Micrurus* Wagler, 1824 from eastern Andes. Range is followed by mean and standard deviation. Sources: A= This work, Feitosa 2006; B= This work, Schmidt 1954, Cunha & Nascimento 1991, Roze 1996, Campbell & Lamar 2004; Feitosa *et al.* 2015; C=This work, Cunha & Nascimento 1989, Silva-Haad 1994, Feitosa *et al.* 2015, Valencia *et al.* 2016; D= Roze 1967, 1996, Campbell & Lamar 2004, Feitosa *et al.* 2015; E=Roze 1967, 1996, Campbell & Lamar 2004; F=This work, Valencia *et al.* 2016; G=Carvalho 2002; H=Feitosa 2006, Feitosa *et al.* 2007; I=This work, Roze 1996, Campbell & Lamar 2004.

Characters	**Sex**	***M. averyi*[A]**	***M. corallinus*[B]**	***M. langsdorffi*[C]**	***M. argaritiferus*[D]**	***M. medemi*[E]**	***M. ornatissimus*[F]**	***M. pacaraimae*[G]**	***M. paraensis*[H]**	***M. putumayensis*[I]**
Ventral scales	M	190–198 (193.2±3.1)	185–215 (200.9±6.1)	201–210 (206.2±2.5)	205–212	190–203	161–225 (202.7±9.9)	201	184–197 (191.3±3.6)	197–208 (201.1±3.8)
	F	201–216 (207.6±4.9)	198–288 (215.5±27.4)	210–219 (222.6±4.3)	212–224	208–221	156–234 (218.1±14.6)	–	186–217 (205.1±7.9)	216–226 (221.2±3.1)
Subcaudal scales	M	40–48 (45±3.1)	38–49 (44.5±2.4)	27–55 (47.8±5.9)	47–48	42–49	34–54 (47.3±3.6)	43	36–54 (47.3±3.4)	47–51 (48.6±1.7)
	F	29–34 (31.8±2.1)	26–42 (31.2±5.2)	29–37 (33.7±2.5)	30–37	30–37	28–40 (33.8±2.7)	–	30–52 (38.0±6.6)	32–35 (33.3±0.9)
Black body rings	M	8–10 (9±0.8)	14–90 (37.5±23.8)	25–67 (43.8±14.7)	36–50	17–27	15–60 (40.4±10.3)	23	12–18 (14.8±1.4)	7–11 (9.1±1.5)
	F	10–13 (11.5±1.0)	20–83 (41.6±20.6)	29–45 (37.6±4.6)	46–68	17–27	20 –67 (45.3±11.5)	–	13–21 (17.1±2.2)	9–12 (10.6±1.2)
Black tail rings	M	6–9 (7.3±1.2)	5–13 (7.4±1.9)	5–14 (9.0±2.1)	7–13	6–9	5–17 (11.8±3.2)	9	5–12 (8.2±1.7)	2–3 (2.4±0.5)
	F	4–7 (5.6±1.1)	4–9 (5.5±2.0)	5–8 (6.4±1.0)	7–13	6–9	2–12 (8.2±2.3)	–	2–11 (6.4±1.9)	2 (2±0.0)
% Tail–Total length	M	14.9–18.1 (16.4±1.4)	11.9–20.3 (14.4±1.3)	14.4–16.2 (14.8±0.9)	–	–	10.3–17.4 (14.8±1.5)	11.8	10–21	15.1–16.0 (15.5±0.3)
	F	7.9–9.3 (8.5±0.5)	6.8–10.9 (8.8±1.3)	7.8–9.9 (8.7±0.6)	8.7–9.4 (.1±0.3)	–	7.9–11.0 (9.1±0.7)	–	9–18	7.5–99 (9.0±0.8)
Left dentary teeth		11	9–12	10–11	10	–	10	–	–	–
Left pterygoid teeth		4–5	4–5	4	7	–	5	–	–	–

Table 5 (continued). Selected characters of monadal coralsnakes of the genus *Micrurus* Wagler, 1824 from eastern Andes. Range is followed by mean and standard deviation. Source: A= This work, Feitosa 2006; B= This work, Schmidt 1954, Cunha & Nascimento 1991, Roze 1996, Campbell & Lamar 2004; Feitosa *et al.* 2015; C=This work, Cunha & Nascimento 1989, Silva-Haad 1994, Feitosa *et al.* 2015, Valencia *et al.* 2016; D= Roze 1967, 1996, Campbell & Lamar 2004, Feitosa *et al.* 2015; E=Roze 1967, 1996, Campbell & Lamar 2004; F=This work, Valencia *et al.* 2016; G=Carvalho 2002; H=Feitosa 2006, Feitosa *et al.* 2007; I=This work, Roze 1996, Campbell & Lamar 2004.

Characters	Sex	*M. averyi*[A]	*M. corallinus*[B]	*M. langsdorffi*[C]	*M. argaritiferus*[D]	*M. medemi*[E]	*M. ornatissimus*[F]	*M. pacaraimae*[G]	*M. paraensis*[H]	*M. putumayensis*[I]
Left palatine teeth		8	7	6–7	7	–	7	–	–	–
Shape of the hemipenis		Long, strongly forked, and non-capitate	Long, forked, and non-capitate	Long, strongly forked, and non-capitate	–	–	Long, strongly forked, and non-capitate	–	Long, strongly forked, and non- capitate	Long, strongly forked, and non- capitate
Hemipenis length by subcaudal scales		15 scales	15–19 scales	14–18 scales	–	–	11 scales	–	15 scales	18 scales
Hemipenis bifurcation length by subcaudal scales		9 scales	12–13 scales	9–12 scales	–	–	7 scales	–	10 scales	12 scales
Spermatic groove length by subcaudal scales		Deep, bifurcated at 9th caudal	Deep, bifurcated at 11th to 13th caudal	Deep, bifurcated at 9th to 12th caudal	–	–	Deep, bifurcated at 7th caudal	–	Deep, bifurcated at 8th or 9th subcaudal	Deep, bifurcated at 10th subcaudal
Surface of spermatic groove edge		Smooth with tiny spines	Smooth with tiny spines	Smooth with tiny spines	–	–	Smooth	–	Smooth	Smooth with tiny spines
Lobe length percentage of total length		ca 40% of total.	27–36% of total length	27–36% of total length	–	–	42% of total length	–	56% of total length	ca 36% of total.

Table 5 (continued). Selected characters of monadal coralsnakes of the genus *Micrurus* Wagler, 1824 from eastern Andes. Range is followed by mean and standard deviation. Source: A= This work, Feitosa 2006; B= This work, Schmidt 1954, Cunha & Nascimento 1991, Roze 1996, Campbell & Lamar 2004; Feitosa *et al.* 2015; C=This work, Cunha & Nascimento 1989, Silva-Haad 1994, Feitosa *et al.* 2015, Valencia *et al.* 2016; D= Roze 1967, 1996, Campbell & Lamar 2004, Feitosa *et al.* 2015; E=Roze 1967, 1996, Campbell & Lamar 2004; F=This work, Valencia *et al.* 2016; G=Carvalho 2002; H=Feitosa 2006, Feitosa *et al*. 2007; I=This work, Roze 1996, Campbell & Lamar 2004.

Characters	**Sex**	***M. averyi*[A]**	***M. corallinus*[B]**	***M. langsdorffi*[C]**	***M. argaritiferus*[D]**	***M. medemi*[E]**	***M. ornatissimus*[F]**	***M. pacaraimae*[G]**	***M. paraensis*[H]**	***M. putumayensis*[I]**
Surface between lobes		–	Ornate with small spines	Ornate with small spines	–	–	Ornament with small spines	–	With small spines	Naked
Hemipenis body ornamentation		Naked on the base up to two thirds of hemipenis body	Naked, without rnamentation up to 3th scale	Naked, without rnamentation up to 5th scale	–	–	Naked, without ornamentation	–	Naked, without ornamentation	Naked on the base, and ornate with small and disperse spine on the body
Basal pocket		Present, well-developed length from base to 10th subcaudal	Present and bare, length from base to 7 th to 8th subcaudal	Present and poorly developed, from base to 8th caudal	–	–	Present and deep, from base to 8th caudal	–	Present and bare, length from base to 8th subcaudal	Undefined
Hemipenis body folds		Absent	Present	Absent	–	–	Absent	–	Present	Present

In males, the first two principal components (PC1 and PC2) explain 72.3% of the morphological variation among *Micrurus* species, indicating that these two axes alone describe a large part of the morphological differences. Male morphometric traits of *M. corallinus*, *M. langsdorffi*, *M. medemi* and *M. ornatissimus* show considerable overlap, indicating limited differentiation among species (Fig. 4), with the greatest contribution of variables BTR (33.9%) and BBR (30.0%) in PC1, and TL (42.3%) and TaL (38.9%) in PC2.

In females, the first two principal components (PC1 and PC2) explain 72.8% of the morphological variation among *Micrurus* species. Considerable overlap is observed among the three species, none of which appears completely separated in an exclusive morphometric space. Variation was primarily influenced by BTR (32.8%) and BBR (26.5%) in PC1, and TL (40.1%) and TaL (36.8%) in PC2. Comparative data on BBR and BTR in males and females are shown in Fig. 5.

Geographic and environmental species delimitation

The geographic distribution and extent of occurrence (EOO) of the three species are visualized in Figs 6–7 and Table 6. *Micrurus corallinus* is widely distributed in South America (~4 573 000 km²),

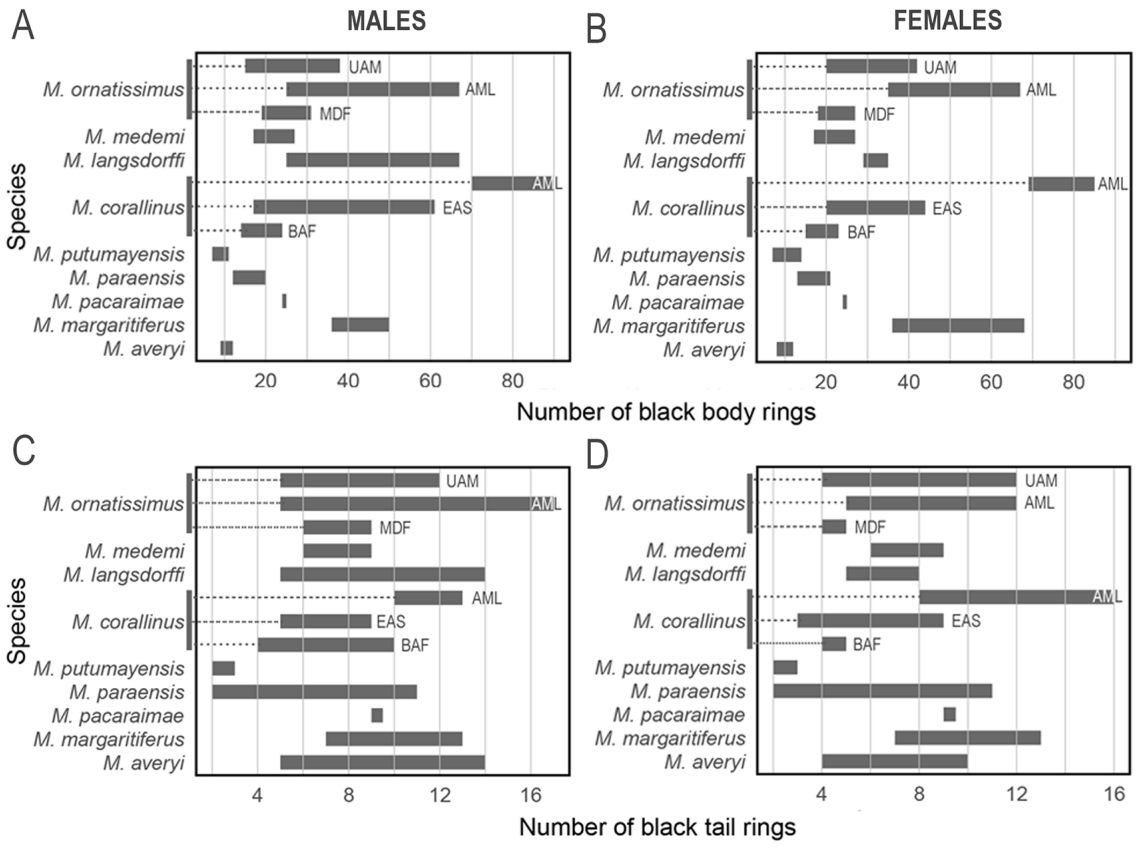

Fig. 5. Segment plot of comparative data showing geographic variation in the range of scale counts for the number of black rings on the body and tail in of *M. corallinus* (Merrem, 1820), *M. ornatissimus* (Jan, 1858) and other cis-Andean monadal *Micrurus* Wagler, 1824 species. **A**, **C**. Males. **B**, **D**. Females. Bioregions abbreviations: BAF = Brazilian Atlantic Forest; LAM = Amazonian lowlands; EAS = Eastern Andean Slopes; UAM = Upper Amazonia; IAV = Inter-Andean Valleys.

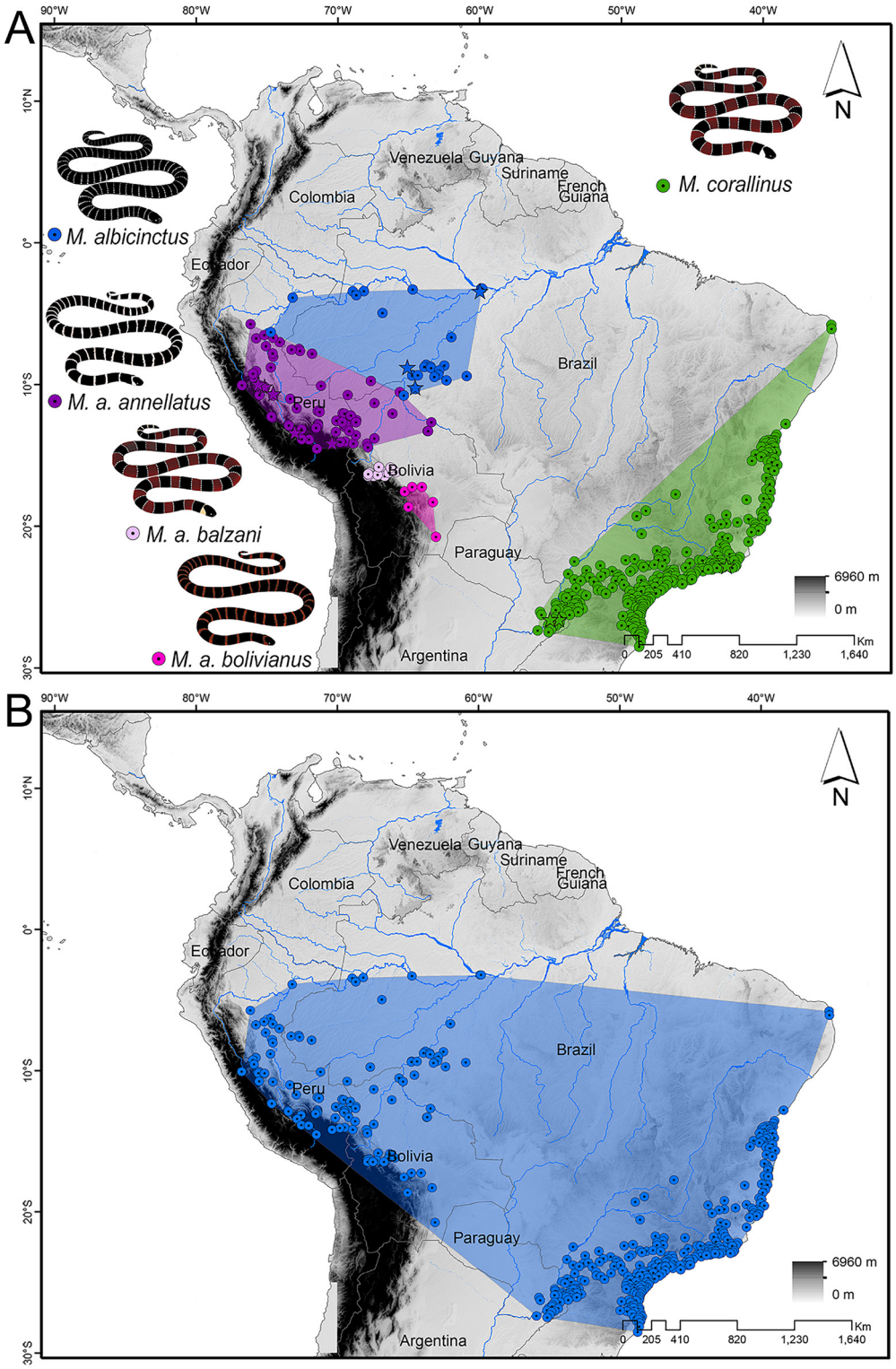

Fig. 6. A. Map showing distribution areas based on minimum convex polygons and locality records for *Micrurus* Wagler, 1824 species currently considered synonyms of *M. corallinus* (Merrem, 1820). **B**. Map shows the consolidated minimum convex polygons for *M. corallinus*, constructed using locality records of the synonymized species. Stars indicate the genetic samples.

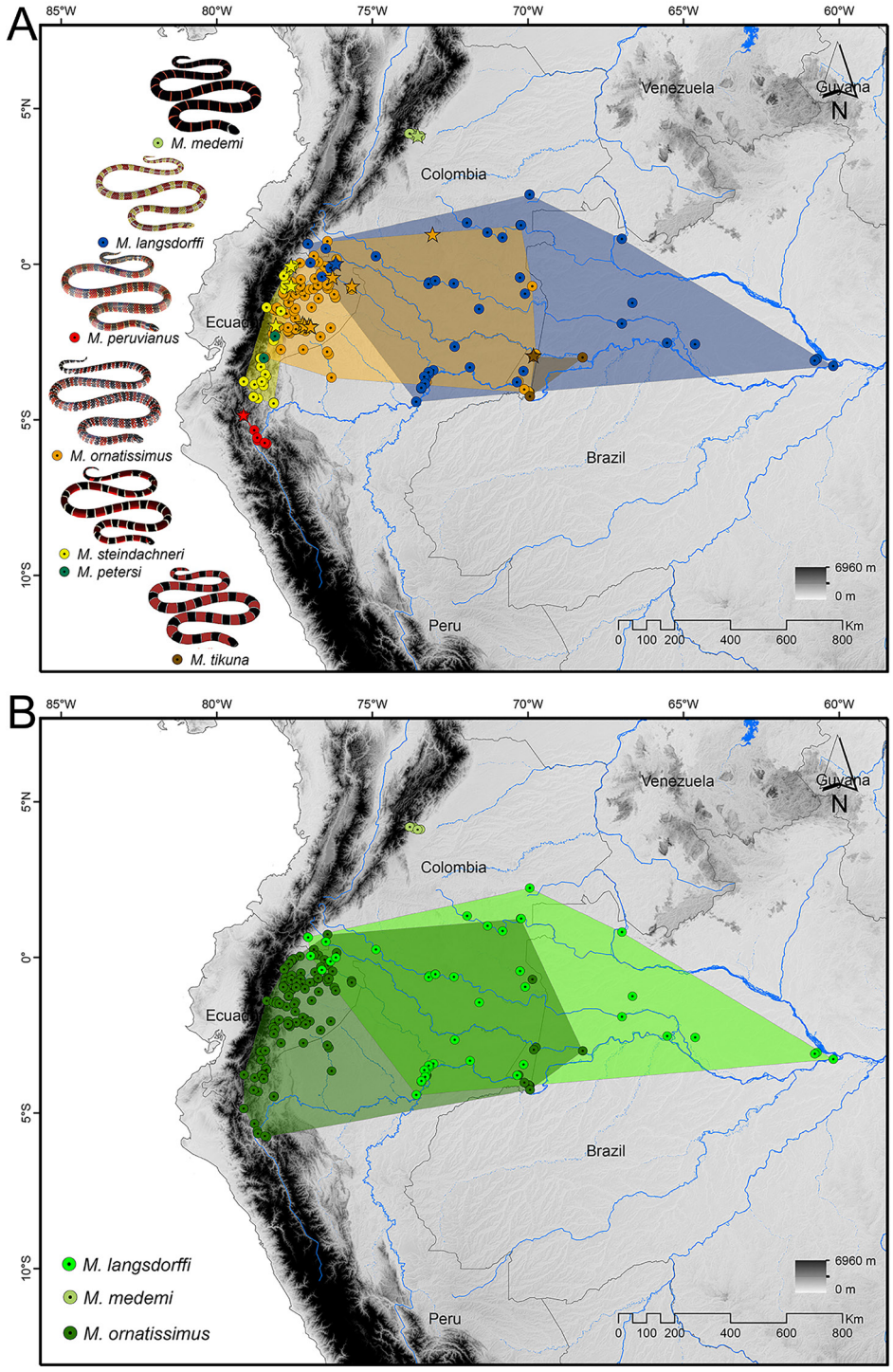

Fig. 7. A. Map showing distribution areas based on minimum convex polygons and locality records for *Micrurus* Wagler, 1824 species currently considered synonyms of *M. ornatissimus* (Jan, 1858), except for *M. langsdorffi* (Wagler, 1824) (light green), and *M. medemi* Roze, 1967 (green olive), which are closest phylogenetic relatives of *M. ornatissimus* (Jan, 1858). **B**. Map shows the consolidated minimum convex polygons for *M. langsdorffi*, *M. medemi* and *M. ornatissimus*, constructed using locality records of the synonymized species. Stars indicate the genetic samples.

Table 6. Descriptive variables and statistics for ecological niche models (ENMs) and their spatial representations for eastern Andean species of the genus *Micrurus* Wagler, 1824. 10 percentile training presence logistic threshold was used as the threshold to define the suitability areas in the models.

	M. corallinus	***M. langsdorffi***	***M. medemi***	***M. ornatissimus***
Bioclimatic variables	3, 4, 5, 6	2, 3, 4, 11	2, 3, 4, 12, 16	11, 12, 14
10 percentile training presence Logistic threshold	0.2733	0.4506	0.2924	0.1415
Mean AUC	1.298	1.334	1.669	1.697
AICc	12829.5	1054.2	197.0	3205.0
wAIC	1.000	0.408	1.000	0.197
Omission rate at 5%	0.045	0.000	0.285	0.026
Predicted model (km^2)	4 574 187	809 498	26 936	679 437
Occurrence area (km^2)	8 135 580	732 908	128.9	557 225

from the south of the Amazon River and consisting of two disjunct populations. The first population occurs throughout the Atlantic Forest in Argentina, Brazil, and Paraguay, with marginal records in the Cerrado biome (Nogueira *et al.* 2019; Campbell & Lamar 2004). The second population is found in the lowland rainforests of the Amazon region in Peru and Brazil, extending along the eastern Andes and into the inter-Andean valleys of Peru and Bolivia. *M. medemi* is restricted to lower montane pluvial forests in the Cordillera Oriental of Colombia, between the departments of Meta and Cundinamarca (~128 km²). Finally, *Micrurus langsdorffi* and *M. ornatissimus* are distributed in the Amazon region (~732 000 km² and ~557 000 km², respectively), between the Amazon and Negro rivers, spanning southeastern Colombia, eastern Ecuador, and western Brazil. However, *M. ornatissimus* also occurs along the Amazonian slopes of the Andes in Ecuador, with an isolated population in the inter-Andean dry forests of southern Ecuador (Fig. 8).

Ecological niche models are shown in the Fig. 8. Descriptive statistics and environmental projections using Linear Discriminant Analysis (LDA) functions of the ENMs are shown in Table 6. Prior group probabilities reflected sample imbalance: *M. corallinus* (70.3%), *M. ornatissimus* (21.8%), *M. langsdorffi* (6.3%), and *M. medemi* (1.6%). Group means showed that *M. corallinus* occupied cooler (21.6°C) and drier areas (annual precipitation 1736 mm) with higher temperature seasonality, whereas *M. langsdorffi* and *M. ornatissimus* were associated with warmer and wetter conditions. The first discriminant function (LD1) explained 81.44% of the between-group variance, and the first two functions together accounted for 97.75%. LD1 was primarily driven by temperature variables, especially mean temperature of the coldest quarter (BIO11), temperature seasonality (BIO4 and BIO7), and annual mean temperature (BIO1). The model achieved an overall classification accuracy of 92.21% (95% CI = 89.93–94.11%) (Table 7), significantly higher than the no-information rate of 70.29% ($P < 0.001$), with a Cohen's kappa of 0.829. Classification performance was strongly supported for *M. corallinus* (sensitivity = 98.12%, precision = 98.53%) and *M. medemi* (sensitivity = 90.91%, precision = 88.3%). Lower sensitivity was observed for *M. langsdorffi* (53.49%), mainly due to misclassification with *M. ornatissimus*. *Micrurus ornatissimus* showed good performance (sensitivity = 84.46%, precision = 85.62%). These results indicate strong climatic niche differentiation, with *M. corallinus* occupying more seasonal and drier environments, whereas *M. langsdorffi* and *M. ornatissimus* share warmer and more humid conditions (Fig. 9).

Taxonomy

Phylum Chordata Haeckel, 1866
Class Reptilia Laurenti, 1768
Order Squamata Oppel, 1811
Suborder Serpentes Linnaeus, 1758
Superfamily Elapoidea Boie, 1827
Family Elapidae Boie, 1827
Genus *Micrurus* Wagler, 1824

Micrurus corallinus (Merrem, 1820)
Figs 10–11

Elaps corallinus Merrem, 1820: 108.
Elaps annellatus Peters, 1871: 402.
Elaps balzani Boulenger, 1898: 130.
Elaps regularis Boulenger, 1902: 402.
Micrurus albicinctus Amaral, 1926: 26, figs 7–10.
Micrurus waehnerorum Meise, 1938: 20.
Micrurus annellatus montanus Schmidt, 1954: 322.
Micrurus annellatus bolivianus Roze, 1967: 7.

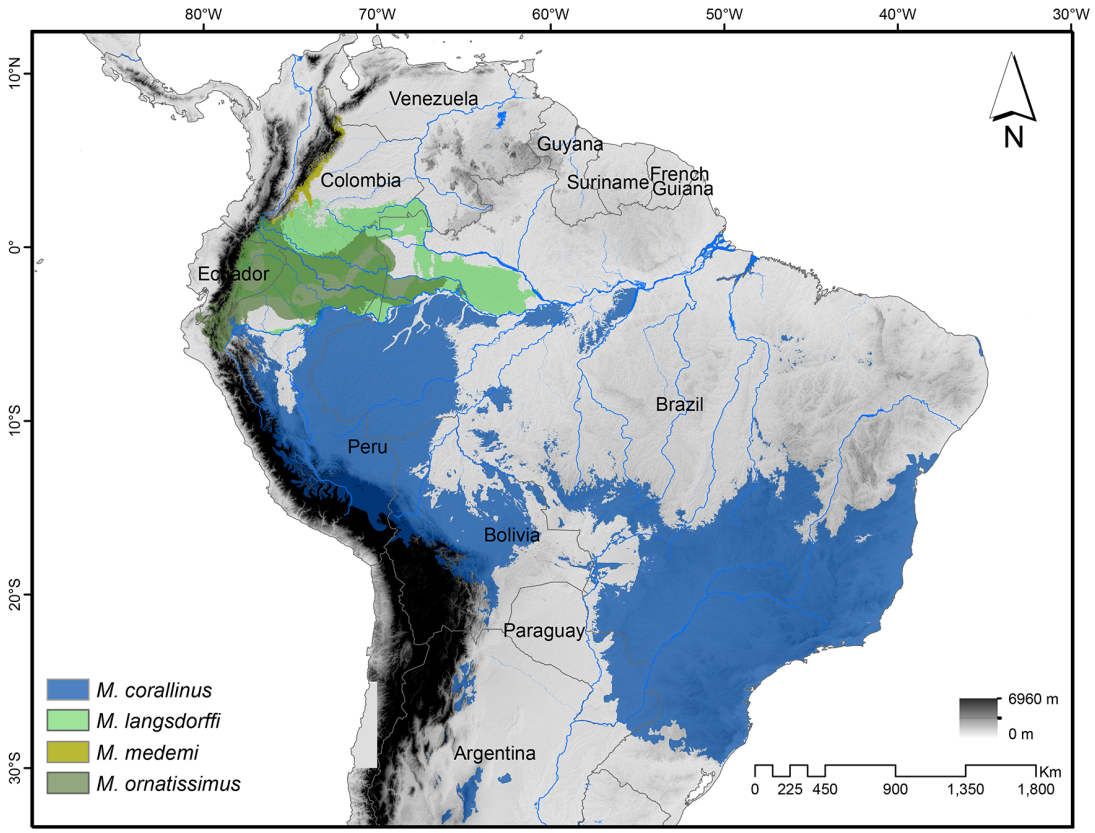

Fig. 8. Maps showing ecological niche models (ENMs), with colored polygons representing environmentally suitable areas for *M. corallinus* (Merrem, 1820), *M. langsdorffi* (Wagler, 1824), *M. medemi* Roze, 1967, and *M. ornatissimus* (Jan, 1858).

Elaps corallinus – Wied-Neuwied, 1820: 108. – Duméril *et al.* 1854: 1208 – Merrem 1820: 180. – Boulenger 1896: 438.
Micrurus balzani – Schmidt 1936: 192.
Micrurus ornatissimus – Schmidt 1936: 191 [in part].
Micrurus annellatus annellatus – Schmidt 1954: 322.
Micrurus annellatus balzani – Roze 1967: 6.
Micrurus bolivianus – da Silva Jr., Buononato, Pires, Feitosa 2021: 131. – da Silva Jr., Feitosa, Pires, Prudente 2021: 223.

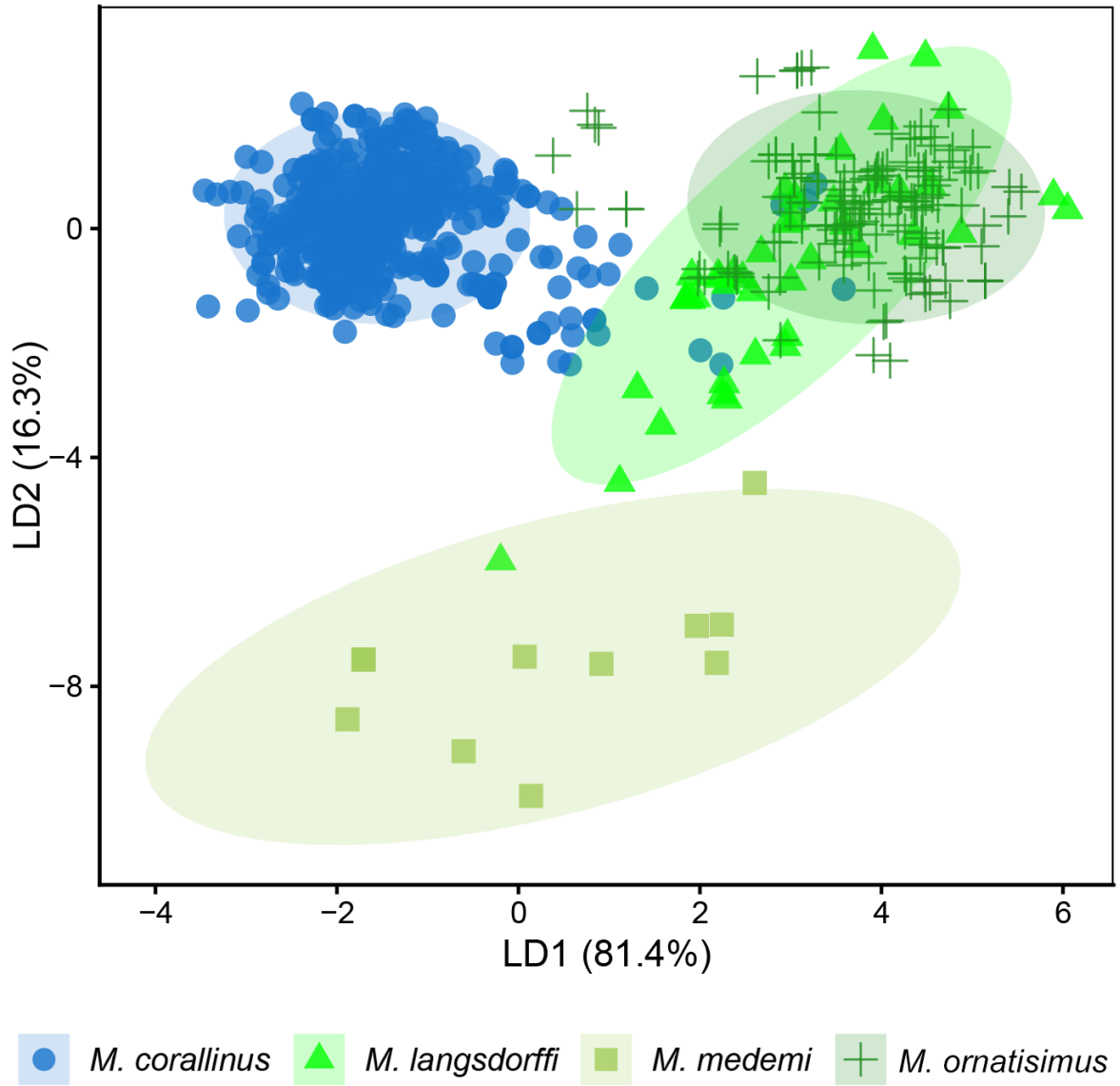

Fig. 9. Discriminant analysis biplot based on bioclimatic variables contributing to the ecological niche models of *Micrurus corallinus* (Merrem, 1820), *M. langsdorffi* (Wagler, 1824), *M. medemi* Roze, 1967, and *M. ornatissimus* (Jan, 1858).

Table 7. Results of successful classification in environmental-space (localities), with percentage in parentheses, assigned to each species of *Micrurus* Wagler, 1824 by discriminant analysis.

	Total 92.2%			
	M. corallinus	***M. langsdorffi***	***M. medemi***	***M. ornatissimus***
M. corallinus	466 (98.1%)	0	0	7
M. langsdorffi	6	23 (53.5%)	1	16
M. medemi	0	2	10 (90.9%)	0
M. ornatissimus	3	18	0	25 (84.5%)

Diagnosis

Micrurus corallinus can be distinguished from all congeners by a unique combination of the following characters: (1) body slender; (2) head slightly longer than wide (HL/HW = 1.2); (3) dorsal scales smooth, 15/15/15, apical pits absent; (4) rostral scale triangular, wider than long (RL/RW = 0.5); (5) internasal scales hexagonal, slightly wider than long (INL/INW = 0.9); (6) loreal scales absent; (7) prefrontal scales hexagonal, as wide as long (PFL/PFW = 1.0); (8) frontal scale hexagonal, longer than wide (FL/FW = 1.7); (9) temporal scales 1+1, occasionally 1+2; (10) one preocular scale on each side; (11) two postocular scales on each side; (12) nasal scale divided; (13) supralabial scales seven on each side, with the third and fourth bordering the orbit; (14) infralabial scales seven on each side, the first four in contact with the anterior chin-shield scales, the first pair in broad contact behind the symphysial; (15) preventral scales 1–4; (16) gular scales arranged in 1–2 rows; (17) chin shields in two pairs, never in contact with the symphysial; (18) symphysial scale wider than long (SL/SW = 0.8); (19) ventral scales 185–215 (mean 200.9±6.1 SD) in males, 198–288 (mean 215.5±27.4 SD) in females; (20) anal plate divided, supracloacal tubercles absent; (21) subcaudal scales divided, 38–49 (mean 45.5±2.4 SD) in males, 26–42 (mean 31.2±5.2 SD) in females; (22) tail-total length ratio 11.9–20.3% (mean 14.4±1.3 SD) in males, 6.8–10.9% (mean 8.8±1.3 SD) in females; (23) teeth: 9–11 dentary, 4–6 pterygoid, and 6–8 palatine.

Etymology

The specific epithet is derived from the Latin '*corallium*', meaning 'coral', and the suffix '*-inus*', meaning 'pertaining to', which alludes to the bright colors of this coralsnake (see Campbell & Lamar, 2004).

Fig. 10 (next page). Illustrations of the variation in dorsal color patterns of the body and tail in *Micrurus* Wagler, 1824. **A–E**. *M. corallinus* (Merrem, 1820). **F–H**. *M. langsdorffi* (Wagler, 1824) **I–K**. *M. medemi* Roze, 1967. **L–P**. *M. ornatissimus* (Jan, 1858). **A**. USNM 253595, holotype, El Tirol, Itapúa, Paraguay. **B**. CORBIDI 14678, Río Mantaro, Tayacaja, Huancavelica, Peru. **C**. USNM247702, Tambopata Reserve, Madre de Dios, Peru. **D**. Unvouchered specimen, Acre, Brazil. **E**. MPEG 19548, Careiro da Várzea, Amazonas, Brazil. **F**. QCAZ 13129, Reserva de Producción Faunística Cuyabeno, Sucumbíos, Ecuador. **G**.Unvouchered specimen, Iquitos, Peru. **H**. BMNH 1946.1.17.21, holotype of *Elaps batessi* Günther, 1868, Pebas, Peru. **I**. AMNH 96988, holotype of *M. medemi*. **J**. UTA-M555, Villavicencio, Meta, Colombia. **K**. UTA-M558, Villavicencio, Meta, Colombia. **L**. BMNH 1946.1.17.18, holotype of *Elaps buckleyi* Boulenger, 1896, Canelos, Pastaza, Ecuador. **M**. MCZ 175385, holotype of *M. peruvianus* Schmidt, 1936, Perico, Cajamarca, Peru. **N**. USNM 158295, holotype of *M. petersi* Roze, 1967, Plan de Milagro on the trail to Pan de Azúcar, Morona Santiago, Ecuador. **O**. NMW 15750, holotype of *M. steindachneri* (Werner, 1901), Ecuador. **P**. MPEG 19199, holotype of *M. tikuna* Feitosa, Da Silva Jr, Pires, Zaher & Prudente, 2015, Tabatinga, Amazonas, Brazil. Illustrations by G. Corona and J.H. Valencia.

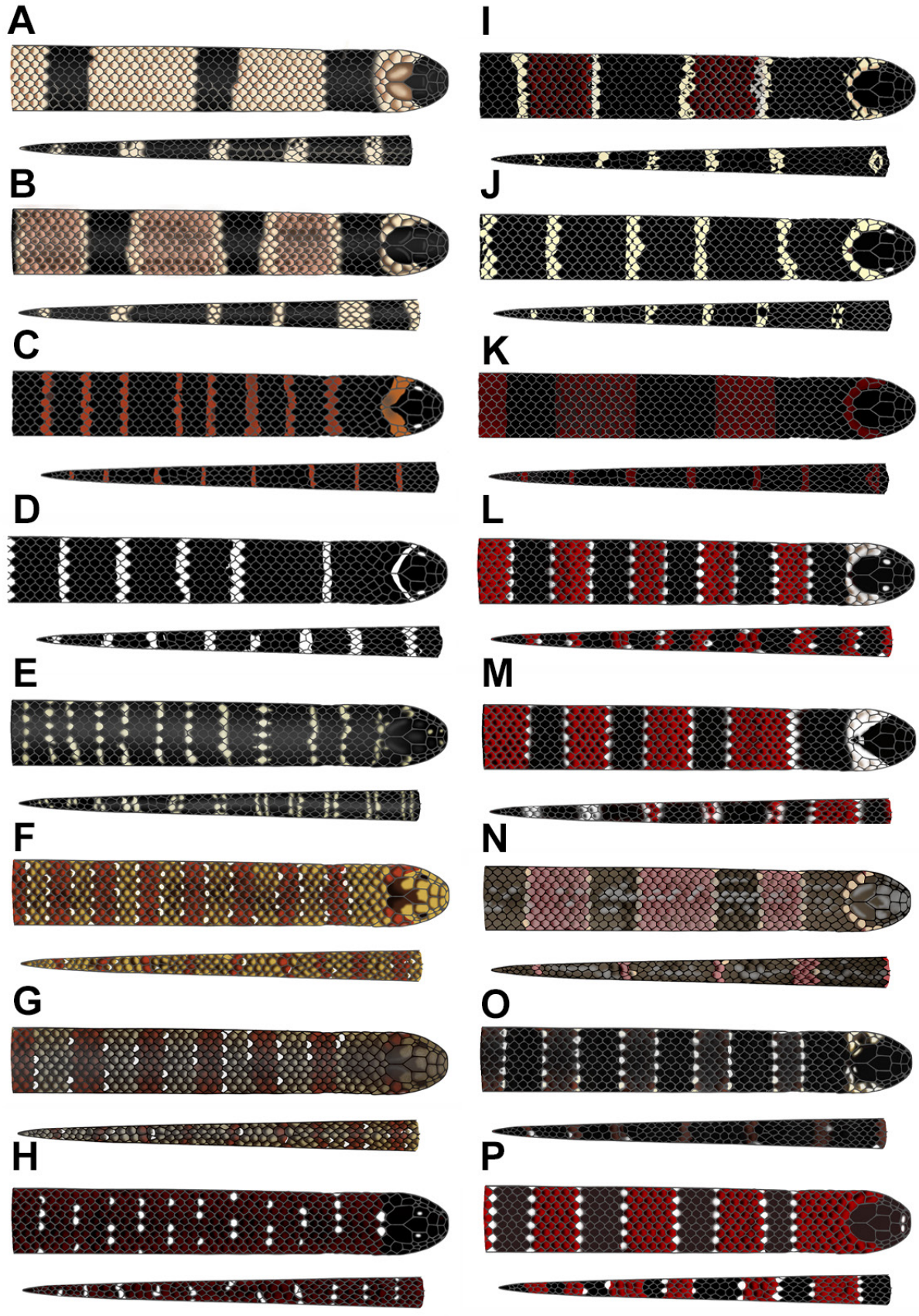
A
B
C
D
E
F
G
H
I
J
K
L
M
N
O
P

Type material

Lectotype (designed by Roze 1966)
BRAZIL • ♀; Rio do Janeiro, Cabo Frio, Campos de Coaytacases, Parahyba; 22.833° S, 42.033° W; unknown date; M. zu Wied-Neuwied leg.; AMNH 3911.

Paralectotype (designed by Roze 1966)
BRAZIL • ♀; same collection data as for lectotype; AMNH 3935.

Other material examined (n = 201)
ARGENTINA – Misiones • 2 ♂♂, 1 ♀; Monte Carlo; 26.571° S, 54.741° W; 1926; J. Haider leg.; FMNH 9371, 9372, 9473.

BOLIVIA – **Beni** • 1 ♂, 1 ♀; Beni; unknown collection data; E.J. Young leg.; AMNH 2975–2976, paratypes of *M. a. annellatus* • 1 ♂; San Carlos, Río Beni; 11.179° S, 66.179° W; 1921; C. Bock leg.; ZMH 396. – **Cochabamba** • 5 ♀♀; Yungas de Cochabamba; 17.406° S, 65.259° W; 1897; Rolle and J. Steinbach leg.; NHW 26992; CM 2758–2759, paratypes of *M. annellatus bolivianus* • 1 ♀; same collection data as for preceding; MSNG 28874, holotype of *Elaps balzani*. – **Chuquisaca** • 1 ♀; Charobamba River, about 50 km northeast of Zudañez; 18.677° S, 65.051° W; 29 May 1897; Rolle leg.; ZMH 2706e, holotype of *M. annellatus bolivianus*. – **La Paz** • 1 ♀; Achipiri; 15.166° S, 68.233° W; 1897; Rolle leg.; NHW 27060c • 1 ♀; Chulumani; 16.408° S, 67.527° W; 2 Aug. 1903; P.O. Simones leg.; BMNH 1946.1.17.2, type of *Elaps regularis* • 1 ♂; same collection data as for preceding; 1934; L. Cárdenas leg.; USNM 98890 • 2 ♂♂; La Paz; 16.509° S, 68.191° W; unknown date; D. Jaeger leg.; ZSM 16/1924a, b • 1 ♀; Larecaja; 15.5° S, 68.333° W; 1897; Rolle leg.; ZMH 2706d • 1 ♂; Pando; 11.030° S, 68.769° W; unknown date; K.P. Schmidt leg.; UNAS 82. – **Unknow locality** • 2 ♂♂, 1 ♀; unknown collection data; NHW 18218.1, 18219.2; ZSM 207/0

BRAZIL – **Espírito Santo** • 1 ♀; Espírito Santo; 19.297° S, 40.453° W; unknown collection data; MCZ 17856 • 1 ♀; Santa Leopoldina; 20.100° S, 40.527° W; 1918; J. Müller leg.; ZSM • 1 ♀; Vitória, Colônia Santa Isabel; 20.544° S, 41.160° W; 1918; J. Müller leg.; ZSM • 2 ♀♀; Santa Teresa; 19.932° S, 40.598° W; 23 Feb. 1940; C. Ruschi leg.; MNRJ 959, 960. – **Goiás** • 1 ♀; Goiás; 15.9207° S, 48.927° W; unknown collection data; MCZ 3489. – **Mato Grosso** • 1 ♂; northern or central Mato Grosso; unknown date; C. Rondon leg.; type of *M. albicinctus*; MNRJ 376. – **Minas Gerais** • 1 ♂; São Syriaco, near Serra Providência; 19.878° S, 43.876° W; unknown collection data; MCZ 5568. – **Paraná** • 2 ♂♂, 1 ♀; Foz do Iguaçu; 25.516° S, 54.585° W; unknown collection data; MNRJ 1002, 1003 • 2 ♂♂, 1 ♀; Paranaguá;

Fig. 11 (next page). Illustrations of the variation in head color patterns in lateral, dorsal, and ventral views for *Micrurus*. **A–E**. *M. corallinus* (Merrem, 1820). **F–H**. *M. langsdorffi* (Wagler, 1824). **I–K**. *M. medemi* Roze, 1967. **L–P**. *M. ornatissimus* (Jan, 1858). **A**. USNM 253595, holotype of *M. corallinus*, El Tirol, Itapúa, Paraguay **B**. CORBIDI 14678, Río Mantaro, Tayacaja, Huancavelica, Peru. **C**. USNM247702, Tambopata Reserve, Madre de Dios, Peru. **D**. Unvouchered specimen, Acre, Brazil. **E**. MPEG 19548, Careiro da Várzea, Amazonas, Brazil. **F**. QCAZ 13129, Reserva de Producción Faunística Cuyabeno, Sucumbíos, Ecuador. **G**. Unvouchered specimen, Iquitos, Peru. **H**. BMNH 1946.1.17.21, holotype of *Elaps batessi* Günther, 1868, Pebas, Peru. **I**. AMNH 96988, holotype of *M. medemi*. **J**. UTA-M555, Villavicencio, Meta, Colombia. **K**. UTA-M558, Villavicencio, Meta, Colombia. **L**. BMNH 1946.1.17.18, type of *Elaps buckleyi* Boulenger, 1896, Canelos, Pastaza, Ecuador. **M**. MCZ 175385, holotype of *M. peruvianus* Schmidt, 1936, Perico, Cajamarca, Peru. **N**. USNM 158295, holotype of *M. petersi* Roze, 1967, Plan de Milagro on the trail to Pan de Azúcar, Morona Santiago, Ecuador. **O**. NMW 15750, holotype of *M. steindachneri* (Werner, 1901), Ecuador. **P**. MPEG 19199, holotype of *M. tikuna* Feitosa, Da Silva Jr, Pires, Zaher & Prudente, 2015, Tabatinga, Amazonas, Brazil. Illustrations by G. Corona and J.H. Valencia.


A
B
C
D
E
F
G
H
I
J
K
L
M
N
O
P

25.514° S, 48.522° W; unknown collection data; MNRJ 558, 961, 962. – **Rio de Janeiro** • 1 ♀; Rio de Janeiro; 22.360° S, 42.718° W; unknown date; M. zu Wied-Neuwied leg.; ZSM 42/1926 • 3 ♀♀; same collection data as for preceding; 1877; H. Massini leg.; NHMB 2287–2289 • 10 ♀♀; same collection data as for preceding; unknown date and collector; MCZ 1374, 1374a, 1374b, 2648, 2648a–2648e, 2923 • 1 ♀; Andaraí; 22.922° S, 43.247° W; 1883; H. Massini leg.; NHMB 2285 • 1 ♂, 2 ♀♀; Barro Branco; 22.633° S, 43.244° W; 1941; C. Passarelli leg.; MNRJ 950, 953, 955 • 1 ♀; same collection data as for preceding; unknown date and collector; MNRJ 1004 • 1 ♀; Guanabara, Tijuca; 23.000° S, 43.333° W; unknown date and collector; MNRJ 1539 • 2 ♂♂, 1 ♀; Paraty; 23.219° S, 44.716° W; unknown date and collector; MNRJ 1000, 1001, 2708 • 2 ♀♀; Serra do Mar, Serrinha; 22.033° S, 41.693° W; Aug. 1938; C. Kulhom leg.; MNRJ 725, 956. – **Rio Grande do Sul** • 3 ♂♂, 6 ♀♀; Rio Grande do Sul; unknown collection data; MCZ 20826, 20828–20835 • 1 ♀; Santo Antônio, Guaporé; 28.789° S, 51.917° W; unknown date; J. Haseman leg.; CM 341. – **Santa Catarina** • 1 ♀; Santa Catarina; 26.928° S, 49.364° W; unknown date; Q.C. Jordan leg.; ANSP 6789 • 1 ♀; same collection data as for preceding; C. Stejner leg.; FMNH 11624 • 3 ♀♀; same collection data as for preceding; unknown date and collector; FMNH 37202, 37203, 37733 • 2 ♀♀; same collection data as for preceding; MCZ 20822, 20824 • 3 ♀♀; Blumenau; 26.916° S, 49.071° W; unknown date and collector; MCZ 17755, 17756, 17758 • 6 ♀♀; Hansa; 26.425° S, 49.243° W; 1928; W. Ehrhardt leg.; BMNH 1928.11.5.141–1928.11.5.146 • 3 ♀♀; Humboldt; 26.487° S, 49.063° W; unknown date and collector; UMMZ 62564, 62736; MNRJ 968 • 5 ♂♂, 7 ♀♀; Humboldt; 26.487° S, 49.063° W; 1915; W. Ehrhardt leg.; MNRJ 648, 965, 967, 968, 970, 973–975, 978, 980, 983, 995 • 2 ♀♀; Jaraguá; 26.481° S, 49.084° W; 14 Apr 1941; unknown collector; FMNH 37204, 37205 • 1 ♀; Joinville; 26.304° S, 48.846° W; 1906; Ehrhardt leg.; MTD 1906 • 1 ♂, 10 ♀♀; 1915; C. Dalibour leg.; MNRJ 966, 988–995, 997, 999 • 2 ♀♀; São Bento; 26.249° S, 49.383° W; unknown date and collector; MCZ 20842, 27682. – **São Paulo** • 15 ♂♂, 12 ♀♀; São Paulo; unknown collection date; UMMZ 12696, 17857, 17859, 17861, 20837–20839, 20841, 62734, 62737–62739, 62741–62743, 62757, 63025; AMNH 5751, 5752; IRSNB 62; MTD 9420c; MCZ 12695, 16675, 17858, 17860, 20836, 20840 • 1 ♂; Batatais; 20.886° S, 47.585° W; 8 May 1922; Vital Brazil leg.; BMNH 1908.5.22.7 • 1 ♂; Bauru; 22.350° S, 49.024° W; 1901; unknown collector; MNHN 187.67 • 1 ♀; São Sebastião; 23.800° S, 45.401° W; 1902; W. Rosenberg leg.; BMNH 1902.7.28.89. – **Unknow locality** • 3 ♂♂, 3 ♀♀; unknown collection data; AMNH 3935, ANSP 6786, IRSNB 62E, 62J, 304, MCZ 3205.

PERU – **Arequipa** • 1 ♀; Arequipa; unknown date; P. Oviedo leg.; FMNH 40199. – **Ayacucho** • 1 ♀; Huanuachayo; 12.114° S, 75.124° W; unknown date and collector; LSUMZ 26880 • 1 ♂; Pajonal; 5.265° S, 79.674° W; Jun. 1929; W.F. Walker leg.; MCZ 45913. – **Cajamarca** • 1 ♂; Chanchamayo; 11.123° S, 75.370° W; 29 May 1908; C. Schunke leg.; BMNH 1908.5.29.39. – **Cusco** • 1 ♀; Marcapata Valley; 13.587° S, 70.977° W; 29 May 1902; G. Ockenden leg.; BMNH 1902.5.29.191 • 1 ♂, 1 ♀; same collection data as for preceding; unknown date; C. Kalinowski leg.; FMNH 40223, 62942. – **Huancavelica** • 1 ♀; Tayacaja, Colcabamba, Río Mantaro; 12.293° S, 74.689° W; 9 Jul. 2014; L. Echevarría leg.; CORBIDI 14678 • 1 ♀; Andaymarca, Chupto; 12.299° S, 74.649° W; 1 Jul. 2014; L. Echevarría leg.; CORBIDI 14647 • 2 ♀♀; Andaymarca, Fundición; 12.293° S, 74.660° W; 18 Sep. 2014; L. Echevarría leg.; CORBIDI 13724, 13646 • 1 ♂; Colcabamba, Pichiu; 12.361° S, 74.624° W; 18 Sep. 2013; C.Z. Landauro leg.; CORBIDI 13646 • 1 ♀; Surcubamba, Jatuspata; 12.259° S, 74.690° W; 3 Jul. 2014; C.Z. Landauro leg.; CORBIDI 13726. – **Huánuco** • 1 ♀; Hacienda Pampayacu; 9.550° S, 75.900° W; 17 Jul. 1936; W.F. Walker leg.; MCZ 42417 • 1 ♀; Pozuzo; 10.064° S, 75.545° W; 1871; unknown collector; ZMB 7185, type of *M. annellatus*. – **Junín** • 1 ♀; La Merced; 11.062° S, 75.332° W; unknown date; R. Reinhard leg.; ZSM [1] • 1 ♂; San Ramón; 11.121° S, 75.358° W; unknown date; J.M. Schunke leg.; FMNH 152312. – **Loreto** • 1 ♀; Alto Pisqui; 7.654° S, 75.035° W; 29 Oct. 1906; H. Bassler leg.; AMNH 52311 • 1 ♀; Cashiboya; 7.683° S, 74.937° W; unknown date; H. Bassler leg.; AMNH 52701 • 1 ♀; Iquitos; 3.740° S, 73.250° W; 1925; H. Bassler leg.; AMNH 52586 • 1 ♀; Monte Alegre, Pachitea; 10.105° S, 75.864° W; unknown date; H. Bassler leg.; AMNH 53036 • 3 ♀♀; Pampa Hermosa; 7.196° S, 75.295° W; unknown date; H. Bassler leg.; AMNH 53555, 55451, 55977 • 1 ♀;

Pisqui Plain, mont front above; 7.654° S, 75.035° W; 28 Oct. 1929; H. Bassler leg.; AMNH 52895 • 1 ♂; Tapiche–Utiquinia, Brazil frontier; unknown locality; H. Bassler leg.; AMNH 52068 • 1 ♀; Rancho Viejo & Vito; 1894; unknown collector; NHW 13390 • 1 ♂, 1 ♀; Sierras de Contaya; 7.172° S, 74.521° W; unknown date; H. Bassler leg.; AMNH 52066, 53373, 53375. – **Madre de Dios** • 1 ♀; Puerto Maldonado; 12.579° S, 69.191° W; Aug. 1921; H. Bassler leg.; AMNH 56145. – **Puno** • 1 ♂, 1 ♀; Carabaya; 13.653° S, 70.240° W; May–Jun. 1903 and May 1907; G. Ockenden leg.; BMNH 1903.6.30.5, 1907.5.7.7 • 1 ♀; Juliaca, Santo Domingo Mine; 15.508° S, 70.135° W; unknown date; H.H. Keamps leg.; AMNH 2957 • 1 ♂; Santo Domingo; 15.508° S, 70.135° W; unknown date; Dr. Itori leg.; FMNH 40222 • 1 ♂; about 10 km north of Santo Domingo Mine, Camp 4; 15.414° S, 70.147° W; 2 Nov. 1941; C. Sanborn leg.; FMNH 40221, type of *M. annellatus montanus* • 1 ♂; Sandia, Pajchani Trail to Río Llauri; 15.449° S, 69.257° W; unknown date; unknown collector; UMMZ 86164 • 1 ♀; Sandia, San Ignacio; 14.073° S, 68.981° W; 3 Oct. 1951; H.H. Heller leg.; FMNH 68590. – **San Martín** • 1 ♀; Río Huallaga; 5.006° S, 76.004° W; Nov. 1930; H. Bassler leg.; AMNH 52718 • 1 ♂, 1 ♀; Tarapoto, Río Mayo; 6.596° S, 76.312° W; unknown date; unknown collector; INSP 422, 445 • 1 ♂; Hacienda Matara, Apurímac; 13.741° S, 72.899° W; Nov. 1941; F. Samanez leg.; FMNH 40224. – **Ucayali** • 1 ♀; 15 km of Ucayali, Río Callería, colonia Callería; 8.401° S, 74.541° W; 1961; B. Malkin leg.; CAS 25 • 1 ♂, 1 ♀; Fundo Sinchono; 9.080° S, 75.770° W; Jun.–Jul. 1944; J.G. Sanders leg.; USNM 119016–119017 • 1 ♀; Yarinacocha; 8.249° S, 74.663° W; unknown date; T. Richard leg.; LSUMZ 26881. – **Unknow locality** • Unknown locality; AMNH 2827.

Description

Coloration. Tricolor (red–white/yellow–black) and bicolor (reddish/white–black) patterns. Dorsal coloration with 14–90 black rings in males (mean = 31.6±21.8 SD) and 20–83 in females (mean = 41.6±20.6 SD). Accessory black rings are absent. The nuchal black ring is 4–7 dorsal scale rows long, sometimes bordered by a sequence of white spots, and usually connected to the black hood by one or two dorsal scale rows. Black rings measure 3–6½ dorsal scale rows dorsally and 1–2 scales ventrally. Red rings tend to be longer along the vertebral region and usually bear black spots on each scale, except in juveniles. Red rings are 2.5–5 dorsal scale rows long, similar in length to the black rings, and occasionally reaching up to 13 dorsal scales at mid-dorsum. Ventrally, they are slightly reduced, measuring 2–4 scales in length. In juveniles, the red dorsal scales are immaculate or may bear irregular black spots or tips, whereas the red ventral scales are immaculate. Some melanistic individuals have completely black scales within the red rings, causing them to fuse with adjacent black rings on both the dorsum and venter. White or yellow rings are 1–1.5 dorsal scale rows long, usually composed of fused or separated spots, with each scale exhibiting brown spots on the anterior edge. Ventrally, these rings are one scale long and may be indistinguishable in some individuals. Head coloration is black, covering the posterior or anterior internasals, prefrontals, frontal, preoculars, postoculars, and parietals. The occipital band may be present or absent; when present, it is white, yellowish, or reddish, covering the entire head or including the temporals, three supralabials, and one dorsal scale row. The occipital band is either separated from the first black ring by a sequence of white spots or connected to it by one or two scales. Tail coloration: males have 5–14 black rings (mean = 8.1±2.4 SD), while females have 3–16 (mean = 4.8±1.4 SD). These rings measure 2–7 dorsal scale rows in length and 2–6 scales ventrally. Red rings or bands are 1–3 dorsal scale rows long dorsally and 1–3 scales long.

Hemipenial morphology. Based on CORBIDI 13646, MPEG 19548 (partially everted), and USNM 253595. Additional data were sourced from Feitosa *et al.* (2006), Da Silva *et al.* (2021), and the original descriptions by K. P. Schmidt (MNRJ 376, type of *M. albicinctus*) and J. Roze (IB 15089; NHW 18219.1, previously identified as *M. waehnerorum* Meise, 1938; AMNH 53375; FMNH 40221, 56141, previously identified as *M. annellatus*). Hemipenis deeply bilobed between the 11th and 13th subcaudal scales, non-capitate. The sulcus spermaticus is deep, bifurcated at the base of the lobes, centripetal, and curved along the lobes, reaching the apices. The margins of the sulcus are thin and bordered by minute spines.

The long lobes (about 26–46% of the total hemipenial length) are subcylindrical, tapering distally into sharply pointed tips, and are ornamented with small to medium-sized spines densely arranged in irregular longitudinal rows, larger between the ninth and sixteenth subcaudals, and gradually decreasing in size toward the apex of the lobes. Lobular spines are thinner and more numerous on the asulcate side of the organ. The distal half of the hemipenial body is ornamented with small, irregularly arranged spines that gradually increase in size proximodistally, whereas the proximal region of the hemipenis is naked. On the asulcate surface of the hemipenial body, spines are restricted to the area near the bifurcation of the lobes. A distinct naked basal pocket is present but poorly developed (Fig. 12).

Variation. Populations of *Micrurus corallinus* are polymorphic in both dorsal coloration patterns and scutellation. Based on morphological characteristics, *M. corallinus* can be grouped into three geographically structured assemblages for analytical purposes: (1) populations associated with the Brazilian Atlantic Forest (BAF), (2) those from the Amazonian lowlands (AML), and (3) those from the Andes (AND), including lower montane wet and cloud forests. Populations from the Amazon rainforest exhibit the highest degree of variability. Dorsal coloration patterns include both monadal and bicolor forms. In some Amazonian populations, the red rings are completely melanized, giving the snake a bicolor dorsal coloration (the *M. albicinctus* pattern). Populations of *M. corallinus* from the Andes and the Atlantic Forest also share a typical monadal coloration, characterized by a sequence of black rings bordered by pale rings (white or yellow), followed by red rings two to three times the width of the black ones (the *M. annellatus annellatus* pattern). However, Andean populations usually exhibit a bicolor dorsal pattern of black and white or red/orange rings (the *M. a. balzani* and *M. a. bolivianus* patterns). Geographic variation in the morphological characters of *Micrurus corallinus* is summarized in Table 8.

Differential diagnosis

Micrurus corallinus shares several characteristics with other cis-Andean monadal species of the genus *Micrurus* (Table 5, Fig. 5), including the number of dorsal scale rows (15–15–15); supralabials (7–7, with the 3rd and 4th contacting the eye); infralabials (7–7, with the first four contacting the first pair of chin shields); preoculars (1–1); postoculars (2–2); and temporals (1+1). It has two pairs of chin shields, which never contact the symphysial scale, and the symphysial is wider than long. The hemipenis is strongly forked, with an unornamented body. The dorsal coloration of *M. corallinus* includes monadal or bicolor patterns, except in *M. averyi* Schmidt, 1939, *M. pacaraimae* Morato de Carvalho, 2002, *M. paraensis* Cunha & Nascimento, 1973, and *M. remotus* Roze, 1987, which exhibit only monadal coloration, and in *M. margaritiferus* Roze, 1967 and *M. putumayensis* Lancini, 1962, which show only a bicolor pattern. Additionally, *M. corallinus* lacks the accessory black rings present in *M. sangilensis*. The number of ventral scales in males (185–215) and females (198–288), and subcaudal scales in males (38–49) and females (26–42), falls within the range of most *Micrurus* species. The number of black body rings (BBR) in males (14–90) and females (20–83) is within the range of most species, except in *M. averyi* (9–12 and 8–12, respectively) and *M. putumayensis* (7–11 and 9–12, respectively). Similarly, the number of black tail rings (BTR) in males (5–13) and females (3–9) falls within the range of most species, except in *M. putumayensis* (2–3 in both sexes).

Micrurus corallinus is distinguished from other cis-Andean monadal species by the following characteristics (differences in parentheses). It differs from *M. averyi* by having red rings up to three or four times longer than the black rings, the presence of nuchal rings, distinctive parietal rings, and a greater number of black body rings (BBR) in males (14–90) and females (20–83). In contrast, *M. averyi* has red rings up to six times longer than the black rings, an almost entirely black head, no parietal rings, bands, or spots, and fewer BBR (9–12 in males, 8–12 in females). *Micrurus corallinus* differs from *M. margaritiferus* by having 4–6 pterygoid teeth (*M. margaritiferus* has seven). It differs from *M. medemi* by the absence of ornamental markings above the cloaca (*M. medemi* has one or more yellow caudal rings containing dorsally diamond-shaped black blotches beginning above the cloaca). It is

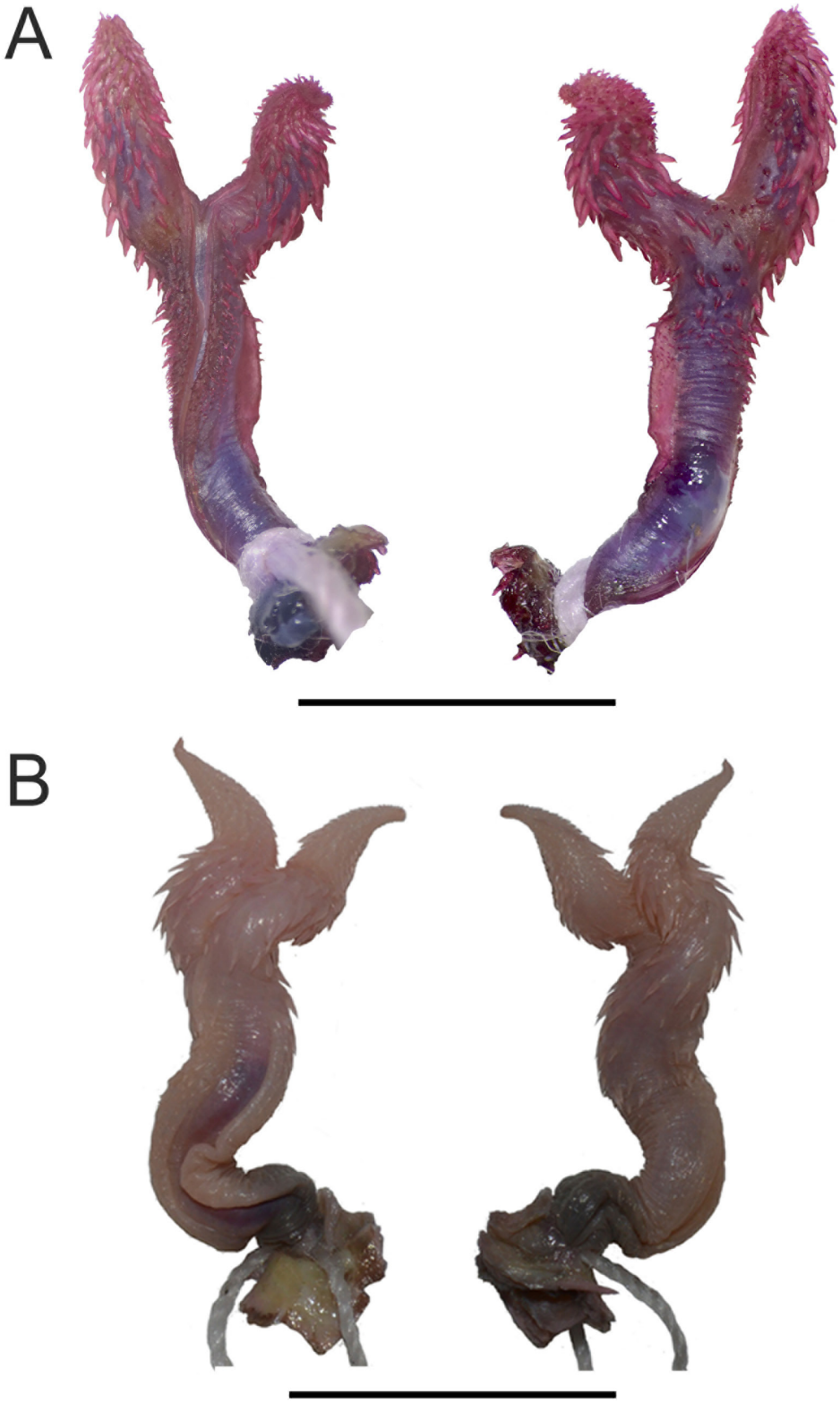

Fig. 12. Sulcate and asulcate sides of the hemipenes. **A**. *Micrurus corallinus* (Merrem, 1820) (CORBIDI 13646). **B**. *M. ornatissimus* (Jan, 1858) (FHGO 9818). Scale bars = 5 mm.

Table 8. Geographic variation of morphometric and scutellation data for *Micrurus corallinus* (Merrem, 1820) and *M. ornatissimus* (Jan, 1858). The range is followed by the mean and standard deviation.

		Micrurus corallinus			***Micrurus ornatissimus***		
Characters	**Sex**	**Andean region**	**Amazon lowlands**	**Brazilian Atlantic Forest**	**Upper Amazon**	**Inter-Andean valleys**	**Amazon lowlands**
Ventral scales	M	208–210 (215.6±15.1)	196–210 (204.1±4.9)	197–229 (221.1±6.6)	184–219 (205.2±9.0)	199–230 (212.6±12.5)	161–225 (216.7±6.8)
	F	224–232 (228±3.03)	197–229 (221.1±6.6)	185–215 (203.8±6.1)	224–234 (229.4±2.8)	202–230 (210.0±11.6)	156–230 (201.5±9.8)
Subcaudal scales	M	45–46 (45.5±0.70)	27–55 (47.6±4.7)	42–50 (44.6±1.8)	42–49 (45.5±2.3)	34–47 (40.6±4.9)	39–54 (48.4±2.9)
	F	32–33 (32.6±0.54)	29–48 (34.7±3.7)	20–33 (29.9±1.8)	29–36 (32.1±2.3)	28–36 (30.7±3.1)	30–40 (34.4±2.3)
Black body rings	M	21–22 (21.5±0.70)	25–90 (55.4±19.6)	14–24 (17.1±1.7)	15–38 (31.4±6.5)	16–31 (21.6±5.2)	27–60 (45.1±6.5)
	F	21–23 (22.2±0.83)	29–90 (43.1±15.4)	15–25 (19.8±1.6)	20–42 (31.7±7.0)	26–31 (27.7±1.9)	35–67 (50.5±7.9)
Black tail rings	M	6–8 (7±1.41)	5–14 (9.8±2.1)	5–8 (6.2±0.8)	5–12 (9.0±1.9)	5–7 (6.2±0.7)	6–17 (13.2±2.4)
	F	3–4 (3.8±0.44)	5–16 (7.1±2.2)	3–6 (7.1±2.2)	2–7 (5.1±1.6)	4–7 (5.2±1.1)	6–12 (9.2±1.4)
% Tail–Total length	M	11.3–16.9 (14.1±3.96)	13.4–16.2 (14.9±0.8)	12.0–15.1 (14.2±0.8)	13.7–16.6 (14.8±0.7)	10.3–14.5 (12.8±1.6)	10.4–17.4 (15.0±1.5)
	F	8.4–9.8 (9.1±0.5)	7.0–9.9 (8.6±0.6)	7.6–9.7 (8.5±0.4)	8.0–9.6 (8.6±0.5)	9.0–9.8 (9.3±0.3)	7.9–11.0 (9.2±0.7)
Nuchal ring		Present	Present	Present	Present	Present	Present/ absent
Accessory black rings		Absent	Absent	Absent	Absent	Absent	Absent

distinguished from *M. langsdorffi* and *M. ornatissimus* by having hemipenes with a bare basal pocket that begins just above the base of the organ and extends laterally along the body, well below the bifurcation point of the spermatic groove (*M. langsdorffi* and *M. ornatissimus* have a poorly developed, completely naked basal pocket that begins just above the base of the organ and continues laterally along the body to below the bifurcation point of the spermatic groove). *Micrurus corallinus* differs from *M. paraensis* and *M. pacaraimae* by having red rings of similar length to the black rings or up to 3.5 times their length (*M. paraensis* and *M. pacaraimae* have red rings three to five times longer than the black rings). Finally, *M. corallinus* differs from *M. putumayensis* by having a greater number of BBR in males (14–90) and females (20–83), black tail rings (BTR) in males (5–13) and females (3–9), and a hemipenis extending up to 14 scales in length (*M. putumayensis* has 7–11 BBR in males, 9–12 in females, 2–3 BTR in both sexes, and a hemipenis up to 18 scales in length) (Fig. 5). Additionally, a detailed comparison of morphological characters is presented in Table 5.

Micrurus langsdorffi (Wagler, 1824)
Figs 10–11

Micrurus langsdorffi Wagler, 1824: 10, pl. 2 fig. 2.
Elaps imperator Cope, 1868: 110.
Elaps Batesii Günther, 1868: 428, pl 17–18.
Micrurus mimosus Amaral, 1935: 226, fig. 1.

Elaps Langsdorfi – Jan 1858: 517.
Micrurus langsdorffi – Amaral 1930: 111, 230. – Schmidt 1936: 191.
Micrurus langsdorffi langsdorffi – Roze 1967: 30; 1989: 328. – Peters & Orejas-Miranda 1970: 211.

Diagnosis

Micrurus langsdorffi can be distinguished from all congeners by the unique combination of the following characteristics: (1) body slender; (2) head usually as long as wide (HW/HL = 1.1); (3) dorsal scale rows 15–15–15, smooth, without apical pits; (4) rostral scale triangular, wider than high (RW/RH = 1.8); (5) internasal scales hexagonal, wider than long (INW/INL = 1.4); (6) loreal scale absent; (7) prefrontal scales hexagonal, often slightly longer than wide (PFL/PFW = 0.9); (8) frontal scale single, longer than wide (FL/FW = 1.3); (9) temporal scales 1+1, occasionally 1+2; (10) preocular scale one on each side; (11) postocular scales two on each side, occasionally three; (12) nasal scale divided; (13) supralabial scales seven on each side, with the third and fourth bordering the orbit; (14) infralabial scales seven on each side, the first four in contact with the anterior chin shields, the first pair in contact with each other; (15) preventral scales 1–2; (16) gular scales arranged in 1–3 rows; (17) chin shields in two pairs; (18) symphysial scale longer than wide (ML/MW = 0.5); (19) ventral scales 201–210 (mean 206.2±2.5 SD) in males, 210–219 (mean 222.6±4.3 SD) in females; (20) anal plate divided; supracloacal tubercles absent; (21) subcaudal scales divided, 27–55 (mean 47.8±5.9 SD) in males, 29–37 (mean 33.7±2.5 SD) in females; (22) tail-to-total length ratio 14.4–16.2% (mean 14.8±0.9 SD) in males, 7.8–9.9% (mean 8.7±0.6 SD) in females; (23) teeth: 10–11 dentary, 4 pterygoid, and 6–7 palatine.

Type material

Holotype
BRAZIL – **Amazonas** • 1 ♂; Rio Japurá; 1.811° S, 66.558° W; 1817–1820; J. von Spix leg.; ZSBS 2250/0.

Other material examined (n = 47)
BRAZIL – **Amazonas** • 1 ♀; unknown collection data; IB 5470 • 1 ♂; Rio Japurá; 1.811° S, 66.558° W; 1817–1820; J. von Spix leg.; lectotype of *M. langsdorffi*; ZSM 2250/0 • 1 ♀; Manaus; 3.101° S, 59.901° W; unknown date; J. Bach leg.; BMNH 1897.12.29.17 • 1 ♂; São Paulo de Olivença; 3.467° S, 68.946° W; unknown date; F. Waehner leg.; MTD, IB 32492 • 1 ♂; same locality data as for preceding; 1882; Standigen leg.; NHW 18219.1, 18220.1 • 1 ♀; Solimões, Porto Afonso; 2.735° S, 66.737° W; 1952; A. Hoge leg.; IB 15084 • 1 ♂; Solimões, Tefé; 3.347° S, 64.709° W; unknown date; A. Hoge leg.; IB 15089.

COLOMBIA – **Amazonas** • 1 ♀; Leticia; 4.203° N, 69.935° W; unknown date; unknown collector; MCZ 49006 • 1 ♂; Río Apaporis; 0.770° S, 70.299° W; 1952; J. Cabrera leg.; MCZ 53240. – **Caquetá** • 1 ♀; Puerto Boy; 0.250° N, 74.891° W; H. Nicéforo María leg.; MLS 14. – **Guaviare** • 1 ♀; Miraflores, Río Vaupés; 1.331° N, 71.953° W; 1965; C. Hutchinson leg.; AMNH. – **Putumayo** • 1 ♂; Puerto Rocío, Río Putumayo; unknown date; H. Bassler leg.; AMNH 53139 • 1 ♀; Río Putumayo; 0.2508° N, 74.891° W; 1934; Fray Miguel leg.; holotype of *Elaps mimosus* IB 8902. – **Vaupés** • 2 ♀♀; Río Comeña, afluente margen izquierdo del Río Piraparana; 0.004° S, 70.542° W; 5 Jul. 1976; unknown collector; INS 227, 288.

ECUADOR – **Sucumbíos** • 1 ♀; Limoncocha; 0.408° S, 76.620° W; 20 Oct. 1964; C. Boweri leg.; UIMNH 61033 • 1 ♂; Reserva de Producción Faunística Cuyabeno; 0.004866° S, 76.173° W; 15 Dec. 2014; J. Freire leg.; QCAZ 13129 • 1 ♀; Pacayacu; 0.182° S, 76.072° W; unknown date; M. Yanez leg.; DHMECN 9130.

PERU – **Loreto** • 1 ♂; Iquitos, San Antonio, Río Itaya; 3.745° S, 73.237° W; unknown date; H. Bassler leg.; AMNH 52801 • 1 ♀; Iquitos; 3.743° S, 73.251° W; unknown date; MBUCV 3732 • 5 ♂♂, 8 ♀♀; Iquitos; same collection data as for preceding; H. Bassler leg.; AMNH 52355, 53258, 53872, 54068, 54089, 54195, 54253, 54748, 54944, 54964, 54994, 55007, 55074; paratypes of *M. langsdorffi* • 7 ♂♂, 3 ♀♀; Mishana; 3.928° S, 73.556° W; Mar.–Nov. 1972; P. Soini leg.; TCWC 1513(PS), 42195, 45360, 45361, 46392–46395, 46398, 46400 • 1 ♂, 3 ♀♀; Morropón; 3.723° S, 73.288° W; Jan.–Nov. 1973; P. Soini leg.; TCWC 45359, 46396, 46397, 46399 • 1 ♀; Pebas; 3.321° S, 71.858° W; 1864; C. Hauxwell leg.; holotype of *Elaps batesii* BMNH 1946.1.17.21 • 1 ♀; Pebas; 3.321° S, 71.858° W; 1867; J. Orton leg.; ANSP 6794 • 1 ♀; Río Napo, Río Marañón; 3.452° S, 72.760° W; 1864; J. Orton leg.; type of *Elaps imperator* ANSP 6793.

Description

Coloration. Patterns of coloration were taken from Roze (1996), Campbell & Lamar (2004), and Valencia *et al.* (2016). Tricolor (red/brown–white–yellow) and bicolor (reddish–yellowish) patterns are observed. Dorsal coloration: 25–67 red rings in males and 25–67 in females, usually melanized in adult specimens. Accessory black rings are absent. The nuchal ring is absent; instead, some specimens present a sequence of white dots. Red rings are 3–8 dorsal scale rows long, and ventrally they are 3–6 scales long. Yellow rings are 3–6 dorsal scale rows long, up to twice shorter than red rings, and slightly longer along the vertebral region. Some melanistic individuals have completely dark brown scales within the red rings, causing them to fuse with adjacent white rings. Ventrally, red rings are 4–10 scales long. White spots are 1–1½ dorsal scale rows long, usually formed by sequences of fused or separated spots, and slightly longer towards the ventral region. Ventrally, these rings are one scale long. Head coloration is reddish, orange, or tan; the snout is usually dark but may be tan or yellow, and this coloration often includes the first 2–4 pairs of supralabials, the frontal, supraoculars, postoculars, and parietals. A pair of white spots may be present, usually on the supraoculars or prefrontals, but sometimes also including each internasal, each anterior temporal, and each sixth supralabial. The temporals and posterior 2–3 supralabials are generally red with extensive dark pigmentation. Red rings on the tail number 5–14 in both males and females, with 5–8 dorsal scale rows long and 4–8 scales ventrally. Red rings or bands are 4–9 dorsal scale rows long (Figs 10–11).

Hemipenial morphology. Based on the original descriptions by J. Roze (AMNH 52975, AMNH 54195, AMNH 53140, MCZ 53240). Everted hemipenes are slender, reaching the 14th–18th subcaudals, bifurcated at the 9th–12th, deeply bilobed, and non-capitate. The sulcus spermaticus bifurcates at the base of the lobes, at the level of the 9th–12th subcaudals, and is centripetal, curved, and shallow, with very thin margins bordered by tiny spines. The sulcus branches have a centrifugal medial orientation, extending toward the apex of each lobe. The capitular groove is indistinct. The lobes are elongated (approximately 36% of the total hemipenial length), tapering distally into pointed tips. The distal half of the lobes forms the capitular region, ornamented with small to medium-sized spines densely arranged in longitudinal and irregular rows, decreasing in size toward the apex. The proximal half of the lobes consists of elongated, scattered spines and papillae. The asulcate side bears longer and more numerous spines. The basal region of the hemipenis extends to the 8th–12th subcaudals, with a few minute spines distally, while the rest remains completely naked. The basal pocket is naked and extends along the lateral surface of the hemipenial body; the lateral fold is absent.

Variation. *Micrurus langsdorffi* exhibits polychromatic variation (Soini 1974), which does not appear to follow a geographic pattern. Specimens exhibit monadal and bicolored patterns. The holotype (ZSBS

2250/0) shows the most atypical pattern, with dorsal rings incomplete ventrally. In some specimens, head coloration varies from brown to yellow or orange, with or without a sequence of white spots posterior to the parietal scales. The morphological characteristics of *M. langsdorffi* are summarized in Table 8.

Differential diagnosis

Micrurus langsdorffi shares with other cis-Andean monadal species of the genus *Micrurus* (Table 5, Fig. 5) the following characteristics: number of dorsal scale rows (15–15–15); number of supralabials (7–7, with the 3rd and 4th contacting the eye); number of infralabials (7–7, with the first four contacting the first pair of chin-shield scales); number of preoculars (1–1); number of postoculars (2–2); number of temporals (1+1); two pairs of chin-shields, never in contact with the symphysial; and symphysial scale wider than long; accessory black rings absent. The number of ventral scales in males (201–210) and females (210–219), as well as the number of subcaudal scales in males (27–55) and females (29–37), overlaps the range of all monadal coralsnakes, with the exception of the ventral scales of males in *M. averyi* (190–198). The number of black body rings in males (25–67) and females (29–45) is within the range of most species, except in *M. averyi* (8–10 in males and 10–13 in females), *M. medemi* (17–27 in both sexes), *M. pacaraimae* (23 in males), and *M. putumayensis* (7–11 in males and 9–12 in females). The number of black tail rings in males (5–14) and females (5–8) is within the range of most species, except in *M. putumayensis* (2–3 in both males and females).

Micrurus langsdorffi differs from all other cis-Andean coralsnakes by the absence of black dorsal rings; instead, the dorsal pattern consists of red, yellow, brown, or tan rings (Table 5, Figs 10–11). Additionally, a detailed comparison of morphological characters is provided in Table 5.

Micrurus medemi Roze, 1967
Figs 10–11

Micrurus psyches medemi Roze, 1967: 41, fig. 14.

Micrurus medemi – Roze 1994: 20.

Diagnosis

Micrurus medemi can be distinguished from all congeners by a unique combination of the following characters (diagnosis taken from Roze 1967, 1996; Campbell & Lamar 2004; Caicedo-Portilla & Lynch 2015; Feitosa *et al.* 2015): (1) body slender; (2) head usually as long as wide; (3) dorsal scales smooth, 15/15/15, apical pits absent; (4) rostral scale triangular, wider than high; (5) internasal scales hexagonal, wider than long; (6) loreal scales absent; (7) prefrontal scales hexagonal, one and a half times longer than the internasals; (8) frontal scale hexagonal, longer than wide; (9) temporal scales 1+1, occasionally 1+2; (10) preocular scales one on each side; (11) postocular scales two on each side; (12) nasal scales undivided; (13) supralabial scales seven on each side, with the third and fourth bordering the orbit; (14) infralabial scales, first pair in broad contact behind the symphysial; (15) preventral scales 1–3; (16) gular scales arranged in 1–3 rows; (17) chin-shields in two pairs, never in contact with the symphysial; (18) symphysial scale longer than wide; (19) ventral scales 190–203 in males, 208–221 in females; (20) anal plate divided, supracloacal tubercles absent; (21) subcaudal scales divided, 42–49 in males, 30–37 in females; (22) tail one-third longer in males than in females; (23) teeth: unknown.

Etymology

The specific epithet is a patronym honoring Dr Count Friedrich Johann von Medem, better known among his friends as 'Federico,' a German naturalist who dedicated much of his effort to the study of amphibians and reptiles of Colombia, especially turtles and crocodiles (Roze 1967; Campbell & Lamar 2004).

Type material

Holotype

COLOMBIA – **Meta** • ♂; Villavicencio; 4.1533° N, 73.642° W; 1950; H. Nicéforo María leg.; AMNH 96988.

Paratypes

COLOMBIA – **Meta** • 2 ♂♂, 3 ♀♀; same collection data as for holotype; MLS 1516, 1517, 1513, 1515, 1580 • 1 ♂; same collection data as for holotype; 1951; IB 7208 • 1 ♂; Villavicencio, Río Ocoa; 4.108° N, 73.546° W; Feb. 1950; H. Nicéforo María leg.; MLS 1512 • 1 ♂; Villavicencio, Río Guatequio; 4.153° N, 73.549° W; Feb. 1951; F. Medem leg.; FMNH 74371.

Description

Patterns of coloration were taken from Roze (1967), Roze (1996), and Campbell & Lamar (2004). Tricolor pattern (red–white or yellow–black–white–red).

Dorsal coloration. 17–27 black rings in males and females. Melanized individuals have 40–42 black rings. Accessory black rings are absent. The nuchal black ring is usually 7–12 dorsal scales long, connected or separated from the black hood by one or two dorsal scale rows. Black rings are 4½–11 dorsal scale rows long, ventrally 3–6½ scales long. Red rings are 3½–10 dorsal scale rows long, slightly shorter than black rings, and slightly longer along the vertebral region, with black spots on each scale, except in juveniles. Some melanistic individuals have completely black scales within the red rings, causing them to fuse with adjacent black rings. Ventrally, red rings are 4–11 scales long. White, yellow, or reddish rings are 1–1½ dorsal scale rows long, usually formed by sequences of fused or separated spots, and slightly longer towards the ventral region. Ventrally, these rings are one scale long and may be indistinguishable in some individuals. Head coloration is black, covering the posterior or anterior internasals, prefrontals, frontal, preoculars, postoculars, and parietals. Some individuals show light or reddish spots on the supraoculars or prefrontals. The occipital band is usually yellowish, including the temporals, three supralabials, and one dorsal scale row, each with a black or dark brown border. Black rings on the tail number 6–9 in males and females, with 3–8 dorsal scale rows long and 3–7 scales ventrally. Red rings or bands are 1–3 dorsal scale rows long and 1–3 scales long ventrally (Figs 10–11).

Hemipenial morphology. Unknown.

Variation. Previously defined by Roze (1996) and Campbell & Lamar (2004), and included in the coloration section for this species.

Differential diagnosis

Micrurus medemi shares with other cis-Andean monadal species of the genus *Micrurus* (Table 5, Fig. 5) the following characteristics: number of dorsal scale rows (15–15–15); number of supralabials (7–7, with the 3rd and 4th contacting the eye); number of infralabials (7–7, with the first four contacting the first pair of chin-shield scales); number of preoculars (1–1); number of postoculars (2–2); number of temporals (1+1); two pairs of chin-shields, never in contact with the symphysial; and symphysial scale wider than long. Like other coralsnakes, *M. medemi* exhibits monadal or bicolor patterns, except in *M. averyi*, *M. pacaraimae*, *M. paraensis*, and *M. remotus*, which only have monadal coloration, and only the bicolor pattern is found in *M. margaritiferus* and *M. putumayensis*. Additionally, *M. medemi* lacks accessory black rings, except in *M. sangilensis*. The number of ventral scales in males (190–203) and females (208–221), as well as the number of subcaudal scales in males (42–49) and females (28–40), overlaps the range of all monadal coralsnakes, with the exception of ventral scales in females of *M. putumayensis* (197–232). The number of black body rings (BBR) in males and females (17–27) is within the range of most species, except in *M. averyi* (8–10 in males and 10–13 in females) and *M. putumayensis* (7–11 in

males and 9–12 in females). The number of black tail rings (BTR) in males and females (6–19) is within the range of most species, except in *M. putumayensis* (2–3 in both males and females).

Micrurus medemi is distinguished from other cis-Andean monadal species by having one or more yellow caudal rings containing dorsally diamond-shaped black blotches, starting above the cloaca, as well as by the following characteristics (Table 5, Figs 10–11). Additionally, a detailed comparison of morphological characters is provided in Table 5.

Micrurus ornatissimus (Jan, 1858)
Figs 10–11

Elaps ornatissimus Jan, 1858: 521.
Elaps buckleyi Boulenger, 1896: 416, pl. 22 fig. 1
Elaps steindachneri Werner, 1901: 249.
Micrurus corallinus Dunn, 1923: 186.
Elaps fasslii Werner, 1927: 249.
Micrurus peruvianus Schmidt, 1936: 193.
Micrurus tikuna Feitosa *et al.,* 2015, figs 1–5, 8–9.

Micrurus buckleyi – Amaral 1930: 110, 128.
Micrurus ornatissimus – Schmidt 1936: 191.
Micrurus langsdorffi ornatissimus – Roze 1967: 30.
Micrurus steindachneri petersi – Roze 1967: 45.
Micrurus steindachneri steindachneri – Roze 1967: 43.
Micrurus steindachneri orcesi – Roze 1967: 43.
Micrurus petersi – Roze 1983: 333.

Diagnosis

Micrurus ornatissimus can be distinguished from all congeners by the unique combination of the following characteristics: (1) body slender; (2) head usually as long as wide (HW/HL = 1.0); (3) dorsal scales 15/15/15, smooth, without apical pits; (4) rostral scale triangular, wider than high (RW/RH = 1.6); (5) internasal scales hexagonal, slightly wider than long (INW/INL = 1.1); (6) loreal scales absent; (7) prefrontal scales hexagonal, often slightly wider than long (PFL/PFW = 0.9); (8) frontal scale single, longer than wide (FL/FW = 1.5); (9) temporal scales 1+1; (10) preocular scales one on each side; (11) postocular scales two on each side; (12) nasal scale divided; (13) supralabial scales seven on each side, with the third and fourth bordering the orbit; (14) seven infralabial scales, the first four in contact with anterior chin-shield scales, the first pair in contact with each other; (15) preventral scales 1–3; (16) gular scales arranged in 1–3 rows; (17) chin-shields in two pairs; (18) symphysial scale longer than wide (ML/MW = 0.6); (19) ventral scales 161–225 (mean 202.3±9.7 SD) in males, 156–234 (mean 217.1±14.7 SD) in females; (20) anal plate divided, supracloacal tubercles absent; (21) subcaudal scales divided, 39–54 (mean 47.8±3.0 SD) in males, 28–40 (mean 33.7±5.2 SD) in females; (22) tail-to-total length ratio 10.4–17.4% (mean 14.9±1.4 SD) in males, 7.8–10.9% (mean 9.1±0.7 SD) in females; (23) teeth: 10 dentary, 5 pterygoid, and 7 palatine.

Type material

Syntypes

ECUADOR – **Pastaza** • Canelos; 1.589° S, 77.7465° W; unknown date; C. Buckley leg.; BMNH 1946.1.17.17; holotype of *Elaps buckleyi*.

BRAZIL – **Pará** • Pará; 6.207° S, 52.702° W; unknown date; C. Stevens leg. BMNH 1946.1.17.18; holotype of *Elaps buckley*.

Other material examined (n = 70)

BRAZIL – **Pará** • 1 ♂; Pará; 6.207° S, 52.702° W (wrong locality); unknown date; C. Stevens leg. BMNH 1946.1.17.18; holotype of *Elaps buckleyi*.

ECUADOR – **Morona Santiago** • 1 ♀; 1 mile S of Plan de Milagro on trail to Pan de Azúcar; 3.05° S, 78.483° W; 16 Aug. 1968; J. Peters leg.; USNM 458295; holotype of *M. petersi* • 1 ♂, 1 ♀; Chiguaza; 2.020° S, 77.970° W; unknown date; B. Pazmiño leg.; USNM 232421, 232422 • 1 ♀; Macas; 2.316° S, 78.116° W; 21 Jan. 1929; C. Fugler leg.; MCZ 100950; paratype of *M. petersi* • 1 ♂, 1 ♀; Macas; 2.307° S, 78.113° W; Sep. 1930; A. Feyer leg.; AMNH 28846, ZSM 268/1913 • 2 ♂♂; Macas vicinity; 2.3298° S, 78.131° W; unknown date; A. Feyer leg.; AMNH 35819, 35820 • 1 ♂; Macuma; 2.149° S, 77.701° W; Nov. 1964; unknown collector; UIMNH 61637 • 1 ♀; Mendez; 2.683° S, 78.316° W; unknown date; J. Peters leg.; USNM 232494 • 1 ♂; Sucúa; 2.454° S, 78.167° W; 6 Jan. 1988; O. González leg.; QCAZ 1130 • 1 ♂; Sucúa; 2.466° S, 78.166° W; 1975; unknown collector; USNM 283969 • 3 ♂♂; Taisha, Achuents; 2.203° S, 77.716° W; Aug. 1998–Nov. 2011; D. Holmes leg.; FHGO 2215, 2241, 6358 • 4 ♂♂; Taisha, Amazonas; 2.143° S, 77.709° W; Jul. 2007–Nov. 2011; D. Holmes leg.; FHGO 5624, 5632, 7137, 8997 • 3 ♂♂; Taisha, Kiim; 2.750° S, 77.216° W; May 1994–Jul. 1995; D. Holmes leg.; FHGO 1191, 2241, 2271 • 7 ♂♂; Taisha, Macuma; 2.144° S, 77.700° W; Nov. 2008–Dec. 2011; D. Holmes leg.; FHGO 2210, 3434, 4231, 5938, 7314, 7234, 7235, 8966 • 1 ♂; Taisha, Paantim; 2.133° S, 77.650° W; 2 Jul. 2007; D. Holmes leg.; FHGO 5634 • 1 ♂; Taisha, Tumpaim; 2.154° S, 77.727° W; 20 Jun. 1998; D. Holmes leg.; FHGO 2238 • 1 ♂; Taisha, Uwi; 2.155° S, 77.716° W; 8 Sep. 1999; D. Holmes leg.; FHGO 1999. – **Napo** • 2 ♂♂, 3 ♀♀; Loreto; 0.692° S, 77.311° W; unknown date; C. Mena leg.; USNM OV2687, OV4215, 232426, 232427, 2324241 • 1 ♂; Reserva Biológica Colonso Chalupas; 0.932° S, 77.903° W; 15 Dec. 2011; A. Barahona leg.; FHGO 8843 • 2 ♀♀; Santa Rosa, El Chaco; 0.201° S, 77.690° W; 29 Oct. 2010; C. Reyes leg.; DHMECN 9256, 9255 • 1 ♂; Shiripuno; 1.00° S, 77.083° W; 23 Aug. 1997; J. Touzet leg.; FHGO 1637. – **Orellana** • 2 ♀♀; Tiputini, Kupi; 0.685° S, 76.739° W; 4 Oct. 2008; J. Valencia leg.; FHGO 6371 • 1 ♂; Orellana, Hotel Auca; 0.4716° S, 76.984° W; 25 Feb. 1991; J. Touzet; FHGO 284 • 1 ♀; Parque Nacional Yasuní; 0.674° S, 76.396° W; 27 Jul. 1997; S. Ron leg.; QCAZ 6565 • 1 ♀; Parque Nacional Yasuní, via Pompeya Sur – Iro, km 38; 0.653° S, 76.451° W; 5 Dec. 1994; S. de la Torre leg.; QCAZ 7558 • 1 ♂; Parque Nacional Yasuní; Vía Pompeya Sur – Iro, km 105; 0.967433° S, 76.222° W; 25 Nov. 1994; M. Read; QCAZ 2706 • 1 ♂; Río Suno; 0.616° S, 77.4° W; unknown date and collector; USNM OV54 • 2 ♂♂; Tiputini; 0.667° S, 76.741° W; 1 Oct. 2008; J. Valencia leg.; FHGO 6347, 6357. – **Pastaza** • 1 ♂; Alto Río Bobonaza; 1.466° S, 77.883° W; unknown date; J. Peters leg.; USNM OV4619 • 1 ♂, 1 ♀; Canelos; 1.589° S, 77.7465° W; unknown date; C. Alzamora leg.; USNM OV500, 232434 • 1 ♀; Canelos; 1.589° S, 77.7465° W; unknown date; BMNH 1946.1.17.17; lectotype of *Elaps buckleyi* • 1 ♂; cruce Shell-Mera; 1.5° S, 78.05° W; unknown date and collector; USNM 287944 • 1 ♂; Pukuang; 19 Nov. 2007; D. Holmes leg.; FHGO 6234 • 1 ♀; Río Bufeo, bajo Bobonaza; 2.333° S, 76.667° W; unknown date; J. Olalla leg.; USNM OV4617 • 5 ♀♀; Río Copataza; 1.830° S, 77.670° W; unknown date; J. Olalla leg.; USNM OV4620, 232423, 232430, 232431, 232432 • 4 ♀♀; Río Pastaza; 2.048° S, 77.607° W; unknown date and collector; AMNH 49092, 49095, UMMZ 88917, 88918 • 1 ♀; Río Pastaza, E Ecuador; 2.048° S, 77.607° W; R. Blomberg leg.; NHRM 3163(6) • 1 ♂; Río Villano; 1.500° S, 77.330° W; unknown date; USNM 232435. – **Sucumbíos** • 1 ♀; Limoncocha; 21 Oct. 1964; C. Boweri leg.; UIMNH 61038 • 1 ♂; Limoncocha, Yamanunka; 0.303° S, 76.659° W; Jul. 2007; C. Tobar leg.; DHMECN 9092 • 1 ♀; Río Aguarico, San Pablo de Kantesiya; 11 Jan. 1994; D. Payaguaje leg.; QCAZ 2866. – **Tungurahua** • 1 ♀; cerca de Abitagua; 1.438° S, 78.179° W; unknown date; J. Olalla leg.; USNM OV6077 • 1 ♀; Baños; 1.398° S, 78.429° W; Sep. 1930; paratype of *M. steindachneri orcesi*, AMNH 35881 • 1 ♂; Baños; 1.398° S, 78.429° W; unknown date; holotype of *M. steindachneri*, NHMW 15750 • 2 ♀♀; Baños, Meta trail; 1.398° S, 78.429° W; Sep. 1930; holotype of *M. steindachneri orcesi*,

UMMZ 88922, 88923 • 1 ♂; cerros de Abitagua, 30 km W of Baños; 1.438° S, 78.179° W; unknown date; W. Clarke McIntyre leg.; UMMZ 91566; paratype of *M. steindachneri* • 1 ♂; San José de Chimbo; F. Steindachner leg.; NHMW 13383.1 • 1 ♀; Río Pastaza; 1.414° S, 78.256° W; unknown date; W. Clarke McIntyre leg.; UMMZ 88921; paratype of *M. steindachneri* • 3 ♀♀; San Francisco cerca Baños, Río Pastaza; 1.391° S, 78.408° W; W. Clarke McIntyre leg.; UMMZ 88924, 88925, 88926; paratypes of *M. steindachneri.* – **Unknow locality** • 1 ♂; unknown date of collection; USNM OV • 1 ♀; E Ecuador; unknown date of collection; H. Feyer leg.; ZSM 268/1913, NHRM 3163.

PERU – **Loreto** • 1 ♀; Andoas, Río Pastaza; 2.906° S, 76.397° W; unknown date; H. Feyer leg.; AMNH 49077 • 1 ♀; Puerto Caramacha, lower Río Tigre; unknown date; H. Bassler leg.; AMNH 53202 • 1 ♀; Santa Rosa, Río Tigre; 3.383° S, 74.948° W; unknown date; J. Olalla leg.; AMNH 49169 • 1 ♀; Iquitos, Lago Rimachi; 4.453° S, 76.692° W; 2 Jul. 1957; L. Eyzaguirre leg.; UNMSM 303.

Description

Coloration. Tricolor pattern (red–white or yellow–black–white–red). Dorsal coloration: 15–60 black rings in males (mean 42.1±8.6 SD), 20–67 in females (mean 45.8±12.8 SD). Accessory black rings are absent. The nuchal black ring is rarely absent; when present, its shape is highly variable, appearing as a spot, band, or a complete or incomplete ring (Figs 9–10). The complete black nuchal ring is usually 3–7 dorsal scale rows long and is typically connected to the black hood by one or two dorsal scale rows. Black body rings are 2–2½ dorsal scale rows long, and ventrally they are 1–2 scales long. Red rings are 2–6½ dorsal scale rows long, occasionally nearly twice as wide as the black rings, and slightly longer along the vertebral region, with black spots on each scale, except in juveniles. Some melanistic individuals have completely black scales within the red rings, causing them to fuse with adjacent black rings. Ventrally, red rings are 1½–8 scales long. White or yellow rings are 1–1½ dorsal scale rows long, usually formed by sequences of fused or separated spots, each scale with brown spots on the anterior edge. Ventrally, these rings are one scale long and are indistinguishable in some individuals. Additionally, ventrally, red rings are 2–11 scales long, lacking spots or borders. Head coloration is black, covering the posterior or anterior internasals, prefrontals, frontal, preoculars, postoculars, and parietals. Some individuals may show light or reddish spots on the supraoculars or prefrontals. The occipital band is usually reddish, including the temporals, three supralabials, and one dorsal scale row, and is separated from the first black ring by a sequence of white spots. Tail coloration: black rings on the tail range from 5–17 in males (mean 12.2±2.9 SD) and 2–12 in females (mean 8.2±2.3 SD). These black rings are 2–7 dorsal scale rows long, and ventrally they are 2–6 scales long. Red rings or bands are 1–3 dorsal scale rows long, and ventrally they are 1–3 scales long.

Variation. The substantial individual variation shown by this species in coloration and scutellation is analyzed in this work. *Micrurus ornatissimus* exhibits a typical monadal color pattern (black rings bordered by red or yellow, followed by red rings). The main difference among populations is the length of the red rings, which are usually longer than the black rings. Consistent with the plasticity of these characters, *M. ornatissimus* can be divided into three populations: (1) those associated with the Upper Amazon (UAM), (2) those associated with the inter-Andean Valleys (IAV), and (3) those from the Amazon lowland (AML). Populations from the inter-Andean Valleys and along the eastern Andean slopes overlap in their range of black body ring counts. In some Andean populations, the red rings are heavily marked with black tips (*M. steindachneri* pattern). Furthermore, head coloration in some specimens is grayish (*M. petersi* pattern). In Amazonian rainforest populations, head ornamentation is highly variable. For instance, the nuchal black ring may be absent (*M. tikuna* pattern) or present as a spot, band, or complete/incomplete ring. The geographic variation in the morphological characteristics of *M. ornatissimus* is shown in Table 8.

Differential diagnosis

Micrurus ornatissimus shares with other cis-Andean monadal species of the genus *Micrurus* (Table 5, Fig. 4) the following characteristics: number of dorsal scale rows (15–15–15); number of supralabials (7–7, with the 3rd and 4th contacting the eye); number of infralabials (7–7, with the first four contacting the first pair of chin-shield scales); number of preoculars (1–1); number of postoculars (2–2); number of temporals (1+1); two pairs of chin-shields, never in contact with the symphysial; symphysial scale wider than long; and a hemipenis body without ornamentation. Among the monadal coralsnakes, *M. corallinus*, *M. paraensis*, *M. pacaraimae* and *M. remotus* are the only species that do not exhibit a bicolor dorsal coloration pattern. The number of ventral and subcaudal scales in males and females overlaps with that of all monadal species. Additionally, the number of black body rings (BBR) in males (15–60) and females (20–67) falls within the range of most species, except for *M. averyi* (8–10 in males and 10–13 in females) and *M. putumayensis* (7–11 in males and 9–12 in females). The number of black tail rings (BTR) in males (5–17) and females (2–12) is within the range of all species, except in males of *M. putumayensis* (2–3).

Micrurus ornatissimus is distinguished from other cis-Andean monadal species by the following characteristics (differences in parentheses): *M. ornatissimus* differs from *M. averyi* by having red rings up to three times longer than the black rings, nuchal rings present, distinctive parietal rings, and a greater number of body rings in males (15–60) and females (20–67) (in *M. averyi*, red rings are up to six times longer than the black rings, the head is almost entirely black, and there are no parietal rings or bands; black body rings are 8–10 in males and 10–13 in females). *Micrurus ornatissimus* differs from *M. langsdorffi* in having a typical monadal coloration with a sequence of black–white/yellow–red rings (in *M. langsdorffi*, the dorsal coloration is bicolored or tricolored, with yellow, brown, or maroon rings replacing the black rings). *Micrurus ornatissimus* differs from *M. margaritiferus* in having a typical modal coloration and five pterygoid teeth (in *M. margaritiferus*, the dorsal coloration is bicolor and there are seven pterygoid teeth). *Micrurus ornatissimus* differs from *M. medemi* by the absence of ornamental shapes above the cloaca (in *M. medemi*, one or more of the yellow caudal rings contain diamond-shaped black blotches dorsally, beginning above the cloaca). *Micrurus ornatissimus* differs from *M. corallinus* in having five pterygoid teeth, a smooth surface on the spermatic groove edge, and a surface between lobes ornamented with small spines (in *M. corallinus*, there are four pterygoid teeth, the surface of the spermatic groove edge is smooth with tiny spines, and the surface between lobes is naked). *Micrurus ornatissimus* differs from *M. paraensis* and *M. pacaraimae* in having red rings of similar length to, or up to three times the length of, the black rings (in *M. paraensis* and *M. pacaraimae*, the red rings are three to five times longer than the black rings). Finally, *M. ornatissimus* differs from *M. putumayensis* by a greater number of black body rings (BBR) in males (15–60) and females (20–67), a greater number of black tail rings (BTR) in males (5–17), and a hemipenis body lacking ornamentation (in *M. putumayensis*, BBR is 7–11 in males and 9–12 in females, BTR is 2–3 in males, and the hemipenis body is naked at the base and ornamented with small, dispersed spines). Additionally, a detailed comparison of morphological characters is shown in Fig. 4 and Table 5.

Hemipenial morphology

Based on FHGO 2210 and 9818. Additional data were sourced from Silva-Haad (1994), Feitosa *et al.* (2015), Valencia *et al.* (2016), and the original descriptions by J. Roze (AMNH 52253, UMMZ 88924, 91566, previously identified as *M. steindachneri*). Everted hemipenes are slender, reaching the 11th subcaudal, bifurcated at the 7th, deeply bilobed, and non-capitate. The sulcus spermaticus bifurcates at the base of the lobes, at the level of the 7th subcaudal, and is centripetal, curved, and shallow, with very thin sulcus margins bordered by tiny spines. The sulcus branches have a centrifugal medial orientation, extending toward the apex of each lobe. The capitular groove is indistinct. The lobes are elongated (approximately 42% of total hemipenial length), tapering distally into pointed tips. The distal half of the lobes forms the capitular region, ornamented with small to medium-sized spines densely arranged

in longitudinal and irregular fringes, which decrease in size toward the apex. The proximal half of the lobes consists of a series of elongated, scattered spines. The asulcate side has longer and more numerous spines. The basal region of the hemipenis extends to the 7th subcaudal, with a few minute spines distally, while the rest remains completely naked. The basal pocket is naked and extends along the lateral surface of the hemipenial body (Fig. 11).

Discussion

Our results, obtained through the review of different lines of evidence, suggest that morphology-based taxonomy has overestimated species boundaries in monadal coralsnakes. Consequently, the generally conservative nature and overlap in traditional meristic and scalation characters within monadal *Micrurus* species needs the inclusion of additional features in taxonomic studies. For instance, although color pattern has been considered a valuable taxonomic character in *Micrurus* (e.g., Di Bernardo 2007; Pires *et al.* 2014; Feitosa *et al.* 2015; Bernarde *et al.* 2018), our study demonstrates that species exhibit considerable plasticity in coloration.

Genetic diversity

The uneven success in amplifying degraded DNA templates underscores the challenges frequently encountered when working with historical or poorly preserved specimens, which may limit the completeness of multilocus datasets. Despite these limitations, our results provide important insights into the genetic diversity of *Micrurus* species. The markedly higher nucleotide diversity observed in *cytb* and *ND4* is consistent with the generally faster evolutionary rate of mitochondrial genes relative to nuclear loci. Both genes are protein-coding regions of the mitochondrial genome known to accumulate substitutions more rapidly, enhancing their utility for detecting recent population differentiation and phylogeographic structure. This is consistent with prior studies demonstrating the utility of *cytb* and *ND4* in phylogenetic and phylogeographic analyses of reptiles, including coralsnakes (e.g., Jowers *et al.* 2019). In contrast, the low diversity values observed in the nuclear markers *NT3* and in the ribosomal gene *16S* reflect their slower substitution rates and higher evolutionary constraints. These differences in variability among loci support the combined use of mitochondrial and nuclear genes to capture both recent and deeper evolutionary signals within *Micrurus* lineages (Townsend *et al.* 2008).

Despite the low variation observed in these markers, the presence of both homozygous and heterozygous genotypes in the *NT3* dataset add valuable genetic resolution. The inclusion of these data still holds potential for improving species delimitation frameworks through multilocus approaches. Overall, the observed genetic variation across loci highlights the importance of carefully selecting markers based on their evolutionary rates and specific research objectives, as well as the utility of incorporating nuclear markers, even those with lower variation, alongside mitochondrial data to gain a more comprehensive understanding of species boundaries and evolutionary history.

Phylogenetic relationships

Over the past two decades, integrative taxonomy has significantly enhanced the quality and reproducibility of species characterization by employing a comprehensive framework that integrates diverse data types and methodologies to delimit and describe taxa (Dayrat 2005; Will *et al.* 2005). For certain species groups, relying solely on morphological traits is insufficient to accurately recognize and delineate species boundaries (Carstens *et al.* 2013). Furthermore, identifying sister or cryptic species requires additional lines of evidence, such as molecular data, ecological niche modeling, morphometrics, haplotype networks, and biogeographic approximations (Dayrat 2005; Pires & Marinoni 2010; Schlick-Steiner *et al.* 2010; Peterson & Soberón 2012; Vences *et al.* 2024). For instance, taxonomic research on the genus *Micrurus* has historically been challenging due to the large number of described species and

subspecies, many of which remain poorly defined. In many cases, these taxa are known only from type specimens (e.g., *M. petersi*, *M. pacaraimae*, *M. tikuna*) or a very limited number of specimens (e.g., *M. boicora* Bernarde, Turci, Abegg & Franco, 2018, *M. diana* Roze, 1983, *M. nattereri* Schmidt, 1952). This complexity is compounded by the fact that interspecific color patterns in *Micrurus* tend to be both conservative and highly variable (Campbell & Lamar 2004), which has historically misled taxonomists, even when relatively large sample sizes are available (e.g., Reyes-Velasco *et al.* 2020).

Our phylogenetic analyses, based on both nuclear and mitochondrial loci, revealed low levels of genetic divergence among *Micrurus* species from the eastern slopes of the Andes in South America. Low genetic divergence was observed among *M. albicinctus*, *M. corallinus* and *M. annellatus annellatus*, *M. a. balzani* and *M. bolivianus* (sensu Da Silva *et al.* 2021), as well as among *M. ornatissimus*, *M. peruvianus*, *M. steindachneri* and *M. tikuna*. Based on these results and our species delimitation analyses, we propose the recognition of four major lineages: (1) *M. corallinus*, with *M. albicinctus* and *M. annellatus* complex as junior synonyms; (2) *M. ornatissimus*, with *M. peruvianus*, *M. steindachneri* and *M. tikuna* as junior synonyms; and (3) The distinctiveness of *M. langsdorffi* and *M. medemi* as evolutionary lineages warrants its recognition as a separate species (Fig. 1).

Our phylogeny includes a sample of the problematic specimen MPEG20348 (field series LJV6756) from the Ituxi River, Amazonas, Brazil. This specimen was previously identified as *Micrurus remotus* by Campbell & Lamar (2004: plate 170). Because the specimen was never examined firsthand, its identification relied exclusively on the coloration depicted in the photograph, leading to an unsupported extension of the known range of *M. remotus* into the Brazilian Amazon, specifically in the southern portion of Amazonas State. This contrasts with previous publications (e.g., Roze 1989, 1996), which restricted the species to the portion of the Guiana Shield near the border region of Brazil, Colombia and Venezuela. The specimen has also been identified as *M. langsdorffi*, although its coloration differs markedly from that species. Other coralsnake species occurring in the Ituxi River region include *M. hemprichii* and *M. spixii*, both of which belong triadal group. In fact, specimen MPEG20348 closely resembles specimens of *M. annellatus* with typical monadal pattern, and its presence in the area probably represents one of the few known Brazilian populations of this species distributed south of the Amazon River.

We also included the sequence of *Micrurus corallinus* CPEB 051 (GenBank accession AF228424), obtained from Jurujuba, Niterói, Rio de Janeiro, Brazil. This old sequence was generated from an early clone in *Escherichia coli* (da Silva & Sites 1999) which can introduce artificial mutations, such as point mutations, insertions, or deletions, not present in the natural genome. We identified these artifacts were subsequently identified and removed through manual alignment. Although we included this sequence to determine its phylogenetic position relative to other *M. corallinus* samples, particularly those from Paraguay, we did not use it for further analyses because its reliability is compromised by the cloning-induced changes. In fact, inclusion of this sequence tends to artificially inflate *p*-distance values among other *M. corallinus* samples.

The bPTP and ASAP support the species delimitation proposed in this work. However, within the *Micrurus corallinus* low support values suggest that the genetic differentiation observed more likely represents intraspecific variation rather than interspecific divergence, supporting the recognition of *M. corallinus* as a single species. Overall, the limited resolution provided by this single-locus dataset indicates that the results should be interpreted cautiously and complemented with morphological and multilocus evidence.

The haplotype networks reveal a marked contrast between mitochondrial and nuclear markers. Mitochondrial genes (*16S*, *ND4*, *cytb*) consistently recovered two deeply divergent and non-overlapping

lineages: one composed exclusively of *Micrurus corallinus*, and another containing all haplotypes of *M. langsdorffi*, *M. medemi* and *M. ornatissimus*. The latter form a single, compact cluster connected by few mutational steps, indicating shallow mitochondrial differentiation and a shared evolutionary history among these nominal taxa. In contrast, *M. corallinus* forms a clearly independent mitochondrial lineage separated by multiple mutational steps, consistent with long-term geographic isolation south of the Amazon River.

Nuclear markers show the opposite pattern. *NT3* exhibits a star-like topology with a central haplotype shared by all three taxa and peripheral variants differing by only 0–3 mutational steps, reflecting minimal nuclear divergence. The lack of structure in the nuclear dataset suggests extensive allele sharing among *Micrurus corallinus*, *M. medemi* and *M. ornatissimus*, attributable to incomplete lineage sorting, recent divergence, or historically large effective population sizes, conditions that commonly delay nuclear differentiation in coralsnakes (M. Jowers pers. comm.).

Morphology

We hypothesize that coloration appears stable throughout ontogeny; however, multiple distinct color patterns may arise and change over time as individuals adapt to environmental conditions and ecological interactions. Although in this study we analyzed four species exhibiting color polymorphism, a phenomenon in which a species displays discrete color morphs that can be distinguished from one another, polymorphism is also evident in other monadal coralsnakes, such as *Micrurus dumerilii* (Schmidt 1954; Roze 1996; Campbell & Lamar 2004; Harvey *et al.* 2003). One of the most striking examples of this phenomenon is the polymorphic ground snake species *Atractus elaps* (Günther, 1858) from the Amazon region (Savage 1960), which can display uniform coloration with small bands or spots, black bands arranged in dyads, monads, or tetrads, as well as longitudinal red bands that vary in length from very short to large (Savage 1960; Dixon *et al.* 1976; Arteaga *et al.* 2024). Some individuals exhibit both banded and longitudinal patterns (Savage 1960; Arteaga *et al.* 2024).

On the other hand, hemipenial morphology and osteology have proven to be valuable sources of information in systematic studies, even in groups that exhibit highly conservative external morphology (e.g., Slowinski 1995; Passos & Fernandes 2005; Nascimento *et al.* 2019). Both character sets are useful for disentangling the *Micrurus* species complex; however, they remain underexplored, probably due to the scarcity of specimens available for several species and the technical difficulties involved in everting hemipenes, which is particularly challenging in monadal coralsnakes because of the fragility of their structures and ornaments. Some authors have suggested that hemipenial morphology in *Micrurus* is highly conserved (e.g., Slowinski 1995; Roze 1996; Feitosa *et al.* 2007). In contrast, we found subtle differences between *M. corallinus* and *M. ornatissimus*, for instance in the length of the basal pocket and the presence or absence of a fold on the body of the everted hemipenis, traits highlighted by Feitosa (2006) for *M. albicinctus* and for a specimen erroneously identified as *M. langsdorffi* (MPEG 18235), as well as by Valencia *et al.* (2016) for *M. ornatissimus*. The specimen MPEG 18235 is identified as *M. corallinus* under the current taxonomic arrangement. In any case, we recommend a thorough evaluation of geographic and elevational variation in hemipenial morphology across widely distributed species such as *M. corallinus*, *M. langsdorffi* and *M. ornatissimus*, as this approach may reveal additional interspecific differences that have so far gone unnoticed.

Aside from a few South American *Micrurus* species, osteological studies have focused primarily on tooth counts and have been based on a limited number of specimens (e.g., Passos & Fernandes 2005; Feitosa *et al.* 2007). A more comprehensive osteological analysis is therefore needed for the genus *Micrurus*, as tooth count differences among species show considerable overlap or remain unknown for some taxa, such as *M. medemi*. Expanding these analyses to include additional *Micrurus* species would be highly valuable for identifying diagnostic cranial features and assessing the extent of morphological variation

within the genus. A broader comparative framework could reveal previously overlooked characters that contribute to a better understanding of species boundaries and phylogenetic relationships in *Micrurus*.

Distinguishing monadal coralsnake species has proven challenging due to the morphological plasticity observed in the group. Whenever possible, we identified externally visible diagnostic traits recognizable through direct observation. However, in several cases, reliable distinguishing features are restricted to hemipenial morphology in males or differences in tooth counts. For example, identifying diagnostic traits for *M. medemi* has been particularly difficult, as this species is poorly represented in biological collections and available data are largely limited to coloration and scalation patterns, which overlap with those of several congeners. In contrast, *M. langsdorffi* can be readily distinguished from other monadal coralsnakes by its remarkable coloration.

Spatial and environmental delimitation

The distribution patterns of *Micrurus corallinus*, *M. ornatissimus* and *M. medemi* reveal clear ecological differentiation, primarily driven by temperature-related bioclimatic variables. While *M. corallinus* and *M. ornatissimus* occupy broad, largely non-overlapping ranges in the Atlantic Forest and Amazon regions, respectively, *M. corallinus* also includes marginal records in the Cerrado biome. In contrast, *M. medemi* is restricted to montane forests of eastern Colombia, likely reflecting a narrower thermal tolerance and specialization to cooler, more stable environments. Ecological differences between *M. ornatissimus* and *M. langsdorffi* appear minimal, as their ranges broadly overlap across the Amazon Basin, with the main distinction arising from the presence of *M. ornatissimus* populations in the Andean foothills.

Although *Micrurus corallinus*, *M. langsdorffi* and *M. ornatissimus* inhabit broadly similar biomes within the Amazonian domain and adjacent foothill environments, the discriminant analysis reveals that *M. corallinus* and the other two species occupy distinct environmental niches, primarily differentiated by thermal and precipitation variables. The first discriminant function (LD_1), dominated by temperature-related variables such as mean annual temperature and temperature seasonality, effectively separates *M. corallinus* from *M. langsdorffi* and *M. ornatissimus*, but does not distinguish between the latter two, which are mainly associated with precipitation variables. *Micrurus corallinus* is associated with warmer and more thermally stable environments typical of the lowland Amazon and Atlantic Forest, whereas *M. langsdorffi* and *M. ornatissimus* occur in slightly cooler and more thermally variable regions situated between the Amazon and Negro rivers. The second discriminant axis (LD_2), influenced mainly by precipitation of the driest quarter and annual precipitation, suggests that *M. langsdorffi* and *M. ornatissimus* tolerate more seasonal or moderately drier conditions compared to *M. corallinus*, which is restricted to consistently humid forests. This pattern implies that even within similar biomes, these species are ecologically segregated along fine-scale climatic gradients. Such microclimatic differentiation may represent adaptive responses to distinct hydrological and thermal regimes on opposite sides of major Amazonian rivers or across elevation transitions at the Andean interface. These findings reinforce that riverine and topographic barriers not only shaped historical allopatry between *M. corallinus* and the pair *M. langsdorffi–M. ornatissimus*, but also contributed to maintaining ecological divergence through climatic specialization. This supports previous hypotheses that temperature and moisture gradients act as strong ecological filters for Amazonian herpetofauna (Santos *et al.* 2020; Guayasamin *et al.* 2024), sustaining niche partitioning even among closely related coralsnake species.

Terribile *et al.* (2021) analyzed the distribution patterns of Brazilian and southern South American coralsnakes using macroecological models (MEMs) and ENMs, identifying the highest species richness in the Amazon biome, with 8.3 to 14 species predicted in central Amazonia. However, under the current taxonomic revisions proposed in this study, the estimated species richness is substantially reduced. The authors note that ENMs tend to overpredict species richness by assuming that all climatically suitable areas can be occupied, overlooking ecological and historical constraints. Conversely, underpredictions

may arise from insufficient sampling in regions such as the Amazon. Despite these limitations, the congruence between predicted and observed patterns (i.e., documented species records) supports the role of climate as a major driver of coralsnake distribution (Terribile *et al.* 2021). These findings contrast with global studies that emphasize evolutionary history as the main predictor of elapid diversity, underscoring the importance of 'deconstructive' approaches that focus on ecologically and evolutionarily cohesive groups (e.g., Terribile *et al.* 2009).

ENMs identify geographic regions where environmental conditions are suitable for the occurrence of a species (Peterson & Soberón 2012). However, in the case of coralsnakes, ENMs likely indicate areas with environmental conditions that support species interactions with other fauna for specific behaviors (e.g., predation, foraging, courtship, male-male combat, copulation) within the necessary time frames for these activities. Notably, coralsnakes appear to be closely associated with leaf-cutter ants and termite nests. Due to the unique structure, size, and construction of ant and termite mounds, these microhabitats can provide suitable conditions for various ecological functions in reptiles, including serving as breeding sites with stable temperature and humidity (Knapp & Owens 2008; Vaz-Ferreira *et al.* 1970), foraging grounds and food resources (Gandolfi & Rocha 1996; Flemming & Loveridge 2003), and refuges for temporary or permanent shelter (Duleba & Ferreira 2014).

Although observations of specialized interactions involving coralsnakes within these microhabitats are not recent, they remain poorly studied. Dunn (1954) documented records of coralsnakes found inside anthills in Panama. Vaz-Ferreira *et al.* (1970, 1974) reported interactions of *Micrurus frontalis* (Duméril, Bibron & Duméril, 1854) with *Acromyrmex* Mayr, 1865 leaf-cutter ants in Uruguay. Similarly, Moreira *et al.* (2009) and Duleba & Ferreira (2014) reported individuals of *M. frontalis* inside underground termite mounds in Mato Grosso do Sul and Goiás, Brazil, respectively. We have observed similar interactions with leaf-cutter ants in *M. apiatus* (Jan, 1858), *M. elegans* (Jan, 1858), and *M. tener* (Baird & Girard, 1853) in Mexico and Guatemala, and in *M. nigrocinctus* (Girard, 1854) across Central America. Additionally, in the central Amazon region of Ecuador, we observed these interactions with unidentified ants in *M. helleri* Schmidt & Schmidt, 1925, *M. ornatissimus* (Jan, 1858), *M. narduccii* (Jan, 1863), and *M. obscurus* (Jan, 1872). It is likely that other species exhibit similar behaviors, but further research is needed to confirm this. Ants and termites tolerate the presence of coralsnakes in their nests without exhibiting aggressive behavior, which may serve as a strategy to deter predatory reptiles, such as worm lizards (Duellman 1978) or blindsnakes (Martins & Oliveira 1998; Kley & Brainerd 1999; Cundall & Greene 2000; Kley 2001; Mizuno & Kojima 2015), which prey on ants and termites but are, in turn, part of the diet of coralsnakes.

Furthermore, coralsnakes likely utilize these nests as shelters and for egg protection, similar to other documented interactions with ants and termites (Criddle 1937; Carpenter 1953; Vaz-Ferreira *et al.* 1970, 1974; Pisani 2009; Nagy *et al.* 2017). If these interactions are widespread among coralsnake species, developing predictive models based on nest microenvironments may be highly complex, as these environments feature distinct thermoregulatory systems and microclimates compared to the surrounding forest. These social insects maintain specialized thermoregulation systems, resulting in internal microclimates with restricted temperature and humidity ranges (Jones & Oldroyd 2006). It is still premature to fully understand the impact that the use of refuges may have on the conservation of Amazonian coralsnakes. However, in the context of climate change, shifts in soil moisture could alter the populations of other fossorial prey species, such as amphisbaenians and caecilians, which would likely affect coralsnakes, as snakes in general are highly dependent on prey density (Shine & Madsen 1997). These fine-scale interactions highlight limitations in correlative models and emphasize the need for ecological detail, particularly for poorly known species. Addressing these gaps is essential to overcoming Wallacean shortfalls and improving conservation strategies for elusive taxa like coralsnakes (Hortal *et al.* 2015; Terribile *et al.* 2018).

Although *Micrurus corallinus*, *M. langsdorffi*, and *M. ornatissimus* inhabit broadly similar biomes within the Amazonian domain and adjacent foothill environments, discriminant analysis reveals that *M. corallinus* and the other two species occupy distinct environmental niches, primarily differentiated by thermal and precipitation variables. The first discriminant function (LD_1), dominated by temperature-related variables such as mean annual temperature and temperature seasonality, effectively separates *M. corallinus* from *M. langsdorffi* and *M. ornatissimus*, but does not distinguish between the latter two, which are mainly associated with precipitation variables. *Micrurus corallinus* is associated with warmer and more thermally stable environments typical of the lowland Amazon and Atlantic Forest, whereas *M. langsdorffi* and *M. ornatissimus* occur in slightly cooler and more thermally variable regions situated between the Amazon and Negro rivers.

The second discriminant axis (LD_2), influenced mainly by precipitation of the driest quarter and annual precipitation, suggests that *M. langsdorffi* and *M. ornatissimus* tolerate more seasonal or moderately drier conditions compared to *M. corallinus*, which is restricted to consistently humid forests. This pattern implies that even within broadly similar biomes, these species are ecologically segregated along finescale climatic gradients. Such microclimatic differentiation may represent adaptive responses to distinct hydrological and thermal regimes on opposite sides of major Amazonian rivers or across elevational transitions at the Andean interface. These findings reinforce that riverine and topographic barriers not only shaped historical allopatry between *M. corallinus* and the pair *M. langsdorffi–M. ornatissimus*, but also contributed to maintaining ecological divergence through climatic specialization. This supports previous hypotheses that temperature and moisture gradients act as strong ecological filters for Amazonian herpetofauna, sustaining niche partitioning even among closely related coralsnake species (e.g., Terribile *et al.* 2009; Terribile *et al.* 2021).

Micrurus ornatissimus is widely distributed in the Amazon region of Ecuador (throughout the Amazonian provinces), Peru (northern Loreto Department), Colombia (Amazonas, Guainía, Putumayo, and Vaupés departments), and Brazil (a small portion of Amazonas State), between the Amazon and Negro rivers. In addition, populations of *M. ornatissimus* extend into montane and cloud forests along the Andean slopes, including the sub-Andean Cordilleras del Cóndor and Kutukú. *Micrurus ornatissimus* is sympatric with *M. langsdorffi* in the Amazonian lowlands of Ecuador, Colombia, Brazil, and Peru; it is also sympatric with *M. margaritiferus* in Santa Rosa, Cajamarca, Peru (Koch *et al.* 2018), and probably with *M. putumayensis* in the vicinity of Iquitos, Peru.

The ENM projections reveal an extensive area along the eastern foothills of the Colombian Andes where environmental conditions appear suitable for the occurrence of *M. medemi* populations. At the southern limit of the predicted distribution, specifically within the Department of Caquetá, there is a potential area of overlap with *M. langsdorffi* and *M. ornatissimus*, although confirmed records of *M. medemi* remain restricted to the vicinity of Villavicencio. A wide area of overlap between *M. langsdorffi* and *M. ornatissimus* occurs in the Amazon region of Colombia, Ecuador, and Peru. Meanwhile, in the northern most Peruvian Andes, within the Marañón Valley, particularly near Santa Rosa, Department of Cajamarca, environmentally suitable conditions suggest a potential zone of sympatry between *M. corallinus* and *M. ornatissimus*. Nevertheless, current records indicate that both species occur on opposite sides of the Marañón River.

The distributional patterns of *Micrurus corallinus*, *M. langsdorffi* and *M. ornatissimus* suggest a case of allopatry between the three species. *M. langsdorffi* and *M. ornatissimus* occur in the region between the Negro and Amazon rivers, whereas *M. corallinus* is distributed south of the Amazon River, across the central and southeastern portions of South America. On the other hand, another monadal coralsnake, *M. psyches*, inhabits the northern portion of the South America, above the Negro River. The geographic

ranges of these three species do not overlap, and their distribution limits appear to be strongly associated with major Amazonian rivers.

This pattern is consistent with Wallace's river-barrier hypothesis, which proposes that large rivers in Amazonia act as effective biogeographic barriers, promoting genetic divergence and speciation by limiting dispersal among populations on opposite riverbanks (Wallace 1852; Ayres & Clutton-Brock 1992; Gascon *et al.* 2000). This mechanism has been well documented in a wide variety of taxa, including primates, birds, frogs, and butterflies (e.g., Ávila-Pires 1995; Peres *et al.* 1996; Lougheed *et al.* 1999; Gascon *et al.* 2000; Patton *et al.* 1994; Hayes & Sewlal 2004; Fernandes *et al.* 2013; Fernandes *et al.* 2014). In snakes, such barriers may play a particularly important role in the diversification of *Micrurus*, given their generally low dispersal capacity and strong habitat specificity (Da Silva & Sites 1999). Therefore, the allopatric distribution of *M. corallinus*, *M. langsdorffi–M. ornatissimus*, and *M. psyches* may represent an evolutionary outcome of historical riverine barriers in the Amazon Basin.

Micrurus corallinus, *M. langsdorffi* and *M. ornatissimus* are classified as Least Concern (LC) according to IUCN criteria (IUCN 2024), based on the number of records across South America. We recommend maintaining this classification, as our revised taxonomic evaluation has significantly expanded the known extent of occurrence for both species. Additionally, these species are present in most protected areas within the countries where they have been reported. In contrast, *Micrurus medemi* is the only species classified as Critically Endangered (CR) due to the limited number of recorded specimens and the restricted sampling within its known range. Endemic to Colombia, it is currently the only monadal coralsnake known to inhabit the Municipality of Villavicencio. Its distribution covers approximately 140 km² within an estimated 27 000 km² of suitable habitat. However, it remains unclear whether this distribution gap reflects a true absence or is merely an artifact of sampling bias. Given its restricted range, we consider that *M. medemi* faces a high risk of population decline. Without the implementation of a targeted conservation program, its populations are likely to decrease rapidly.

Taxonomy

The taxonomic history of monadal coralsnakes within the genus *Micrurus* has been marked by persistent ambiguity and instability, primarily due to the high degree of morphological convergence, intraspecific variation, and the limited availability of type material in early descriptions. We revisit and chronologically synthesize the complex taxonomic history of the *Micrurus corallinus*, *M. langsdorffi*, and *M. medemi* lineages, three species that have long posed challenges to systematists due to overlapping diagnostic characters and wide geographic distributions across distinct South American biomes. By examining historical taxonomic treatments, synonymies, and subsequent redefinitions of these taxa, we contextualize the evolution of their current classification and clarify the sources of confusion that have historically obscured their species boundaries.

Micrurus corallinus

Micrurus corallinus has a long and complex taxonomic history, largely due to the overestimation of morphological plasticity or conservatism in earlier classifications. The type species, *Elaps corallinus*, was described over 200 years ago from Rio de Janeiro, Cabo Frio, Brazil (Merrem 1820). In the same year, and using the same type specimen, Wied-Neuwied (1820) also described the species under the name *Elaps corallinus*. However, Merrem's (1820) original proposal was subsequently cited by several authors (e.g., Duméril & Bibron 1854; Boulenger 1896; Jan 1858; Günther 1859). Although Boulenger (1896) included, under the name *E. corallinus*, several other monadal coralsnakes (e.g., *E. ornatissimus* Jan, 1858, *E. bocourti* Jan, 1858 and *E. circinalis* Cope, 1876), likely due to similarities in color pattern, this interpretation was not accepted by other herpetologists of the time. Since its original description, the taxonomic interpretation of *M. corallinus* has undergone several revisions that revealed morphological

variation within the species (e.g., Amaral, 1925; Roze, 1967, 1989, 1996; Campbell & Lamar, 2004) and ultimately restricted its distribution to the Atlantic Forest of Brazil.

The taxonomic history of *Micrurus annellatus* reveals persistent morphological overlap and color variation across Andean and sub-Andean populations in Peru and Bolivia. *Elaps annellatus* was described by Peters (1871) from Pozuzo, Peru (ZMB 7185), and *E. balzani* by Boulenger (1898) from Yungas, Bolivia, both based on black-and-yellow bicolored specimens. *Elaps regularis* was later described by Boulenger (1902) from Chulumani, Bolivia (BMNH 1946.1.17.22), and the type of *E. balzani* is now apparently lost. Schmidt (1954) was the first to propose subspecies within the complex, describing *M. annellatus montanus* from Puno, Peru (FMNH 40221), and distinguishing it from *M. a. annellatus* by the presence of red rings and the length of the parietals. Roze (1967) adopted this classification, incorporated *M. balzani* into the complex without explanation, and described *M. a. bolivianus* from Chuquisaca, Bolivia (ZMH 2706e). Later, Roze (1983) synonymized *M. a. montanus* with *M. a. annellatus*, noting overlap in the diagnostic characters used by Schmidt. Roze (1996) maintained three subspecies: *M. a. annellatus*, *M. a. bolivianus*, and *M. a. balzani*, based mainly on the number of postoculars, although Harvey *et al.* (2003) demonstrated that this trait is polymorphic and unreliable for diagnosis. They also observed that tricolored (black–white–red) patterns occur mainly at higher elevations, whereas bicolored (black–yellow) forms dominate in the lowlands.

Bernarde *et al.* (2012) reported *Micrurus annellatus bolivianus* from the state of Acre, representing both the first record of this taxon in Acre and the only subspecies of the *M. annellatus* complex previously known from Brazil, where it had been recorded exclusively in Amazonas (Hoge & Romano 1969). These authors also documented additional records of *M. a. annellatus*, likewise from Acre. More recently, Da Silva *et al.* (2021) proposed substantial taxonomic changes in monadal coralsnakes affecting several Brazilian species. Among these, they elevated the Brazilian subspecies of the *M. annellatus* complex to full species rank, although they did not provide new data or evidence supporting this taxonomic proposal. Furthermore, and contrary to the interpretation of Bernarde *et al.* (2012), Da Silva *et al.* (2021) restricted *M. bolivianus* to Acre while expanding the distribution of *M. annellatus* to include both Amazonas and Acre. We were unable to identify any evidence supporting these taxonomic changes, which would also imply modifications to the known distributions of the members of the *M. annellatus* group. In any case, our phylogeny includes samples representing all color-pattern variants described for this complex, and based on these results, we propose the synonymy of all members of the *M. annellatus* complex with *M. corallinus*.

Specimens assigned to *M. annellatus* exhibit considerable chromatic variability, including black-and-white, red-and-white, and the typical monadal black–white–red pattern. Such variation indicates that dorsal coloration in this lineage is highly labile and may vary geographically across populations inhabiting the eastern Andean slopes of Peru. Along the eastern foothills of the Andes, dorsal bicolored and monadal patterns appear to intergrade geographically, suggesting that these phenotypes likely represent intraspecific variation rather than discrete taxonomic units. Thus, specimens assigned to *Micrurus annellatus* exhibit marked chromatic variability, including black–white, red–white, and the typical monadal black–white–red dorsal patterns. This diversity indicates that dorsal coloration in this lineage is highly labile and varies geographically among populations inhabiting the eastern slopes of the Andes in Peru. Across the Andean foothills, bicolored and monadal patterns appear to intergrade geographically, suggesting that these phenotypes most likely represent intraspecific variation rather than discrete taxonomic entities. For this reason, in our phylogenetic analyses we associated each sample with the taxon to which it had been previously assigned based on coloration, even though the spatial distribution of these chromatic variants does not strictly correspond to the currently recognized taxonomic distributions.

Micrurus albicinctus has also presented significant taxonomic challenges (Cunha & Nascimento 1991). The species was originally described by Amaral (1926) from the northern region of the former state of Mato Grosso, now part of Rondônia, Brazil. Subsequently, Meise (1938) described *M. waehnerorum* from Paulo de Olivença, Amazonas, Brazil. However, without providing a formal justification, Roze (1967) synonymized *M. waehnerorum* with *M. albicinctus*. Later, Cunha and Nascimento (1982) argued that both *M. albicinctus* and *M. waehnerorum* should be synonymized with *M. ornatissimus*, citing shared morphological variation. This decision, however, generated controversy, and the same authors later acknowledged (Cunha & Nascimento 1991) that their initial conclusion had been based solely on the examination of the holotype of *M. albicinctus*. Consequently, they revalidated both *M. albicinctus* and *M. waehnerorum*, despite not demonstrating clear differences in coloration or morphology. Finally, Roze (1996) once again placed *M. waehnerorum* as a synonym of *M. albicinctus*.

On the other hand, we hypothesize that *M. corallinus* may be closely related to *M. paraensis* due to their geographic proximity (Figs 5, 8) and similarities in hemipenial morphology. However, we acknowledge that the evolutionary relationships within this group remain poorly understood; due to the lack of genetic data for *M. paraensis*, its precise phylogenetic position remains unresolved. Nevertheless, Aird *et al.* (2017) provided venomic and transcriptomic evidence suggesting a close evolutionary relationship between *M. paraensis* and *M. corallinus*.

We also infer the following scenarios based on the distribution of *M. paraensis*, *M. corallinus*, and *M. langsdorffi*: (1) *M. paraensis* represents a distinct species, likely phylogenetically related to *M. corallinus*, and widely distributed in the Brazilian Amazon, where neither *M. corallinus* nor *M. ornatissimus* have been reported; (2) alternatively, *M. paraensis* may correspond to a population of *M. corallinus* inhabiting the central-northern Amazon of Brazil, considering the high morphological plasticity and the similarities in hemipenial morphology observed in *M. corallinus*; (3) the least likely scenario is that *M. paraensis* represents a population of the polymorphic *M. ornatissimus*. The only notable similarity observed between these two species is the variation in the presence or absence of a nuchal band.

Micrurus langsdorffi

Elaps langsdorffi was described by Wagler (1824) from Japurá, Brazil. Among the morphological traits common to coralsnakes, he identified an additional feature that stood out: the presence of small fangs, suggesting that this characteristic placed the species closer to the genus *Micrurus* than to *Elaps*, in which the fangs were assumed to be more prominent. In the same work, Wagler also proposed the genus *Micrurus* to describe *M. spixii*. Currently, *Micrurus* is accepted as the Official Generic Name No. 2144 according to ICZN Opinion 1201, and *M. spixii* is recognized as the type species by monotypy (Campbell & Lamar 2004). However, *E. langsdorffi* was subsequently reassigned to the genus *Micrurus*. The holotype of *M. langsdorffi* (ZSBS 2250/0) exhibits one of the most atypical coloration patterns observed in coralsnakes: the dark and pale brown rings are incomplete, absent on the venter, or may fade years after preservation. Over time, additional specimens of *M. langsdorffi* were collected from various Amazonian localities, leading to the identification of three main morphological variants. These variants were described as separate species: *M. imperator* (Cope, 1868) from the Río Napo, Peru; *M. batesi* (Günther, 1868) from Pebas, northeastern Peru; and *M. mimosus* (Amaral, 1935) from the Río Putumayo, Colombia.

Chromatic variation has likely represented one of the major challenges in the taxonomy of *Micrurus langsdorffi*. The species exhibits marked polychromatism, a condition extensively examined by Soini (1974) and Cunha & Nascimento (1982). However, the occurrence of a bicolored pattern (black and white) was not considered part of the intraspecific variation, as suggested by some authors (e.g., Cunha & Nascimento 1982, 1991; Campbell & Lamar 2004). Detailed examination of specimens reveals that

some individuals display red rings heavily invaded by black pigmentation. In fact, previous authors did not report any specimens exhibiting fully black rings for this species and suggested that such records likely correspond to *M. ornatissimus*.

Micrurus medemi

Micrurus medemi and *M. ornatissimus* are sister species, together forming a clade. *Micrurus medemi* is a coralsnake endemic to Colombia, restricted to the Municipality of Villavicencio (Roze 1967, 1996; Campbell & Lamar 2004). Since its description (Roze 1967), few specimens have been deposited in biological collections, and consequently, there is limited information in the literature (e.g., Roze 1996; Campbell & Lamar 2004; Caicedo-Portilla & Lynch 2015; Montoya-Cruz *et al.* 2021, 2022). This scarcity has generated significant gaps in taxonomic knowledge, including osteology and hemipenial morphology, which are critical for delimiting species within the monadal *Micrurus*, as well as in ecological and biogeographic data. In the Municipality of Villavicencio, *M. medemi* is sympatric with *M. mipartitus*; both species exhibit bicolored dorsal patterns, but *M. mipartitus* can be distinguished by having black and orange rings on the tail and an orange parietal ring.

Small bicolored specimens of *Micrurus medemi* could be confused with *M. spurrelli* (Boulenger, 1914), the senior synonym of *M. nicefori*, from the Colombian Chocó. Schmidt (1955) described *Micrurus nicefori* from a single specimen (MLS571), a juvenile male characterized by a high ventral scale count (244 scales) and numerous alternating black and light rings (52 black body rings). This specimen was obtained by Niceforo María (1942) and was previously assigned to the *M. mipartitus* complex. Roze (1967) questioned the validity of its diagnostic characters and recommended placing it in the synonymy of *M. spurrelli*, due to the remarkable similarities between the two species. We have not had the opportunity to reexamine the specimen in question, but its allocation is reasonably certain based on its description and the fact that additional specimens with these characteristics have not been reported from Villavicencio. Unfortunately, the specimen is lost (J.S. Cárdenas, pers. comm.), so its identity cannot be reconfirmed.

Micrurus ornatissimus

Elaps ornatissimus was described by Jan (1858), with the holotype originally deposited in the Museo di Storia Naturale di Milano, Italy (MSNM), and the type locality cited as "Mexico, Amérique Centrale," which was clearly erroneous, since the species is actually distributed in the Amazon region. Subsequently, *Elaps buckleyi* was described by Boulenger (1896) based on specimens from Canelos, Ecuador and Pará, Brazil. The holotype of *E. ornatissimus* was destroyed during World War II (Roze, 1996). Consequently, Roze (1996) designated specimens BMNH 1946.1.17.17 and BMNH 1946.1.17.18, originally part of the *E. buckleyi* type series, as syntypes of *M. ornatissimus*. Schmidt (1955) later restricted the type locality of *E. ornatissimus* to the Río Putumayo region in Colombia, whereas Cunha and Nascimento (1982) suggested Ecuador or Peru as more plausible origins. Roze (1967) considered *M. ornatissimus* and *M. langsdorffi* as subspecies within the *M. langsdorffi* complex. Furthermore, Cunha and Nascimento (1982) excluded Pará, Brazil, from the distribution of *M. ornatissimus*, a taxonomic interpretation that remains widely accepted (Nogueira *et al.* 2019).

Micrurus peruvianus was originally described by Roze (1967) from Perico, Cajamarca, in the inter-Andean valleys of northern Peru. Subsequently, Kuch and Ayala-Varela (2002) reported the species from Ecuador for the first time, based on a specimen collected near Zumba, in Zamora Chinchipe Province. Valencia *et al.* (2016) later proposed the synonymy of *M. peruvianus* with the polymorphic *M. ornatissimus*, although this reclassification has not been universally accepted. Our phylogenetic results, however, support this taxonomic interpretation. Koch *et al.* (2018) reported several specimens referable to *M. peruvianus* along the Marañón River, within the departments of Amazonas and Cajamarca. In the same region, near the confluence of the Santiago and Marañón Rivers, lies the

type locality of *M. margaritiferus*. Although these two nominal species have not been documented in sympatry, suitable habitat continuity along the Marañón River suggests a potential contact zone where their distributions may overlap. This, in turn, raises the possibility of a close phylogenetic relationship between *M. peruvianus* and *M. margaritiferus*, although the precise position of the latter within *Micrurus* remains unresolved. Records of *M. margaritiferus* from Ecuador (Valencia 2007), previously interpreted as representing a monadal dorsal pattern variant of *M. ornatissimus* (Campbell & Lamar 2004), were reassigned by Valencia *et al.* (2016) to *M. ornatissimus*, following phylogenetic evidence that included specimens exhibiting the same coloration pattern.

Feitosa *et al.* (2015) described *Micrurus tikuna* from the Amazonian regions of Brazil and Colombia, restricting its occurrence to the type localities of Tabatinga, Amazonas, Brazil, and Leticia, Colombia. Morphologically, *M. tikuna* is remarkably similar to *M. ornatissimus*, differing only in two reported features: a lower number of black rings and the absence of a nuchal collar. However, our results indicate that these traits fall within the range of intraspecific variation observed in *M. ornatissimus*. A specimen from Leticia, Colombia (M556), included in our phylogenetic analysis, lacks a nuchal collar and bears 28 black body rings, corresponding precisely to the characteristics attributed to *M. tikuna*. Furthermore, Ecuadorian populations of *M. ornatissimus* exhibit marked variation in the presence, absence, and morphology of the nuchal collar (Valencia *et al.* 2016, Fig. 13), with some specimens completely lacking the collar (FHGO 2210) or showing it as a small or large spot (QCAZ 477; FHGO 939, 1920, 2238, 5624, 5633). Notably, in a captive clutch from a gravid female (FHGO 8966), four of the five hatchlings displayed a complete nuchal ring, while one presented only a large black spot (Valencia *et al.* 2016), further demonstrating the plasticity of this character. Additionally, although Roze (1996) and Campbell & Lamar (2004) reported that *M. ornatissimus* possesses 38–67 black body rings, Jan (1858) noted only 32 in the holotype of *Elaps ornatissimus*, and we examined another specimen (EPN 4621) with 33 black dorsal rings. Taken together, these data show that the diagnostic traits used to distinguish *M. tikuna* are encompassed by the morphological variability of *M. ornatissimus*. Consequently, we regard *M. tikuna* as a junior synonym of *M. ornatissimus*.

Finally, *Elaps steindachneri* was originally described by Werner (1901) based on a single specimen (NMW 15750) from Ecuador. Subsequently, Werner (1927) described *Elaps fasslii* from "Colombia," designating the same specimen (NMW 15750) as the holotype. This was evidently a nomenclatural error, as the specimen had previously been reported from Ecuador, and no verified records of *M. steindachneri* are known from Colombia. Subsequently, Schmidt (1936) erroneously included *M. steindachneri* within a broader concept of *M. langsdorffi*, together with *M. annellatus*, although this arrangement was not universally accepted.

Roze (1967) revised the taxonomic status of populations of *M. steindachneri*, recognizing two distinct subspecies: *M. s. steindachneri* and *M. s. orcesi*. The latter was based on a holotype (UMMZ 88922) collected along the Meta Trail near Baños, Tungurahua Province, Ecuador. In the same publication, Roze (1967) also described *Micrurus steindachneri petersi* (holotype USNM 158295) from "one mile south of Plan de Milagro on the trail to Pan de Azúcar, Morona-Santiago Province, Ecuador." This taxon was later elevated to full species rank as *Micrurus petersi* by Roze (1983), based on additional morphological evidence. Valencia *et al.* (2016) conducted a comprehensive revision of specimens previously referred to the *M. steindachneri* complex from Ecuador and concluded that all morphological characters used to separate the nominal subspecies, or to distinguish *M. petersi* as an independent lineage, overlap extensively among specimens. The pale grayish coloration on the head, considered diagnostic for *M. petersi*, was also observed in other *M. steindachneri* specimens and may represent either a preservation artifact or an atypical color variation. Consequently, although tissue samples of *M. petersi* are not available to determine its phylogenetic position or evolutionary relationships, we also regard *M. petersi* as a junior synonym.

Conclusions

Our integrative analyses combining phylogenetic, haplotype, morphological, and biogeographic evidence reveal four well-supported lineages within monadal coralsnakes, with *M. medemi*, *M. langsdorffi*, and *M. ornatissimus* forming a strongly supported sister-group relationship. Low intraspecific genetic divergence across lineages indicates that several previously recognized taxa, including *M. albicinctus*, *M. annellatus*, *M. peruvianus*, *M. steindachneri*, *M. tikuna* and *M. petersi*, are best regarded as junior synonyms of *M. corallinus* or *M. langsdorffi*. Furthermore, the geographic distributions of *M. corallinus* and *M. ornatissimus* are broader than previously documented, spanning Amazonian lowlands, Andean slopes, and sub-Andean forests, with pronounced dorsal color-pattern variation across populations.

These findings underscore the limitations of relying exclusively on morphological traits for species delimitation in monadal coralsnakes, where characters such as nuchal collars or ring counts exhibit considerable plasticity. By integrating molecular, morphological, and spatial data, this study provides a robust framework for clarifying species boundaries and evolutionary relationships. Such an approach not only resolves longstanding taxonomic ambiguities but also strengthens the foundation for accurate biogeographic and conservation assessments of these elusive South American coralsnakes.

Acknowledgments

We are deeply grateful to all the museum curators and collection managers who allowed us to examine specimens under their care: F.T. Burbrink (AMNH), N. Gilmore (ANSP), D. Gower (BMNH), A. Almendáriz and M. Guerra (EPN), M. Barragán (FHGO), M. Yánez-Muñoz and M. Urgilés (INABIO), David Salazar-Valenzuela (MZUTI), P. Passos (MNRJ), H. Grillischt (NHM), I. Ineich (NMHN), F. Ayala-Varela (QCAZ), and C. Franklin and G. Pandelis (UTA), as well as Paul Székely and Pablo Loaiza (UTPL). C.J. Franklin and G. Pandelis kindly assisted with incoming and outgoing loans from other

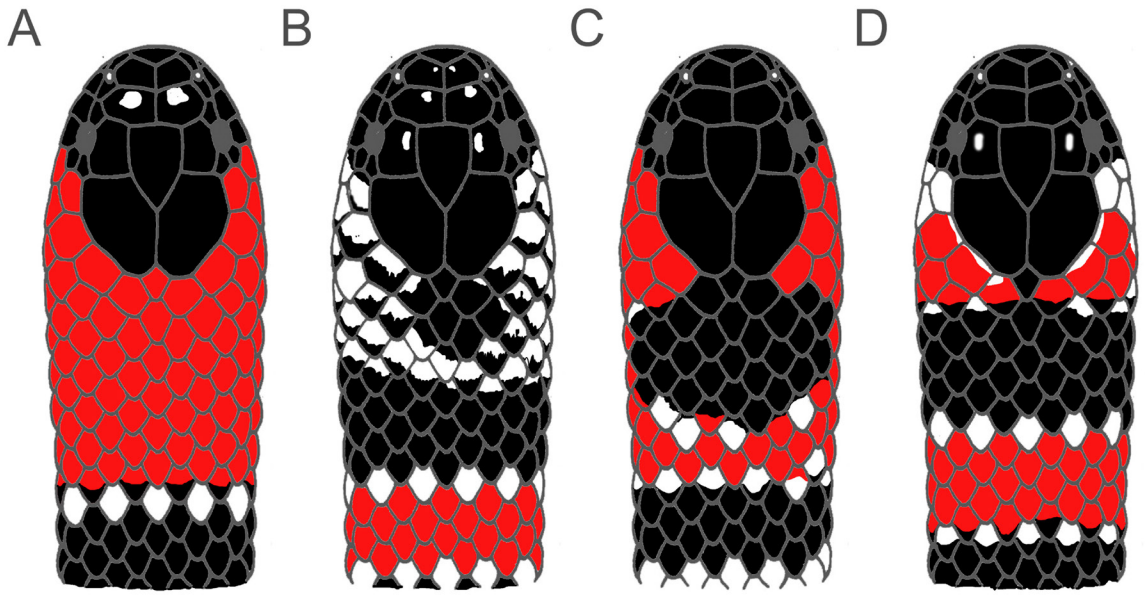

Fig. 13. Variation in the nuchal ring on the head of *Micrurus ornatissimus* (Jan, 1858) sensu stricto. **A**. Absent (MPEG 19199). **B**. Present as a spot (QCAZ 477). **C**. Present as a band or incomplete ring (FHGO 8837). **D**. Present as a complete ring (FHGO 8837). Illustrations by J.H. Valencia.

institutions, making specimens available for our examination at UTA. We are indebted to C. Jaramillo and R. Ibañez (STRI, Círculo Herpetológico de Panamá); R. Murphy, A. Lathrop, and R. MacCulloch (Royal Ontario Museum, Ontario); W.E. Duellman (University of Kansas Biodiversity Institute, Lawrence); Laurie Vitt (University of Oklahoma, via NSF grants DEB-9200779 and DEB-9505518); C.C. Austin and D.L. Dittman (Museum of Natural Science, Louisiana State University); R.W. McDiarmid and S.W. Gotte (Smithsonian Institution, Washington, D.C.); and J.C. Murphy (Field Museum, Science and Education) for providing tissue samples. For laboratory assistance, we thank K. Apunte, E. Dalgo, N. Espinosa de los Monteros, K. Quizphi, G. Reyes-Ortega, H. Stevenson, L. Tipantiza, and M. Vanderborucke. We are also grateful to A. Arteaga, L. Y. Echevarría, D. Holmes, P. Passos, P. Pinna, A.L.C. Prudente, J. Roze, M. Cardoso, and L. Vonnahme for providing photographs. This manuscript was significantly improved by the comments of J.A. Campbell, L. Fadda, K. Garzon-Tello, J.M. Herrera-Lopera, D. Holmes, W. W. Lamar and J. Pablo-Cea. Laboratory work was conducted at several institutions: the Instituto de Biología of the Universidad de Antioquia; the University of Central Florida, where T.A. Castoe generated numerous sequences; the University of Texas at Arlington, where U. Smart, G.C. Sarker, and E. Wostl kindly generated difficult DNA sequences; and the Universidad Regional Amazónica Ikiam, Ecuador. J. Valencia's visits to the UTA and Ikiam laboratories were supported by fellowships from the Secretaría de Ciencia, Humanidades, Tecnología e Innovación (SECIHTI, México), the Instituto de Ecología, A.C., México, and the University of Texas at Arlington, USA. J.H. Valencia's doctoral research is supported by SECIHTI, Mexico, under grant No. 109985. This paper is also based in part upon work supported by the National Science Foundation (grant no. DEB-0416160 to ENS) and the Instituto Bioclon (grant to ENS).

Author contributions

Conceived and designed the analyses: JHV, HMOA, ENS, WQ. Performed the analyses: JHV, HMOA, WQ, BS, ENS. Analyzed the data: JHV, HMOA, AEM, PJV, BS, ENS. Contributed reagents/materials/analysis tools: JHV, HMOA, WQ, OTC, ALN, BS, ENS. Wrote the paper: JHV, HMOA, AEM, OTC, PJV, ENS. Field and museum sampling: JHV, JCA, JCC, OTC, PJV, ENS.

Conflicts of interest

The authors declare that they have no known competing financial interests or personal relationships that could have appeared to influence the work reported in this paper.

References

Aiello-Lammens M.E., Boria R.A., Radosavljevic A., Vilela B. & Anderson R.P. 2015. spThin: an R package for spatial thinning of species occurrence records for use in ecological niche models. *Ecography* 38 (5): 541–545. https://doi.org/10.1111/ecog.01132

Aird S.D., da Silva Jr N.J., Qiu L., Villar-Briones A., Saddi V.A., Pires de Campos M., Grau M.L. & Mikheyev A.S. 2017. Coralsnake venomics: analyses of venom gland transcriptomes and proteomes of six Brazilian taxa. *Toxins* 9 (6): 1–64. https://doi.org/10.3390/toxins9060187

Alkishe A., Cobos M.E., Peterson A.T. & Samy A.M. 2020. Recognizing sources of uncertainty in disease vector ecological niche models: An example with the tick *Rhipicephalus sanguineus sensu lato*. *Perspectives in Ecology and Conservation*, 18 (2): 91–102. https://doi.org/10.1016/j.pecon.2020.03.002

Amaral A. 1925. South American snakes in the collection of the United States National Museum. *Proceedings of the United States National Museum* 67: 1–30.

Amaral A. 1926. Ophidios de Mato Grosso. (Contribuição II para o conhecimento dos ophidios do Brasil). Commissão de Linhas Telegraphicas Estrategicas de Matto Grosso ao Amazonas. História Natural, Zoologia 84: 1–29.

Amaral A. 1930. Lista remissiva dos ophidios da regiao neotropica. *Memorias do Instituto Butantan* 4: 129–271.

Amaral A. 1935. Estudos sobre ophidos neotropicos. XXXIII. Novas especies de ophidios da Colombia. *Memorias do Instituto Butantan* 4: 219–223.

Anderson R.P., Lew D. & Peterson A.T. 2003. Evaluating predictive models of species' distributions: criteria for selecting optimal models. *Ecological Modelling* 162: 211–232. https://doi.org/10.1016/S0304-3800(02)00349-6

Arevalo E., Davis S.K. & Sites Jr J.W. 1994. Mitochondrial DNA sequence divergence and phylogenetic relationships among eight chromosome races of the *Sceloporus grammicus* complex (Phrynosomatidae) in central Mexico. *Systematic Biology* 43 (3): 387–418. https://doi.org/10.1093/sysbio/43.3.387

Arteaga A., Bustamante L. & Vieira J. 2024. *Reptiles of Ecuador*. Khamai Foundation & Tropical Herping. Quito, Ecuador.

Avila-Pires T.C. 1995. Lizards of brazilian Amazonia (Reptilia: Squamata). *Zoologische Verhandelingen* 299: 1–706.

Ayres J.M. & Clutton-Brock T.H. 1992. River boundaries and species range size in Amazonian primates. *American Naturalist* 140: 531–537.

Barve N., Barve V., Jiménez-Valverde A., Lira-Noriega A., Maher S.P., Peterson A.T., Soberón J. & Villalobos F. 2011. The crucial role of the accessible area in ecological niche modeling and species distribution modeling. *Ecological Modelling* 222 (11): 1810–1819. https://doi.org/10.1016/j.ecolmodel.2011.02.011

Bernarde P.S., Batista L.C., Diesel A. & Franco L. F. 2018. A remarkable new species of coralsnake of the *Micrurus hemprichii* species group from the Brazilian Amazon. *Salamandra* 54 (4): 249–258.

Bernt M., Donath A., Jühling F., Externbrink F., Florentz C., Fritzsch G., Pütz J., Middendorf M. & Stadler P. F. 2013. MITOS: improved de novo metazoan mitochondrial genome annotation. *Molecular Phylogenetics and Evolution* 69 (2): 313–319. https://doi.org/10.1016/j.ympev.2012.08.023

Bickford D., Lohman D.J., Sodhi N.S., Ng P.K., Meier R., Winker K., Ingram K.K. & Das I. 2007. Cryptic species as a window on diversity and conservation. *Trends in Ecology and Evolution* 22 (3): 148–155. https://doi.org/10.1016/j.tree.2006.11.004

Booth T.H. 2021. A problem with variable selection in a comparison of correlative and process-based species distribution models: Comments on Higgins *et al.*, 2020. *Ecology and Evolution* 11 (19): 13609–13612. https://doi.org/10.1002/ece3.7496

Boulenger G.A. 1898. A list of the reptiles and batrachians collected by the late Prof. L. Balzan in Bolivia. *Annali del Museo Civico di Storia Naturale di Genova* (2) 19: 128–133

Boulenger G.A. 1896. Catalogue of the Snakes in the British Museum. Trustees of the British Museum (Natural History), London.

Boulenger G.A. 1902. Descriptions of new batrachians and reptiles from the Andes of Peru and Bolivia. *The Annals and Magazine of Natural History* (7) 10 (59): 394–402

Brauner N. & Shacham M. 1998. Role of range and precision of the independent variable in regression of data. *AIChE Journal* 44 (3): 603–611. https://doi.org/10.1002/aic.690440311

Caicedo-Portilla J.R. & Lynch J.D. 2015. Coral de Villavincencio. *Micrurus medemi* Roze, 1967. *In*: Morales-Betancourt M.A., Lasso C.A., Páez V.P. & Bock B.C. (eds) *Libro Rojo de Reptiles de Colombia*: 98–100. Instituto de Investigación de Recursos Biológicos Alexander von Humboldt, Universidad de Antioquia, Bogotá.

Campbell J.A. & Lamar W.W. 2004. *The Venomous Reptiles of the Western Hemisphere. Vol. 1*. Comstock Publishing Associates. Ithaca, New York.

Carpenter C.C. 1953. A study of hibernacula and hibernating associations of snakes and amphibians in Michigan. *Ecology* 34 (1): 74–80.

Carstens B.C., Pelletier T.A., Reid N.M. & Satler J.D. 2013. How to fail at species delimitation. *Molecular Ecology* 22 (17): 4369–4383. https://doi.org/10.1111/mec.12413

Castoe T.A., Streicher J.W., Meik J.M., Ingrasci M.J., Poole A.W., de Koning A.P.J., Campbell J.A., Parkinson C.L., Smith E.N. & Pollock D.D. 2012. Thousands of microsatellite loci from the venomous coralsnake (*Micrurus fulvius*) and variability of select loci across populations and related species. *Molecular Ecology Resources* 12 (6): 1105–13. https://doi.org/10.1111/1755-0998.12000

Cobos M.E., Jiménez L., Nuñez-Penichet C., Romero-Alvarez D. & Simões M. 2018. Sample data and training modules for cleaning biodiversity information. *Biodiversity Informatics* 13: 49–50. https://doi.org/10.17161/bi.v13i0.7600

Cobos M.E., Peterson A.T., Osorio-Olvera L. & Jiménez-García D. 2019a. An exhaustive analysis of heuristic methods for variable selection in ecological niche modeling and species distribution modeling. *Ecological Informatics* 53: 100983. https://doi.org/10.1016/j.ecoinf.2019.100983

Cobos M.E., Peterson A.T., Barve N. & Osorio-Olvera L. 2019b. kuenm: an R package for detailed development of ecological niche models using Maxent. *PeerJ* 7:e6281. https://doi.org/10.7717/peerj.6281

Cope E.D. 1868. An examination of the Reptilia and Batrachia obtained by the Orton expedition to Equador and the Upper Amazon, with notes on other species. *Proceedings of the Academy of Natural Sciences of Philadelphia* 20: 94–140.

Criddle S. 1937. Snakes from an ant hill. *Copeia* 1937 (2): 142–142.

Cundall D. & Greene H.W. 2000 Feeding in snakes. *In*: Schwenk K. (ed.) Feeding: Form, Function and Evolution in Tetrapod Vertebrates: 293–333. Academic Press, London.

Cunha O.R.D. & Nascimento F.P.D. 1982. Ofídios da Amazônia: XVII-Revalidação de *Micrurus ornatissimus* (Jan, 1958) diferenciada de *M. langsdorffi* (Wagler, 1824) e distribuição geográfica das duas espécies (Ophidia: Elapidae). *Boletim do Museu Paraense Emílio Goeldi. Nova Série Zoologia* 116: 1–17.

Cunha O.R.D. & Nascimento F.P.D. 1991. Ofídios da Amazônia. XXII: Revalidação e redescrição de *Micrurus albicinctus* Amaral, de Rondônia, e sobre a validade de *Micrurus waehrerorum* Meise, do Amazonas (Ophidia: Elapidae). *Boletim do Museu Paraense Emílio Goeldi. Nova Série Zoologia* 7 (1): 43–52.

Da Silva Jr N.J. & Sites Jr J.W. 1999. Revision of the *Micrurus frontalis* complex (Serpentes: Elapidae). *Herpetological Monographs*: 142–194.

Da Silva Jr. N.J., Buononato M.A. & Feitosa D. 2016. As cobras-corais do Novo Mundo. Biologia, taxonomia, venenos e envenenamentos. *In*: Da Silva Jr N.J. (ed.) *As cobras-corais do Brasil*: 47–78. Editora da Pontifícia Universidade Católica da Goiás. Goiânia, Brazil.

Da Silva Jr. N.J., Feitosa D.T., Pires G.M. & Prudente A.L.C. 2021. Coralsnake diversity in Brazil. Chapter 5. *In*: Da Silva Jr. N.J, Porras L., Aird S. & Prudente A.L.C (eds) *Advances in Coralsnake Biology with an Emphasis on South America*: 201–251. Eagle Mountain Publishing. Utah, USA.

Dayrat B. 2005. Towards integrative taxonomy. *Biological Journal of the Linnean Society* 85 (3): 407–417. https://doi.org/10.1111/j.1095-8312.2005.00503.x

de Queiroz K.S. 2007. Species concepts and species delimitation. *Systematic Biology* 56 (6): 879–886. https://doi.org/10.1080/10635150701701083

DeSalle R., Egan M.G. & Siddall M. 2005. The unholy trinity: taxonomy, species delimitation and DNA barcoding. *Philosophical Transactions of the Royal Society B: Biological sciences* 360 (1462): 1905–1916. https://doi.org/10.1098%2Frstb.2005.1722

Di Bernardo M., Borges-Martins M. & Silva Jr N.J. 2007. A new species of coralsnake (*Micrurus*: Elapidae) from southern Brazil. *Zootaxa* 1447 (1): 1–26. https://doi.org/10.11646/zootaxa.1447.1.1

Dixon J.R., Thomas R.A. & Greene H.W. 1976. Status of the neotropical snake *Rhabdosoma poeppigi* Jan, with notes on variation in *Atractus elaps* (Günther). *Herpetologica* 32 (2): 221–227.

Dowling H.G. & Savage J.M. 1960. A guide to the snake hemipenis: a survey of basic structure and systematic characters. *Zoologica* 45: 17–28. https://doi.org/10.5962/p.203350

Duellman W.E. 1978. The biology of an equatorial herpetofauna in Amazonian Ecuador. *Miscellaneous Publication. Museum of Natural History, University of Kansas* 65: 1–352.

Duleba S. & Ferreira V.L. 2014. Herpetofauna associated with termite mounds in a pasture, Mato Grosso do Sul State, Brazil. *Herpetological Bulletin* 127: 10–16.

Duméril A.M.C., Bibron G. & Duméril A.H.A. 1854. *Erpetologie generale ou, Histoire naturelle complète des reptiles*. Librairie Encyclopedique de Roret, vol. 7. Paris.

Dunn E.R. 1923. Some snakes from North Western Peru. *Proceedings of the Biological Society of Washington* 36: 185–188.

Dunn E.R. 1954. The Coral Snake "Mimic" Problem in Panamá. *Evolution* 8: 97–102.

Escobar L.E., Lira-Noriega A., Medina-Vogel G. & Peterson A. 2014. Potential for spread of the white-nose fungus (*Pseudogymnoascus destructans*) in the Americas: Use of Maxent and NicheA to assure strict model transference. *Geospatial Health* 9 (1): 221–229. https://doi.org/10.4081/gh.2014.19

Feitosa D.T. 2006. *Morfologia hemipeniana de 11 espécies do gênero Micrurus Wagler, 1824 na Amazônia Brasileira, com redescrição de Micrurus filiformis (Günther, 1859) e Micrurus paraensis Cunha & Nascimento, 1973 (Serpentes, Elapidae)*. MSc thesis. Universidad Federal do Pará. Brazil.

Feitosa D.T., Prudente A.L.C. & Lima A.C. 2007. Redescription and variation of *Micrurus paraensis* Cunha & Nascimento 1973 (Serpentes: Elapidae). *Zootaxa* 1470 (1): 35–46. https://doi.org/10.11646/zootaxa.1470.1.2

Feitosa D.T., Da Silva Jr. N.J., Pires M.G., Zaher H. & Pudente A.L. 2015. A new species of the monadal coral snake of the genus *Micrurus* (Serpentes, Elapidae) from western Amazon. *Zootaxa* 3974 (4): 538–554. https://doi.org/10.11646/zootaxa.3974.4.5

Fernandes A.M., Gonzalez J., Wink M. & Aleixo A. 2013. Multilocus phylogeography of the Wedge-billed Woodcreeper *Glyphorynchus spirurus* (Aves, Furnariidae) in lowland Amazonia: Widespread cryptic diversity and paraphyly reveal a complex diversification pattern. *Molecular Phylogenetics and Evolution* 66 (1): 270–282. https://doi.org/10.1016/j.ympev.2012.09.033

Fernandes A.M., Cohn-Haft M., Hrbek T. & Farias I.P. 2014. Rivers acting as barriers for bird dispersal in the Amazon. *Revista Brasileira de Ornitologia* 22 (4): 363–373. https://doi.org/10.1007/BF03544273

Fick S.E. & Hijmans R.J. 2017. WorldClim 2: new 1 km spatial resolution climate surfaces for global land areas. *International Journal of Climatology* 37 (12): 4302–4315. https://doi.org/10.1002/joc.5086

Flemming P.A. & Loveridge J.P. 2003. Miombo woodland termite mounds: resource islands for small vertebrates? *Journal of the Zoological Society of London* 259: 161–168. https://doi.org/10.1017/S0952836902003084

Frateles L.E., Tavares G., Nakamura G., da Silva Jr. N., Terribile L. & Diniz-Filho J. 2025. The interaction between the Linnean and Darwinian shortfalls affects our understanding of the evolutionary dynamics driving diversity patterns of New World coralsnakes. *Journal of Biogeography* 52(1): 42–54. https://doi.org/10.1111/jbi.15014

Gandolfi S.M. & Rocha C.F. 1998. Orientation of thermoregulating *Tropidurus torquatus* (Sauria: Tropiduridae) on termite mounds in an open area of south-eastern Brazil. *Amphibia-Reptilia* 19: 319–323.

Gascon C., Malcolm J.R., Patton J.L., da Silva M.N., Bogart J.P., Lougheed S.C., Peres C.A., Neckel S. & Boag P.T. 2000. Riverine barriers and the geographic distribution of Amazonian species. *Proceedings of the National Academy of Sciences of the United States of America* 97: 1367213677. https://doi.org/10.1073/pnas.230136397

Grismer L.L., Wood Jr P.L., Le M.D., Quah E.S. & Grismer J.L. 2020. Evolution of habitat preference in 243 species of Bent-toed geckos (Genus *Cyrtodactylus* Gray, 1827) with a discussion of karst habitat conservation. *Ecology and Evolution* 10 (24): 13717–13730. https://doi.org/10.1002/ece3.6961

Guayasamin J.M., Ribas C.C., Carnaval A.C., Carrillo J.D., Hoorn C., Lohmann L.G., Riff D., Ulloa C. & Albert J.S. 2024. Evolution of Amazonian biodiversity: A review. *Acta Amazonica* 54: e54bc21360.

Guisan A., Edwards Jr T.C. & Hastie T. 2002. Generalized linear and generalized additive models in studies of species distributions: setting the scene. *Ecological Modelling* 157 (2–3): 89–100. https://doi.org/10.1016/S0304-3800(02)00204-1

Günther A. 1868. Sixth account of new species of snakes in the collection of the British Museum. *Annals and Magazine Natural History* 1: 413–429. https://doi.org/10.1080/00222936808695725

Gutberlet Jr R.L. & Harvey M.B. 2004. The evolution of New World venomous snakes. *In*: Campbell W.L. & Lamar W.W. (eds) *The Venomous Reptiles of the Western Hemisphere, Vol.* 2: 634–682. Comstock Pub. Associates. Ithaca, New York.

Harvey M.B., Aparicio J. & Gonzalez L. 2003. Revision of the venomous snakes of Bolivia: Part 1. The coralsnakes (Elapidae: *Micrurus*). *Annals of the Carnegie Museum 72*: 1–52. https://doi.org/10.5962/p.215087

Hayes F. E. & Sewlal J.A. 2004. The Amazon River as a dispersal barrier to passerine birds: effects of river width, habitat and taxonomy. *Journal of Biogeography* 31 (11): 1809–1818.

Hoang D.T., Chernomor O., Von Haeseler A., Minh B.Q. & Vinh L.S. 2018. UFBoot2: improving the ultrafast bootstrap approximation. *Molecular Biology and Evolution* 35 (2): 518–522. https://doi.org/10.1093/molbev/msx281

Hoge A.R. & Romano S.A. 1969. Espécies registradas para o Brasil (Serpentes). *Ciência e Cultura* 21(2): 454.

Hortal J., de Bello F., Diniz-Filho J.A., Lewinsohn T.M., Lobo J.M. & Ladle R.J. 2015. Seven shortfalls that beset large-scale knowledge of biodiversity. *Annual Review of Ecology*, *Evolution, and Systematics* 46: 523–549. https://doi.org/10.1146/annurev-ecolsys-112414-054400

Hurtado J.P., Ramirez M.V., Gómez F.J.R., Fouquet A. & Fritz U. 2021. Multilocus phylogeny clarifies relationships and diversity within the *Micrurus lemniscatus* complex (Serpentes: Elapidae). *Salamandra* 57 (2): 229–239.

IUCN. 2024. The IUCN Red List of Threatened Species. Ver. 2024-2. Available from https://www.iucnredlist.org [accessed 6 Dec. 2024].

Jan G. 1858. Plan d'une iconographie descriptive des ophidiens et description sommaire de nouvelles espèces de serpents. *Revue et Magasin de Zoologie Pure et Appliquée* 10: 514–527.

Jones J.C. & Oldroyd B.P. 2006. Nest thermoregulation in social insects. *Advances in Insect Physiology* 33: 153–191. https://doi.org/10.1016/S0065-2806(06)33003-2

Jörger K.M. & Schrödl M. 2013. How to describe a cryptic species? Practical challenges of molecular taxonomy. *Frontiers in Zoology* 10 (1): 1–27. https://doi.org/10.1186/1742-9994-10-59

Jowers M.J., Garcia-Mudarra J.L., Charles S.P. & Murphy J.C. 2019. Phylogeography of West Indies Coralsnakes (*Micrurus*): Island colonisation and banding patterns. *Zoologica Scripta* 48 (3): 263–276. https://doi.org/10.1111/zsc.12346

Jowers M.J., Smart U., Sánchez-Ramírez S., Murphy J.C., Gómez A., Bosque R.J., Sarker G.C., Noonan B.P., Faria J.F., Harris H.D., da Silva N.J., Prudente A.L., Weber J., Kok P.J., Rivas G.A., Jadin R.C., Sasa M., Muñoz-Mérida A., Moreno-Rueda G. & Smith E.N. 2023. Unveiling underestimated species diversity within the Central American coralsnake, a medically important complex of venomous taxa. *Scientific Reports* 13 (11674): 1–11. https://doi.org/10.1038/s41598-023-37734-5

Kalyaanamoorthy S., Minh B.Q., Wong T.K., Von Haeseler A. & Jermiin L.S. 2017. ModelFinder: fast model selection for accurate phylogenetic estimates. *Nature Methods* 14 (6): 587–589. http://doi.org/10.1038/nmeth.4285

Katoh K. & Standley D.M. 2013. MAFFT multiple sequence alignment software version 7: improvements in performance and usability. *Molecular Biology and Evolution* 30 (4): 772–780. https://doi.org/10.1093/molbev/mst010

Kley N.J. 2001. Prey transport mechanisms in blindsnakes and the evolution of unilateral feeding systems in snakes. *American Zoologist* 41: 1321–1337. https://doi.org/10.1093/icb/41.6.1321

Kley N.J. & Brainerd E.L. 1999. Feeding by mandibular raking in a snake. *Nature* 402: 369–370. https://doi.org/10.1038/46460

Knapp C.R. & Owens A. 2008. Nesting Behavior and the use of termitaria by the Andros Iguana (*Cyclura cychlura cychlura*). *Journal of Herpetology* 42: 46–53. https://www.jstor.org/stable/40060481

Koch C., Venegas P.J., Santa Cruz R. & Böhme W. 2018. Annotated checklist and key to the species of amphibians and reptiles inhabiting the northern Peruvian dry forest along the Andean valley of the Marañón River and its tributaries. *Zootaxa* 4385 (1): 1–101. https://doi.org/10.11646/zootaxa.4385.1.1

Kuch U. & Ayala-Varela F. 2002. First record of *Micrurus peruvianus* Schmidt, 1936 from Ecuador. *Herpetozoa* 15 (3/4): 182–183

Kumazawa Y. & Nishida M. 1993. Sequence evolution of mitochondrial tRNA genes and deep–branch animal phylogenetics. *Journal of Molecular Evolution* 37 (4): 380–398. https://doi.org/10.1007/bf00178868

Leigh J.W. & Bryant D. 2015. POPART: full-feature software for haplotype network construction. *Methods in Ecology and Evolution* 6 (9): 1110–6.

Lomonte B., Rey-Suárez P., Fernández J., Sasa M., Pla D., Vargas N., Bénard-Valle N., Sanz L., Corrêa-Netto C., Núñez V., Alape-Girón A., Alagón A., Gutiérrez J.M. & Calvete J.J. 2016. Venoms of *Micrurus* coral snakes: Evolutionary trends in compositional patterns emerging from proteomic analyses. *Toxicon* 122: 7–25. https://doi.org/10.1016/j.toxicon.2016.09.008

Lougheed S.C., Gascon C., Jones D.A., Bogart J.P., & Boag P.T. 1999. Ridges and rivers: a test of competing hypotheses of Amazonian diversification using a dart-poison frog (*Epipedobates femoralis*). *Proceedings of the Royal Society of London. Series B: Biological Sciences* 266 (1431), 1829–1835.

Maddison W.P. & Maddison D.R. 2019. Mesquite: a modular system for evolutionary analysis. Ver. 3.70. Available from https://www.mesquiteproject.org/ [accessed 12 Apr. 2026].

Marques O. & Sazima I. 2021. The natural history of New World coralsnakes. *In*: Silva Jr. N.J., Porras L.W., Aird S.D. & Prudente A. (eds.) *Advances in Coralsnakes Biology: with an Emphasis on South America*: 275–290. Eagle Mountain Publishing. Eagle Mountain, Utah.

Martins M. & Oliveira M.E. 1998. Natural history of snakes in forests of the Manaus region, Central Amazonia, Brazil. *Herpetological Natural History* 6 (2): 78–150.

Meise W. 1938. Eine neue Korallenschlange aus dem Amazonasgebiet. *Zoologischer Anzeiger* 123: 20–22.

Merrem B. 1820. *Versuch eines Systems der Amphibien. Marburg*. Germany.

Mizuno T. & Kojima Y. 2015. A blindsnake that decapitates its termite prey. *Journal of Zoology* 297 (3): 220–224. http://doi.org/10.1111/jzo.12268

Montoya-Cruz A., Mancera-García D. & Díaz-Flórez R. 2021. Defensive behavior by a Villavicencio coralsnake, *Micrurus medemi* Roze 1967 (Squamata: Elapidae), in Colombia. *Reptiles & Amphibians* 28 (3): 483–484. https://doi.org/10.17161/randa.v28i3.15719

Montoya-Cruz A., Díaz-Flórez R., & Mancera-García D. 2022. A new departmental and elevational record for the Villavicencio Coralsnake, *Micrurus medemi* Roze 1967 (Squamata: Elapidae), in Colombia. *Reptiles & Amphibians* 29 (1): 189–190. https://doi.org/10.17161/randa.v29i1.16329

Moreira L., Fenolio D., Silva H. & Silva Jr N. 2009. A preliminary list of the Herpetofauna from termite mounds of the Cerrado in the Upper Tocantins river valley. *Papéis Avulsos de Zoologia* 49: 183–189. https://doi.org/10.1590/S0031-10492009001500001

Nagy Z. T., Dekoninck W., De Block F., Yeo K., Silue K.S. & Delsinne T. 2017. Oviposition of the snake *Thelotornis kirtlandii* in a parabiotic ant nest. *Salamandra* 53(1): 167–170.

Nascimento L.R., Silva Jr N.J., Feitosa D.T. & Prudente A.L. 2019. Taxonomy of the *Micrurus spixii* species complex (Serpentes, Elapidae). *Zootaxa* 4668 (3): 370–392. https://doi.org/10.11646/zootaxa.4668.3.4

Nascimento L.R., Graboski R., Silva Jr. N.J. & Prudente A.L. 2024. Integrative taxonomy of *Micrurus ibiboboca* (Merrem, 1820) (Serpentes, Elapidae) reveals three new species of coral snake. *Systematics and Biodiversity* 22 (1): 2315958. https://doi.org/10.1080/14772000.2024.2315958

Niceforo M.H. 1942. Los ofidios de Colombia. *Revista de la Academia Colombiana de Ciencias Exactas, Físicas y Naturales* 5 (17): 84–101.

Nogueira C.C., Argôlo A.J., Arzamendia V., Azevedo J.A., Barbo F.E., Bérnils R.S., Bolochio B., Borges-Martins M., Brasil-Godinho M., Braz H., Buononato M., Cisneros-Heredia D., Colli G., Costa H., Franco F., Giraudo A., Gonzalez R., Guedes T., Hoogmoed M., Marques O. & Martins M. 2019. Atlas of Brazilian snakes: verified point-locality maps to mitigate the Wallacean shortfall in a megadiverse snake fauna. *South American Journal of Herpetology* 14: 1–274. https://doi.org/10.2994/SAJH-D-19-00120.1

Noonan B.P. & Chippindale P.T. 2006. Vicariant origin of Malagasy reptiles supports Late Cretaceous Antarctic land bridge. *The American Naturalist* 168 (6): 730–741. https://doi.org/10.1086/509052

Olson D.M., Dinerstein E., Wikramanayake E.D., Burgess N.D., Powell G.V., Underwood E.C., D'Amico J.A., Itoua I., Strand H.E., Morrison J.C., Loucks C.J., Allnutt T.F., Ricketts T.H., Kura Y., Lamoreux J.F., Wettengel W.W., Hedao P. & Kassem K.R. 2001. Terrestrial ecoregions of the world: a new map of life on Earth. *Bioscience* 51 (11): 933–938. https://doi.org/10.1641/0006-3568(2001)051[0933:TEOTWA]2.0.CO;2

Osorio-Olvera L., Lira-Noriega A., Soberón J., Peterson A.T., Falconi M., Contreras-Díaz R.G., Martínez-Meyer E., Barve V. & Barve N. 2020. *ntbox*: An r package with graphical user interface for modelling and evaluating multidimensional ecological niches. *Methods in Ecology and Evolution* 11 (10): 1199–1206. https://doi.org/10.1111/2041-210X.13452

Padial J.M., Miralles A., De la Riva I. & Vences M. 2010. The integrative future of taxonomy. *Frontiers in Zoology* 7 (1): 1–14. https://doi.org/10.1186/1742-9994-7-16

Palumbi S.R. 1996. Nucleic acids II: The polymerase chain reaction. *In*: Hillis D.M., Moritz C. & Mable B.K. (eds.) *Molecular Systematics*: 205–207. Sinauer Associates, Massachusetts.

Parkinson C.L., Campbell J.A. & Chippendale P.T. 2002. Multigene phylogenetic analysis of pitvipers with comments on the biogeographical history of the group. *In*: Schuett G.W., Hoggren M., Douglas M.E. & Greene H.W. (eds) *Biology of the Vipers*: 93–110. Eagle Mountain Publishing, Utah.

Patton J.L., Da Silva M.N.F. & Malcolm J.R. 1994. Gene genealogy and differentiation among arboreal spiny rats (Rodentia: Echimyidae) of the Amazon basin: a test of the riverine barrier hypothesis. *Evolution* 48 (4): 1314–1323.

Passos P. & Fernandes D.S. 2005. Variation and taxonomic status of the aquatic coral snake *Micrurus surinamensis* (Cuvier, 1817) (Serpentes: Elapidae). *Zootaxa* 953 (1): 1–8. https://doi.org/10.11646/zootaxa.953.1.1

Peres C.A., Patton J.L., & da Silva M. 1996. Riverine barriers and gene flow in Amazonian saddle-back tamarins. *Folia Primatologica* 67 (3): 113–124.

Peters J.A. & Orejas-Miranda B. 1970. Catalogue of the Neotropical Squamata. Part I. Snakes. *Bulletin of the United States National Museum* 297: 1–347.

Peters W. 1871. Über eine von Hrn. Dr. Robert Abendroth in dem Hochlande von Peru gemachte Sammlung von Amphibien, welche derselbe dem Königl. zoologischen Museum geschenkt hat. *Monatsberichte der Königlichen Preussischen Akademie der Wissenschaften zu Berlin*: 397–404.

Peterson A.T. & Soberón J. 2012. Species distribution modeling and ecological niche modeling: getting the concepts right. *Natureza & Conservação* 10 (2): 102–107. http://dx.doi.org/10.4322/natcon.2012.019

Pires A.C. & Marinoni L. 2010. DNA barcoding and traditional taxonomy unified through integrative taxonomy: a view that challenges the debate questioning both methodologies. *Biota Neotropica* 10: 339–346. https://doi.org/10.1590/S1676-06032010000200035

Pires G.M., Da Silva Jr N.J., Feitosa T.D., Prudente A., Filho G.A. & Zaher H. 2014. A new species of triadal coral snake of the genus *Micrurus* Wagler, 1824 (Serpentes: Elapidae) from northeastern Brazil. *Zootaxa* 3811 (4): 569–584. https://doi.org/10.11646/zootaxa.3811.4.8

Pisani R.G. 2009. Use of an active ant nest as a hibernaculum by small snake species. *Transactions of The Kansas Academy of Science* 112: 113–118. https://doi.org/10.1660/062.112.0215

Phillips S.J., Anderson R.P. & Schapire R.E. 2006. Maximum entropy modeling of species geographic distributions. *Ecological Modelling* 190 (3-4): 231–259. https://doi.org/10.1016/j.ecolmodel.2005.03.026

Puillandre N., Brouillet S. & Achaz G. 2021. ASAP: assemble species by automatic partitioning. Molecular ecology resources, 21(2), 609–620. https://doi.org/10.1111/1755-0998.13281

Quilumbaquín W., Carrera-Gonzalez A. & Ortega-Andrade H.M. 2023. Environmental DNA and visual encounter surveys for amphibian biomonitoring in aquatic environments of the Ecuadorian Amazon. *PeerJ* 11: e15455. https://doi.org/10.7717/peerj.15455

R Core Team. 2022. R: A language and environment for statistical computing. R Foundation for Statistical Computing, Vienna, Austria. Available from https://www.R-project.org/

Rambaut A., Drummond A.J., Xie D., Baele G. & Suchard M.A. 2018. Posterior summarisation in Bayesian phylogenetics using Tracer 1.7. *Systematic Biology* 67 (5): 901–904. https://doi.org/10.1093/sysbio/syy032

Rannala B. 2015. The art and science of species delimitation. *Current Zoology* 61 (5): 846–853. https://doi.org/10.1093/czoolo/61.5.846

Reyes-Velasco J., Adams R.H., Boissinot S., Parkinson C.L., Campbell J.A., Castoe T.A. & Smith E.N. 2020. Genome-wide SNPs clarify lineage diversity confused by coloration in coralsnakes of the *Micrurus diastema* species complex (Serpentes: Elapidae). *Molecular Phylogenetics and Evolution* 147: 106770. https://doi.org/10.1016/j.ympev.2020.106770

Ronquist F., Teslenko M., Van Der Mark P., Ayres D.L., Darling A., Höhna S., Larget B., Liu L., Suchard M.A. & Huelsenbeck J.P. 2012. MrBayes 3.2: Efficient Bayesian phylogenetic inference and model choice across a large model space. *Systematics Biology* 61: 539–542. http://dx.doi.org/10.1093/sysbio/sys029

Rozas J., Ferrer-Mata A., Sánchez-DelBarrio J.C., Guirao-Rico S., Librado P., Ramos-Onsins S.E., & Sánchez-Gracia A. 2017. DnaSP 6: DNA sequence polymorphism analysis of large data sets. *Molecular Biology and Evolution* 34 (12): 3299–3302. https://doi.org/10.1093/molbev/msx248

Roze J.A. 1966. On the synonymy and type specimens of the coral snakes *Micrurus corallinus* and *M. ibiboboca* (*Marcgravii*). *Copeia* 1966 (2): 369–371.

Roze J.A. 1967. A check list of the New World venomous coralsnakes (Elapidae), with descriptions of new forms. *American Museum Novitates* 2287: 1–60.

Roze J.A. 1983. New World coral snakes (Elapidae): a taxonomic and biological summary. *Memorias do Instituto Butantan* 46: 305–338.

Roze J.A. 1989. New species and subspecies of coralsnakes, genus *Micrurus* (Elapidae), with notes on type specimens of several species. *American Museum Novitates* 2932: 1–15.

Roze J.A. 1994. Notes on taxonomy of venomous coral snakes (Elapidae) of South America. *Bulletin of the Maryland Herpetological Society* 30: 177–185.

Roze J.A. 1996. *Coral Snakes of the Americas: Biology, Identification, and Venoms*. Krieger Publishing Company, Malabar, Florida.

Sahlin K., Lim M.C. & Prost S. 2021. NGSpeciesID: DNA barcode and amplicon consensus generation from long-read sequencing data. *Ecology and Evolution* 11 (3): 1392–1398. https://doi.org/10.1002/ece3.7146

Samadi S. & Barberousse A. 2006. The tree, the network, and the species. *Biological Journal of the Linnean Society* 89 (3): 509–521. https://doi.org/10.1111/j.1095-8312.2006.00689.x

Santos C.D., Sarmento H., de Miranda F.P., Henrique-Silva F. & Logares R. 2020. Uncovering the genomic potential of the Amazon River microbiome to degrade rainforest organic matter. *Microbiome* 8: 151. https://doi.org/10.1186/s40168-020-00930-w

Savage J.M. 1960. A revision of the Ecuadorian snakes of the colubrid genus *Atractus*. *Miscellaneous Publications Museum of Zoology*, *University of Michigan* 112: 1–86.

Savage J.M. & Slowinski J.B. 1990. Short note: A simple consistent terminology for the basic colour patterns of the venomous coral snakes and their mimics. *Herpetological Journal* 1: 530–532.

Savage J.M. & Slowinski J.B. 1992. The colouration of the venomous coral snakes (family Elapidae) and their mimics (families Aniliidae and Colubridae). *Biological Journal of the Linnean Society* 45 (3): 235–254. https://doi.org/10.1111/j.1095-8312.1992.tb00642.x

Schmidt K.P. 1936. Preliminary account of coral snakes of South America. *Field Museum of Natural History Publications, Zoological Series* 20: 189–203.

Schmidt K.P. 1954. The annellated coral snake, *Micrurus annellatus* Peters. *Fieldiana, Zoology* 34 (30): 319–325.

Schmidt K.P. 1955. Coral snakes of the genus *Micrurus* in Colombia. *Fieldiana, Zoology* 34: 337–359.

Schlick-Steiner B.C., Steiner F.M., Seifert B., Stauffer C., Christian E. & Crozier R.H. 2010. Integrative taxonomy: a multisource approach to exploring biodiversity. *Annual Review of Entomology* 55: 421–438. https://doi.org/10.1146/annurev-ento-112408-085432

Silva-Haad J.J. 1994. Las *Micrurus* de la Amazonia colombiana: biología y toxicología experimental de sus venenos. *Colombia Amazónica* 7: 41–138.

Sites Jr J.W. & Marshall J.C. 2004. Operational criteria for delimiting species. *Annual Review of Ecology, Evolution, and Systematics* 35: 199–227. https://doi.org/10.1146/annurev.ecolsys.35.112202.130128

Shine R. & Madsen T. 1997. Prey abundance and predator reproduction: rats and pythons on a tropical Australian floodplain. *Ecology* 78 (4): 1078–1086. https://doi.org/10.1890/0012-9658(1997)078[1078:PAAPRR]2.0.CO;2

Slowinski J.B. 1995. A phylogenetic analysis of the New World coralsnakes (Elapidae: *Leptomicrurus*, *Micruroides*, and *Micrurus*) based on allozymic and morphological characters. *Journal of Herpetology* 29 (3): 325–338.

Slowinski J.B. & Keogh J.S. 2000. Phylogenetic relationships of elapid snakes based on cytochrome b mtDNA sequences. *Molecular Phylogenetics and Evolution* 15 (1): 157–164. https://doi.org/10.2307/1564981

Soini P. 1974. Polychromatism in a population of *Micrurus langsdorffi*. *Journal of Herpetology* 8 (3): 267–269. https://doi.org/10.2307/1563184

Streicher J.W., McEntee J.P., Drzich L.C., Card D.C., Schield D.R., Smart U., Parkinson C.L., Jezkova T., Smith E.N. & Castoe T.A. 2016. Genetic surfing, not allopatric divergence, explains spatial sorting of mitochondrial haplotypes in venomous coralsnakes. *Evolution* 70 (7): 1435–1449. https://doi.org/10.1111/evo.12967

Syfert M.M., Smith M.J. & Coomes D.A. 2013. The effects of sampling bias and model complexity on the predictive performance of MaxEnt species distribution models. *PloS ONE* 8 (2): e55158. https://doi.org/10.1371/journal.pone.0055158

Tamura K., Stecher G. & Kumar S. 2021. MEGA11: Molecular Evolutionary Genetics Analysis version 11. *Molecular Biology and Evolution* 38 (7): 3022–3027. https://doi.org/10.1093/molbev/mst197

Terribile L.C., Diniz-Filho J.A., Rodríguez M.Á. & Rangel T.F. 2009. Richness patterns, species distributions and the principle of extreme deconstruction. *Global Ecology and Biogeography* 18 (2): 123–136. https://doi.org/10.1111/j.1466-8238.2008.00440.x

Terribile L.C., Feitosa D.T., Pires M.G., de Almeida P.C., de Oliveira G., Diniz-Filho J.A. & da Silva Jr N. 2018. Reducing Wallacean shortfalls for the coralsnakes of the *Micrurus lemniscatus* species complex: Present and future distributions under a changing climate. *PloS One* 13 (11): e0205164. https://doi.org/10.1371/journal.pone.0205164

Terribile L.C., de Oliveira G., Lima-Ribeiro M.S., Feitosa D.T., Giraudo A.R., Martins M.M., Arzamendia V., Pires M.G., da Silva Jr N., Moura J.C., Franco F.L., Silveira R. & Diniz-Filho J.A. 2021. Macroecology and conservation of South American coralsnakes. *In*: da Silva Jr N., Hoggren M., Porras W.E., Aird S.A. & Prudente L. (eds) *Advances in Coralsnake Biology: with an Emphasis on South America*: 313–332. Eagle Mountain Publishing, Utah.

Townsend T.M., Alegre R.E., Kelley S.T., Wiens J.J. & Reeder T.W. 2008. Rapid development of multiple nuclear loci for phylogenetic analysis using genomic resources: an example from squamate reptiles. *Molecular Phylogenetics and Evolution* 47 (1): 129–142.

Trifinopoulos J., Nguyen L.T., von Haeseler A. & Minh B.Q. 2016. W-IQ-TREE: a fast online phylogenetic tool for maximum likelihood analysis. *Nuclei Acids Research* 44 (W1): W232–W235. https://doi.org/10.1093/nar/gkw256

Valencia J.H. 2007. First record of the coral snake *Micrurus margaritiferus* Roze, 1967 in Ecuador. *Herpetozoa* 19 (3/4): 186–187.

Valencia J.H., Garzón-Tello K. & Barragán-Paladines M.E. 2016. *Serpientes venenosas de Ecuador: Sistemática, taxonomía, historia natural, conservación, envenenamiento y aspectos antropológicos*. Fundación Herpetológicas Gustavo Orcés/ Universidad de Texas, Arlington/Fondo Ambiental Nacional. Quito.

Vaser R., Sović I., Nagarajan N. & Šikić M. 2017. Fast and accurate de novo genome assembly from long uncorrected reads. *Genome Research* 27 (5): 737–746. https://doi.org/10.1101/gr.214270.116

Vaz-Ferreira R., Covelo de Zolessi L. & Achaval F. 1970. Oviposición y desarrollo de ofidios y lacertilios en hormigueros de *Acromyrmex*. *Physis* 29 (79): 431–459.

Vaz-Ferreira R., Covelo de Zolessi L. & Achaval F. 1974. Oviposición y desarrollo de ofidios y lacertilios en hormigueros de *Acromyrmex*. II. *Trabajos del V Congreso Latinoamericano de Zoología* 1: 232–244.

Vences M., Miralles A. & Dufresnes C. 2024. Next-generation species delimitation and taxonomy: Implications for biogeography. *Journal of Biogeography* 51 (9): 1–14. https://doi.org/10.1111/jbi.14807

Venables W.N. & Ripley B.D. 2002. *Modern Applied Statistics with S*, *4th Edition*. Springer, New York.

Wagler J. 1824. *Serpentum Brasiliensium species novae = ou, Histoire naturelle des espèces nouvelles de serpens: and recueillies et observées pendant le voyage dans l'intérieur du Brésil dans les années 1817, 1818, 1819, 1820*. Monachii Typis F.S. Hübschmanni, Munich.

Wallace A.R. 1852. On the monkeys of the Amazon. *Annals and Magazine of Natural History* 14 (84): 451–454. https://doi.org/10.1080/037454809494374

Werner F. 1901. Über Reptilien und Batrachier aus Ecuador und Neu-Guinea. *Verhandlungen der Kaiserlich-Königlichen Zoologisch-Botanischen Gesellschaft in Wien* 51: 593–614.

Werner F. 1927. Neue oder wenig bekannte Schlangen aus dem Wiener naturhistorischen Staatsmuseum. (III Teil). *Sitzungsberichte der Akademie der Wissenschaften Mathematisch-Naturwissenschaftliche Klasse* 135: 243–257.

Wied-Neuwied M. 1820. Über die Cobra Coral oder Cobras Coraes der Brasilianer. *Nova Acta Academiae Caesareae Leopoldino-Carolinae* 10: 105–110.

Will K.W., Mishler B.D. & Wheeler Q.D. 2005. The perils of DNA barcoding and the need for integrative taxonomy. *Systematic Biology* 54 (5): 844–851. https://doi.org/10.1080/10635150500354878

Zaher H. 1999. Hemipenial morphology of the South American xenodontine snakes, with a proposal for a monophyletic Xenodontinae and a reappraisal of colubroid hemipenes. *Bulletin of the American Museum of Natural History* 240: 1–168.

Zhang J., Kapli P., Pavlidis P. & Stamatakis A. 2013. A general species delimitation method with applications to phylogenetic placements. *Bioinformatics* 29 (22): 2869–2876. https://doi.org/10.1093/bioinformatics/btt499

Printed versions of all papers are deposited in the libraries of two of the institutes that are members of the *EJT* consortium: Muséum national d'Histoire naturelle, paris, France and Royal Museum for Central Africa, Tervuren, Belgium. The other members of the consortium are: Royal Belgian Institute of Natural Sciences, Brussels, Belgium; Meise Botanic Garden, Meise, Belgium; Natural History Museum of Denmark, Copenhagen, Denmark; Naturalis Biodiversity Center, Leiden, the Netherlands; Museo Nacional de Ciencias Naturales-CSIC, Madrid, Spain; Leibniz Institute for the Analysis of Biodiversity Change, Bonn - Hamburg, Germany; National Museum of the Czech Republic, prague, Czech Republic; The Steinhardt Museum of Natural History, Tel Aviv, Israël.

Appendix 1 (continued next page). Uncorrected *p*-distances among cis-Andean species of *Micrurus* (Wagler, 1824) based on the mitochondrial gene *ND4* and *cytb*. First page *ND4 second page cytb.*

Taxa	1	2	3	4	5	6	7	8	9	10	11	12	13	14	15	16	17	18	19	20	21	22	23
M._albicinctus_MPEG19548_M192_Careiro_Amazonas_Brazil	-																						
M._albicintus_MPEG20372_M187_rio_Formoso_Rondonia_Brazil	0.0199	-																					
M._annellatus_CORBIDI13726_M823_Huancavelica_Tayacaja_Peru	0.0087	0.0187	-																				
M._annellatus_CORBIDI14678_M822_Huancavelica_Tayacaja_Peru	0.0092	0.0185	0.0000	-																			
M._annellatus_QCAZ3470_La_Convencion_Cusco_Peru	0.0131	0.0199	0.0136	0.0145	-																		
M._annellatus_QCAZ4238_La_Convencion_Cusco_Peru	0.0119	0.0099	0.0112	0.0118	0.0131	-																	
M._corallinus_AF228424.1_Jurujuba_Niteroi_Rio_do_Janeiro_Brazil	0.0296	0.0207	0.0325	0.0325	0.0296	0.0237	-																
M._corallinus_KU289205_M54_PN_San_Rafael_Itapua_Paraguay	0.0185	0.0236	0.0173	0.0184	0.0160	0.0185	0.0030	-															
M._corallinus_USNM253597_M55_JF308715_Itapua_Paraguay	0.0185	0.0236	0.0173	0.0184	0.0160	0.0185	0.0030	0.0000	-														
M._ornatissimus_M558_50_km_E_from_Villavicencio_Colombia	0.0250	0.0323	0.0272	0.0289	0.0262	0.0263	0.0296	0.0296	0.0296	-													
M._ornatissimus_FHGO5938_M989_Tunantsa_Morona_Santiago_Ecuador	0.0317	0.0333	0.0302	0.0302	0.0345	0.0274	0.0364	0.0388	0.0388	0.0129	-												
M._ornatissimus_FHGO6357_M529_Tiputini_Dayuma_Orellana_Ecuador	0.0310	0.0335	0.0309	0.0329	0.0346	0.0274	0.0355	0.0358	0.0358	0.0107	0.0000	-											
M._ornatissimus_FHGO7137_M778_Paantim_Morona_Santiago_Ecuador	0.0316	0.0332	0.0302	0.0302	0.0345	0.0273	0.0363	0.0388	0.0388	0.0129	0.0000	0.0000	-										
M._ornatissimus_FHGO7314_M779_Makuma_Morona_Santiago_Ecuador	0.0317	0.0333	0.0302	0.0302	0.0345	0.0274	0.0364	0.0388	0.0388	0.0129	0.0000	0.0000	0.0000	-									
M._ornatissimus_FHGO9895_M991_Kiim_Morona_Santiago_Ecuador	0.0317	0.0333	0.0302	0.0302	0.0345	0.0274	0.0364	0.0388	0.0388	0.0129	0.0000	0.0000	0.0000	0.0000	-								
M._ornatissimus_QCAZ17641_Aguarico_Cononaco_Orellana_Ecuador	0.0310	0.0335	0.0309	0.0329	0.0346	0.0274	0.0355	0.0358	0.0358	0.0107	0.0000	0.0000	0.0000	0.0000	0.0000	-							
M._peruvianus_QCAZ12512_Zumba_Zamora_Chinchipe_Ecuador	0.0314	0.0343	0.0328	0.0328	0.0314	0.0301	0.0325	0.0355	0.0355	0.0068	0.0115	0.0109	0.0115	0.0115	0.0115	0.0109	-						
M._peruvianus_QCAZ6094_M253_Zumba_Zamora_Chinchipe_Ecuador	0.0301	0.0330	0.0314	0.0314	0.0301	0.0287	0.0296	0.0342	0.0342	0.0055	0.0101	0.0096	0.0101	0.0101	0.0101	0.0096	0.0014	-					
M._steindachneri_QCAZ4758_El_Reventador_Sucumbios_Ecuador	0.0262	0.0335	0.0285	0.0302	0.0274	0.0274	0.0325	0.0308	0.0308	0.0012	0.0144	0.0119	0.0144	0.0144	0.0144	0.0119	0.0082	0.0068	-				
M._steindachneri_QCAZ6307_Rio_Negro_Tungurahua_Ecuador	0.0251	0.0323	0.0273	0.0289	0.0263	0.0263	0.0326	0.0296	0.0296	0.0024	0.0159	0.0131	0.0158	0.0159	0.0159	0.0131	0.0096	0.0082	0.0036	-			
M._steindachneri_QCAZ8509_San_Rafael_Sucumbios_Ecuador	0.0310	0.0347	0.0322	0.0342	0.0322	0.0298	0.0266	0.0345	0.0345	0.0107	0.0072	0.0072	0.0072	0.0072	0.0072	0.0072	0.0096	0.0082	0.0119	0.0131	-		
M._tikuna_M556_Leticia_Amazonas_Colombia	0.0254	0.0323	0.0272	0.0289	0.0266	0.0266	0.0296	0.0296	0.0296	0.0000	0.0129	0.0109	0.0129	0.0129	0.0129	0.0109	0.0068	0.0055	0.0012	0.0024	0.0109	-	
M._medemi_M555_Villavicencio_Meta_Colombia	0.0227	0.0224	0.0223	0.0224	0.0263	0.0167	0.0326	0.0296	0.0296	0.0215	0.0202	0.0227	0.0201	0.0202	0.0202	0.0227	0.0233	0.0219	0.0227	0.0215	0.0251	0.0218	-
M._langsdorffi_QCAZ13129_RPF_Cuyabeno_Sucumbios_Ecuador	0,0250	0,0298	0,0223	0,0237	0,0262	0,0286	0,0325	0,0271	0,0271	0,0262	0,0273	0,0346	0,0273	0,0273	0,0273	0,0346	0,0246	0,0232	0,0274	0,0263	0,0346	0,0205	0,0263

Appendix 1 (continued). Uncorrected *p*-distances among cis-Andean species of *Micrurus* (Wagler, 1824) based on the mitochondrial gene *ND4* and *cytb*. First page *ND4 second page cytb.*

	Taxa	1	2	3	4	5	6	7	8	9	10
1	M._albicinctus_MPEG19548_M192_Careiro_Amazonas_Brazil	-									
2	M._albicintus_MPEG20372_M187_rio_Formoso_Rondonia_Brazil	0.0143	-								
3	M._annellatus_MHNC5676_M712_Puno_Peru	0.0073	0.0176	-							
4	M._annellatus_MHNC 7228, M715, Pasco, Peru	0.0159	0.0174	0.0145	-						
5	M._corallinus_KU289205_M54_Itapua_Paraguay	0.0075	0.0180	0.0077	0.0167	-					
6	M._corallinus_USNM253597_M55_Itapua_Paraguay	0.0071	0.0171	0.0087	0.0173	0.0000	-				
7	M._annellatus_MPEG20348_M182_Amazonas_Brazil	0.0100	0.0201	0.0118	0.0234	0.0149	0.0144	-			
8	M._medemi_M555_Villavicencio_Colombia	0.0258	0.0330	0.0294	0.0292	0.0313	0.0301	0.0358	-		
9	M._ornatissimus_M558_60_km_SO_Villavicencio_Colombia	0.0315	0.0359	0.0353	0.0379	0.0373	0.0359	0.0387	0.0286	-	
10	M._tikuna_M556_Leticia_Colombia	0.0255	0.0329	0.0291	0.0288	0.0327	0.0298	0.0357	0.0000	0.0286	-
11	M._peruvianus_QCAZ6094_M253_Zumba_Zamora_Chinchipe_Ecuador	0.0340	0.0386	0.0378	0.0403	0.0417	0.0383	0.0414	0.0315	0.0029	0.0310

Appendix 2

Other material examined

Micrurus averyi Schmidt, 1939 (n = 9)

BRAZIL – **Amazonas** • 1 ♂ 3 ♀; Manaos, Reserva Ducke; IB 32492, 43192, 43194, 43195 • 2 ♂ 2 ♀; Manaos, WWF, Reserva INPA; MZUSP 8485, 8448, 8449, 8450, 8451.

GUYANA – **Berbice Oriental-Corentyne** • 1♀; Courantyne District, near the Brazilian border; holotype FMNH

Micrurus margaritiferus Roze, 1967

PERU – **Amazonas** • 1 ♀; vicinity of Huampani, Río Cenepa; MVZ 163327. – **Loreto** • 1 ♀; Boca Río Santiago, Río Marañón; AMNH 53362; holotype.

Micrurus putumayensis Lancini, 1962 (n = 11)

BRAZIL – **Amazonas** • 3 ♀♀; Benjamin Constant, Río Javari; MNRJ 1008, 1300, 1542.

PERU – **Loreto** • 5 ♀♀; Centro Unión, lower Río Aucayo ca. 20 km SE of Iquitos; TCWC 45357, 45358, 46408, 47619, 57620 • 2 ♂ 1 ♀; Puerto Socorro, Río Putumayo, 270 km NE of Iquitos; holotype AMNH 110058, 110059, 110060.